องค์ประกอบทางเคมีและฤทธิ์ทางชีวภาพของใบกันภัยมหิดล

นายเฉลิมรัช สุขทัพภ์

วิทยานิพนธ์นี้เป็นส่วนหนึ่งของการศึกษาตามหลักสูตรปริญญาเภสัชศาสตรมหาบัณฑิต
สาขาวิชาเภสัชเวท ภาควิชาเภสัชเวทและเภสัชพฤกษศาสตร์
คณะเภสัชศาสตร์ จุฬาลงกรณ์มหาวิทยาลัย
ปีการศึกษา 2557

CHEMICAL CONSTITUENTS AND BIOLOGICAL ACTIVITIES OF *AFGEKIA MAHIDOLIAE* LEAVES

Mr. Chalermlat Suktap

A Thesis Submitted in Partial Fulfillment of the Requirements
for the Degree of Master of Science in Pharmacy Program in Pharmacognosy
Department of Pharmacognosy and Pharmaceutical Botany
Faculty of Pharmaceutical Sciences
Chulalongkorn University
Academic Year 2014

Thesis Title	CHEMICAL CONSTITUENTS AND BIOLOGICAL ACTIVITIES OF *AFGEKIA MAHIDOLIAE* LEAVES
By	Mr. Chalermlat Suktap
Field of Study	Pharmacognosy
Thesis Advisor	Associate Professor Suchada Sukrong, Ph.D.
Thesis Co-Advisor	Associate Professor Rutt Suttisri, Ph.D.

Accepted by the Faculty of Pharmaceutical Sciences, Chulalongkorn University in Partial Fulfillment of the Requirements for the Master's Degree

.....Dean of the Faculty of Pharmaceutical Sciences
(Assistant Professor Rungpetch Sakulbumrungsil, Ph.D.)

THESIS COMMITTEE

.....Chairman
(Professor Kittisak Likhitwitayawuid, Ph.D.)

.....Thesis Advisor
(Associate Professor Suchada Sukrong, Ph.D.)

.....Thesis Co-Advisor
(Associate Professor Rutt Suttisri, Ph.D.)

.....Examiner
(Associate Professor Surattana Amnuoypol, Ph.D.)

.....Examiner
(Associate Professor Boonchoo Sritularak, Ph.D.)

.....External Examiner
(Piyarat Chareonsap, Ph.D.)

เฉลิมรัช สุขทัพภ์ : องค์ประกอบทางเคมีและฤทธิ์ทางชีวภาพของใบกันภัยมหิดล (CHEMICAL CONSTITUENTS AND BIOLOGICAL ACTIVITIES OF *AFGEKIA MAHIDOLIAE* LEAVES) อ.ที่ปรึกษาวิทยานิพนธ์หลัก: รศ. ภญ. ร.ต.อ. หญิง ดร.สุชาดา สุขหร่อง, อ.ที่ปรึกษาวิทยานิพนธ์ร่วม: รศ. ภก. ดร.รุทธ์ สุทธิศรี, หน้า.

การศึกษาฤทธิ์ต้านออกซิเดชันของสารสกัดจากใบกันภัยมหิดลโดยหาปริมาณการจับอนุมูลอิสระ DPPH และ พลังต้านออกซิเดชันโดยรีดิวซ์หมู่เฟอร์ริก (FRAP) พบว่า สารสกัดเอธิลอะซิเตทและสารสกัดบิวทานอลมีฤทธิ์ต้านออกซิเดชันที่ดี จึงทำการศึกษาต่อโดยสามารถแยกสารในกลุ่มฟลาโวนอยด์ไกลโคไซด์ ได้ 5 ชนิดจากสารสกัดเอธิลอะซิเตทคือสาร juglanin, astragalin, nicotiflorin, isoquercetin และ apigenin-7-*O*-glucuronide ในขณะที่สามารถแยกสารในกลุ่มไฮโดรควิโนนไกลโคซ์ด์ได้ 1 ชนิด คือสาร arbutin จากสารสกัดบิวทานอล พิสูจน์โครงสร้างทางเคมีขององค์ประกอบในพืชเหล่านี้ได้โดยอาศัยเทคนิคทางสเปกโตรสโคปี ได้แก่ UV, IR, MS และ NMR ร่วมกับการเปรียบเทียบกับข้อมูลที่เคยมีรายงานมาก่อนแล้ว สาร juglanin และ nicotiflorin สามารถเร่งการเคลื่อนที่ของเซลล์ไฟโบรบลาสต์ได้เมื่อทดสอบฤทธิ์สมานแผล scratch-wound ในหลอดทดลอง

ภาควิชา	เภสัชเวทและเภสัชพฤกษศาสตร์	ลายมือชื่อนิสิต .....
สาขาวิชา	เภสัชเวท	ลายมือชื่อ อ.ที่ปรึกษาหลัก .....
ปีการศึกษา	2557	ลายมือชื่อ อ.ที่ปรึกษาร่วม .....

5476234933 : MAJOR PHARMACOGNOSY
KEYWORDS: AFGEKIA MAHIDOLIAE / FABACEAE / FLAVONOID GLYCOSIDES / SCRATCH-WOUND HEALING / FIBROBLASTS

CHALERMLAT SUKTAP: CHEMICAL CONSTITUENTS AND BIOLOGICAL ACTIVITIES OF *AFGEKIA MAHIDOLIAE* LEAVES. ADVISOR: ASSOC. PROF. SUCHADA SUKRONG, Ph.D., CO-ADVISOR: ASSOC. PROF. RUTT SUTTISRI, Ph.D., pp.

Antioxidant activities of the extracts of *A. mahidoliae* Burtt et Chermsir (Fabaceae) leaves were evaluated using DPPH radical scavenging and ferric reducing antioxidant power (FRAP) assays. Chemical constituents of the ethyl acetate and *n*-butanol extracts, which displayed strong activities, were further studied. Five flavonoid glycosides, juglanin, astragalin, nicotiflorin, isoquercetin and apigenin-7-*O*-glucuronide, were isolated from the ethyl acetate extract, while a hydroquinone glycoside, arbutin was obtained from the *n*-butanol extract. The chemical structures of these plant constituents were determined by spectroscopic techniques (UV, IR, MS, and NMR), and comparison with previously reported data. Juglanin and nicotiflorin were able to promote the fibroblasts migration in the in vitro scratch-wound healing assay.

Department:	Pharmacognosy and Pharmaceutical Botany	Student's Signature .....
		Advisor's Signature .....
Field of Study:	Pharmacognosy	Co-Advisor's Signature .....
Academic Year:	2014	

ACKNOWLEDGEMENTS

First and foremost, I would like to offer my sincerest gratitude to my advisor, Associate Professor Dr. Suchada Sukrong, for her attention, instruction, and constant encouragement throughout my research study.

I would like to thank my co-advisor, Associate Professor Dr. Rutt Suttisri. I have been helped many times by his guidance, especially in the extraction, isolation and structure determination of natural products.

I would like to express my appreciation to Professor Dr. Hyeong Kyu Lee of the Korea Research Institute of Bioscience and Biotechnology (KRIBB). It is my honor to have the opportunity to work in his laboratory. I also would like to thank all staffs members of Natural Medicine Laboratory, KRIBB for providing facilities and long lasting friendship.

I wish to express my deep appreciation to all member of the thesis committee for their suggestions and comments.

I would like to thank Miss Nareerat Petpiroon for assisting me numerous ways including teaching basic cell culture skills, giving beneficial advice, and valuable friendship.

The present study was financially supported by Ratchadapiseksomphot Endowment Fund of Chulalongkorn University (RES560530157-HR), the 90th Anniversary of Chulalongkorn University Fund (Ratchadapiseksomphot Endowment Fund).

I would like to thank all staff members and graduate students of the Department of Pharmacognosy and Pharmaceutical Botany, Faculty of Pharmaceutical Sciences, Chulalongkorn University for their friendship and help

Finally, I wish to express my special and deepest appreciation to my parents for supporting me throughout my study at Chulalongkorn University.

CONTENTS

Page

Page

Page

LIST OF TABLES

LIST OF FIGURES

LIST OF SCHEMES

CHAPTER I

INTRODUCTION

Afgekia is a genus in the subfamily Papilionoideae of family Fabaceae. Currently, only 3 species of this plant genus have been identified, i.e. *A. filipes* Geesink (Thai name: Kan phai), *A. mahidoliae* Burtt et Chermsir. (Thai name: Kan phai Mahidol) and *A. sericea* Craib (Thai name: Thua paep chang). *A. mahidoliae* is a rare plant that was firstly discovered, in 1967, growing on limestone mountains in the western part of Thailand (Boonkerd, 2001). It was later named "Kan phai Mahidol" to memorialize the surname "Mahidol" of King Bhumibol Adulyadej's mother, and was also chosen to be the symbolic plant of Mahidol University.

A. mahidoliae is a climbing plant having showy, characteristic purplish and whitish inflorescences, suitable for decorative purpose. The plant usually blooms during August to November. No record has been made of its medicinal uses and, although the plant was found nearly 50 years ago, there has been only one previous research on its biological activities and chemical constituents (Chainok, 2007)

As a preliminary screening for this study, the methanol extract of *A. mahidoliae* leaves was subjected to scratch wound assay as a model to evaluate its ability to promote the migration of human keratinocyte (HaCaT) and human dermal fibroblast (CCD-110sk) cell lines. The results showed that the extract was able to promote both keratinocyte and fibroblast migration in the wound healing process. It was thus interesting to try to discover the plant constituents responsible for this activity.

Another integral mechanism in the process of wound healing is antioxidant activity (Schreml *et al.*, 2010; Akkol *et al.*, 2011). After an injury, reactive oxygen species (ROS) are generally produced by immune cells in order to destroy invading microorganisms. However, overproduction of ROS can cause additional tissue damages, and it has therefore been identified as an important feature in the pathogenesis of chronic wound (Schäfer and Werner, 2008; Geethalakshmi *et al.*,

2013). Elimination of ROS by antioxidants may help to reduce these damages and prevent complications such as skin infection, cellulitis, etc. Consequently, in addition to the ability of chemical constituents from the leaves of *A. mahidoliae* to promote fibroblast migration, antioxidant activities of different extracts and compounds isolated from this plant were evaluated in this study.

The purposes of this research were as follows:

1. Separation and isolation of compounds from the leaves of *A. mahidoliae*
2. Identification of the chemical structures of isolated compounds.
3. Determination of biological activities including the ability to promote fibroblast migration and antioxidant activities of isolated compounds.

CHAPTER II

LITERATURE REVIEW

2.1 The genus *Afgekia* and *Afgekia Mahidoliae*

The genus "*Afgekia*", a member of the bean family (Fabaceae), was named after the initials of Arthur Francis George Kerran, an Irish-born plant collector (Boonkerd, 2001). Members of the genus are climbing shrubs, similar to the related genus *Wisteria*. Its compound leaves are imparipinnate with caduceus stipules and stipels. Its inflorescences are axillary or cauliflorous racemes or elongated panicles, with large imbricate-tailed sericeous bracts covering flower buds. The calyx is shortly 5-toothed. The corolla is papilionaceous with equal in length, clawed wings and keels. The stamens are diadelphous with the vexillary stamen free from the other 9 stamens. Its ovary is stipitate, with trichomes and with 2 ovules. The fruits are inflated legumes, dehiscent with thickly woody valves. The ellipsoid, shiny seeds are 1 or 2 per legume (Zhi and Les, 2010)

Up to the present, only three members of the genus *Afgekia* have been identified. Two of these species were identified from samples originally collected in Thailand. The first species, *Afgekia sericea* Craib, was described in 1927 by W. G. Craib from plant specimen collected in Nakhon Ratchasima. *Afgekia mahidoliae* Burtt et Chermsir. was found in 1967 by Mr. Kasem Chantaraprasong in Kanchanaburi and was subsequently described in 1971 (Burtt and Chermsirivathana, 1971). Only *A. sericea* has been used in Thai traditional medicine. Its roots were employed as an ingredient in combination with various herbs for the treatment of chickenpox, while its seeds have been used as a tonic (Chuakul, 1994).

Afgekia mahidoliae is a climber with whitish pubescent, imparipinnately compound leaves. These leaves are arranged alternately. Each compound leaf has 9-11 leaflets. The leaflet is oblong or oblong-ovate, about 2 cm wide and 4 cm long. Its inflorescences are in terminal raceme having pea-shaped, purplish flowers with

purple bracteoles. Its pods are brown, about 2-4 cm wide and 7-9 cm long, with brown hairs. The seeds are black, round-shaped, 1.5 cm in diameter.

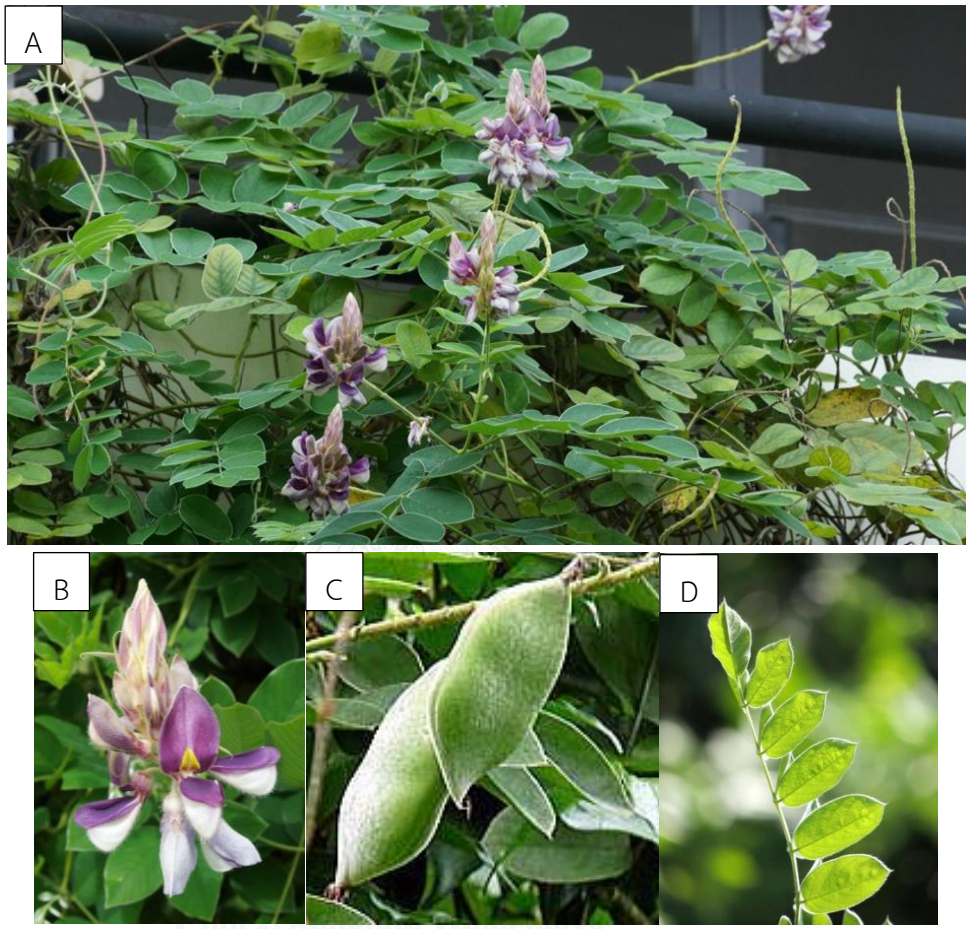

Figure 1 *Afgekia mahidoliae* Burtt et Chermsir. (A) whole plant, (B) inflorescensences, (C) pods, (D) compound leaves (https://www.facebook.com/pitan.singhasaneh/media_set?set=a.10150265828108581.333609.656858580&type=3, From Pitan Singhasaneh, 2014)

A previous research on *A. mahidoliae* has evaluated its leaf, petiole, flower and peduncle extracts for their antibacterial activity against common pathogenic bacteria and DPPH radical scavenging activity. Only its peduncle extract exhibited weak antibacterial activity against the gram-positive *Staphylococcus aureus*, whereas the methanolic extract of its leaves displayed the strongest DPPH radical scavenging activity. Phytochemical investigation of the petroleum ether extract of these leaves

yielded four long-chain hydrocarbon compounds: *n*-pentacosane (1), 1-triacontanol (2), butyldotriacontanoate (3) and *n*-octatriacontanal (4) (Figure 2). Among these isolated constituents, only *n*-octatriacontanal showed weak antioxidant activity against DPPH radical (Chainok, 2007).

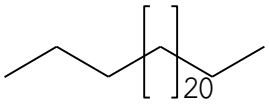

n-pentacosane (1)

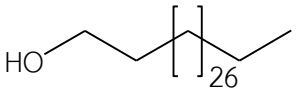

1-triacontanol (2)

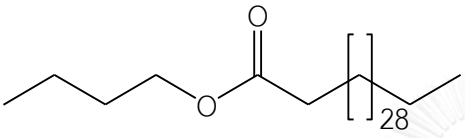

butyldotriacontanoate (3)

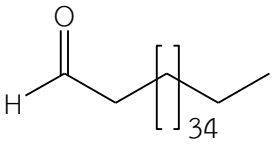

n-octatriacontanal (4)

Figure 2 Chemical compounds previously isolated from *Afgekia mahidoliae*

2.2 Wounds and wound healing

A wound is a type of skin injury which can be defined as the disruption of the anatomical continuity of tissue. Wound may be caused by physical, chemical, thermal or microorganism (Thakur *et al.*, 2011). Open wound usually occurs by sharp-edge object such as knives, needles, nails, whereas closed wound resulted from damaging of tissue under the skin by blunt force trauma (contusions), massive amount of force applied on the skin (crush injury), or damaging of blood vessels leading to accumulation of blood under the skin (hematoma).

Wounds can also be divided into 2 categories: acute and chronic (Demidova-Rice *et al.*, 2012). Examples of common acute wounds are surgical wound without infection and traumatic wound. Acute wound usually proceeds through an orderly and timely reparative process that results in sustained restoration of anatomic and functional integrity. On the contrary, chronic wound usually has at least one detained stage of wound healing. In acute wound, there is a balance in the production and degradation of extracellular matrix and essential components.

However, if this balance is lost and the degradation of these wound healing components is faster than their production, acute wound can develop into chronic wound (Edwards *et al.*, 2004; Schönfelder *et al.*, 2005). In addition, non-healing wounds are prone to develop complications such as skin infections, malignant transformation, and limitation in the movement (Menke *et al.*, 2007).

Wound healing is a multi-factorial process of skin in order to restore itself after injury. The process involves many cellular and biochemical interactions to repair devitalized tissues. There are 3 overlapping stages of wound healing: haemostasis and inflammation, new tissue formation (cell migration and proliferation) and remodeling (Gurtner *et al.*, 2008).

The first stage of wound repair, haemostasis and inflammation, occurs in the wound instantly after injury. Coagulation and haemostasis take place in order to prevent blood and other biological fluid losses, thus the function of vital organs remains unharmed despite the injury (Velnar *et al.*, 2009). The blood clot releases many chemical mediators such as pro-inflammatory cytokines and growth factors i.e. transforming growth factor-β (TGF-β), platelet-derived growth factor (PDGF), fibroblast growth factor (FGF) and epidermal growth factor (EGF). After bleeding is controlled, neutrophils migrate to the wound site for the activation of complement, destruction of microbes and cellular debris. The release of protease and reactive oxygen species at this stage helps to eliminate pathogens, but can cause damages to the surrounding tissues as well. Macrophages work together with neutrophils to release cytokines, which stimulate leucocytes to induce inflammatory response. This first stage occurs for several days after wounding and concludes with the apoptosis of inflammatory cells. The controlling mechanism for this stage is still unclear, although some studies have stated that important anti-inflammatory cytokines such as interleukin 1, TGF-A1 and some bioactive lipids i.e. lipoxins, resolvins, and

cyclopentenone prostaglandin may control this process (Gilroy *et al.*, 2004; Eming *et al.*, 2007).

The second stage, new tissue formation, starts on the third day after wounding and usually overlaps with the first stage. This stage is characterized by the migration and proliferation of fibroblasts, keratinocytes and endothelial cells over the temporary matrix within the wound. The released growth factors such as TGF-β and PDGF induce the migration of fibroblasts from the surrounding tissues into the wound area. Matrix proteins and collagen are then produced and accumulated extracellularly. Collagen, which gives strength and integrity to all tissues and is very important in this and the next stage of wound repair, replaces fibrin and fibronectin network formed during the blood clotting. The extracellular matrix is also necessary and supports further cell migration (Demidova-Rice et al., 2012)

Fibroblasts are formed from nondifferentiated mesenchymal cells within the dermis, which are transformed by the influence of the released cytokines and growth factors (Olczyk *et al.*, 2014). After their migration into the wound, fibroblasts change to myofibroblasts which contain actin bundles and actively extend pseudopodia. Attachment of these cells to fibronectin and collagen in the extracellular matrix, followed by the retraction of these cell extensions, causes the wound to contract. After this event, redundant fibroblasts are destroyed by apoptosis (Baum and Arpey, 2005). The formation of new blood vessels (angiogenesis), in order to provide blood supply and exchange metabolite, is another critical process in the healing of wounds. Crucial regulators including endothelial growth factor A (VEGFA) and fibroblast growth factor 2 (FGF2) are necessary for the stimulation of fibroblasts and endothelial cells to improve capillary growth, collagen production, and formation of granulation tissue at wound site. Epithelialization is another process which happens to reconstruct the epithelium after the injury. This process comprises the separation of keratinocytes from their basement membranes by the action of matrix metalloproteinase enzymes,

their migration to the wound area, proliferation and differentiation. It is a clinical symptom of healing, but does not signify the end of the healing process. The final phase of the process is the remodeling of the granulation tissue (Olczyk *et al*., 2014).

The remodeling phase begins when the rate of collagen synthesis and collagen breakdown is balanced leading to normal healing. The tensile strength of the wound increases continuously in parallel with collagen collection (Clark, 1993). The nature of the tissue is changed by the creation of new tissues. Some immature scars are slowly replaced by fibers. The density of fibroblasts and macrophages is reduced through apoptosis. Finally, the growth of new capillaries stops and metabolic activity at the site decreases, resulting in fully matured scar with high tensile strength.

2.3 Natural products and wound healing

Evaluation of the effectiveness of natural products in wound healing may be conducted either in *in vitro* or *in vivo* assay models. For *in vivo* models, many kinds of animal skin were used such as pig, mouse, rat and rabbit. Both incision and excision models of wound healing are frequently used as study models. The former is practical for the measuring of tensile strength which is an indication of improved collagenation, while the latter is suitable for histological evaluation. For *in vitro* models, two mammalian cell types, keratinocytes and fibroblasts, are used for the investigation of cellular behaviors. Currently, the two most common assays used in the study of cell migration are Boyden chamber-based trans-membrane assay and scratch wound assay. The latter assay is more convenient and economical than other assays (Liang *et al.*, 2007). The important advantage of this method is that the process mimics to some extent the migration of cells *in vivo* as well as the behavior of the cells during migration. It is also appropriate for the study of the regulation of cell migration by their interaction with extracellular matrix as well as cell-cell interaction. Another advantage is the opportunity to observe cells under microscope,

which might be useful for the analysis of intracellular signaling during migration (Tsala *et al.*, 2013).

Various natural products have been used in traditional medicine as wound healing agents and a large number of research articles have reported on wound healing potentials of plant extracts (Fronza *et al.*, 2009; Balekar *et al.*, 2012; Zubair *et al.*, 2012). In Thai traditional medicine, many plants have been employed in the treatment for wounds. Examples of plants found growing in Thailand that have been studied for wound healing activity are *Chromolaena odorata*, *Celosia argentea, Aloe vera* and *Centella asiatica*.

Chromolaena odorata (family Compositae) is a shrub commonly found throughout the country. In many tropical countries, its fresh leaves, or its decoction, have been traditionally used for the treatment of leech bite, soft tissue wounds and burn wounds. The use of its extract have been reported to enhance hemostasis and blood coagulation, and its stimulatory effect on the formation of granulation tissue and wound epithelialization were demonstrated clinically and histologically. Its leaf extract also enhanced fibroblasts and epithelial cell proliferation. Its phenolic acid and flavonoid contents also possessed powerful antioxidant activity that might protect skin cells against oxidative damage and enhance wound healing (Phan *et al.*, 1996; Phan *et al.*, 2001). Moreover, 70% ethanol extract of its leaves promoted mouse fibroblasts migration and proliferation (Pandith *et al.*, 2013).

Celosia argentea (family Amaranthaceae) is a decorative plant which has been used in traditional medicine to treat skin sores, ulcers, eruptions and mouth ulcers. Its leaf extract also possessed antimicrobial activity, which might prevent the wound bed from becoming infected. Its ethanolic leaf extract demonstrated ability to accelerate wound closure by promoting fibroblast motility and proliferation in rat burn model. The effect might result from mitogenic and motogenic promotion of dermal fibroblasts by the extract (Priya *et al.*, 2004).

Aloe vera (family Liliaceae) is a well-known tropical medicinal plant usually found growing in dry climate. The inside of its leaves contains mucilaginous tissue, called *Aloe vera* gel, which is promoted to be employed as a treatment for burn

wounds (Maenthaisong *et al.*, 2007). Although there are several reports on the wound healing property of *Aloe vera* gel, its mechanism in wound repair is unclear. Possible mechanism of its gel for wound repair might involve the increase in the number of macrophages, neutrophils and fibroblast cells (Takzare *et al.*, 2009). The gel could also stimulate gap junctional intercellular communication and proliferation of human dermal fibroblasts in diabetes mellitus patients, where FGF-2 is the target of activation (Atiba *et al.*, 2011).

Centella asiatica (family Umbelliferae) is a medicinal herb commonly used in the treatment of various skin diseases and wounds. In rats, the alcoholic extract of its leaves was able to increase cellular proliferation, wound breaking strength in wound incision model, wet and dry granulation tissue weights, granulation breaking tissue strength, collagenation and hydroxyproline content at the wound bed, resulting in increasing rates of wound contraction and epithelialization (Suguna *et al.*, 1996; Shetty *et al.*, 2006). In addition, its aqueous extract also enhanced corneal epithelium wound healing (Ruszymah *et al.*, 2012). Another study in rats to evaluate the effect of different *Centella asiatica* extracts in burn and incision wound models showed that all extracts (hexane, ethyl acetate, methanol and aqueous extracts) displayed wound healing effects in both wound models, and the ethyl acetate extract was the most active one (Somboonwong *et al.*, 2012).

Although there have been many reports on the wound healing effect of plant extracts, only a handful of phytochemical compounds have been identified as having wound healing activity. Different groups of natural products such as alkaloids, terpenoids, phenylpropanoids were reported to modulate wound repair through different mechanisms.

Even though alkaloid is a group of natural constituents that has been known to possess various biological activities, the number of studies which demonstrated the wound healing activity of these compounds is not as much as expected and might be due to their known cytotoxicity. Examples of alkaloids that have been reported as wound healing agents are the carbazole alkaloids mahanine (5), mahanimbicine (6) and mahanimbine (7) isolated from *Murraya koenigii*. These

alkaloids can protect the injury site from infections as well as elevate the rate of connective tissue formation (Nagappan *et al.*, 2012). Taspine (8), an alkaloid obtained from *Croton lechleri*, enhanced the chemotaxis of fibroblasts and accelerated wound healing in the early phases (Porras-Reyes *et al.*, 1993).

Terpenoids such as asiaticoside (9), a bioactive saponin glycoside from *Centella asiatica*, promoted the migration of human dermal fibroblasts (aHDFs) and human epidermal keratinocytes (aNHEKs) (Lee *et al.*, 2012). Moreover, the compound could promote angiogenesis and displayed wound healing ability in both acute and chronic in vivo models. Hydroxyproline and collagen contents, tensile strength and epithelialization were also increased after application of asiaticoside solution to the wound (Shukla *et al.*, 1999). Asiatic acid, which is the triterpenoid aglycone of asiaticoside, was also active in wound healing and in the management of keloid scars. The compound could suppress TGF-β1-induced collagen and PAI-1 expression in keloid fibroblasts through PPAR-γ activation (Bian *et al.*, 2013). The structure-wound healing activity relationship of asiatic acid has been studied (Jeong, 2006). Two sesquiterpenoids, epi-alpha-bisabolol (10) and alpha-bisabolol (11), and a monoterpenoid, alpha-terpineol (12), isolated from Peperomia galioides, were able to promote wound healing through the formation of scar tissue (Villegas *et al.*, 2001). The triterpenoids cycloastragenol (13), astragaloside IV (14), and cyclocanthoside E (15) were reported to promote migration of fibroblasts at concentrations of 1, 10 and 10 ng/ml, respectively (Sevimli-Gür *et al.*, 2011). Some iridoid glycosides, for instance, aurucin (16), scopolioside A (17), scrophuloside A (18) and scrovalentinoside (19), have demonstrated different actions on the healing of wounds. Aurucin solution promoted early re-epithelialization and collagen matrix formation of oral mucosal, and therefore has a potential to be used as a topical agent for oral wound healing (Shim *et al.*, 2007). The other three iridoid glycosides could stimulate the growth of human dermal fibroblasts (Stevenson *et al.*, 2002).

Flavonoids are secondary metabolites most widely found in many higher plant families. Treatment of wounds with flavonoids and polyphenolic compounds can be considered as a strategy for wound healing both *in vitro* and *in vivo*. Catechin

derivatives such as epicatechin-3-*O*-gallate (20) and 4′-*O*-methylepicatechin-3-*O*-gallate (21) demonstrated promising wound healing effects in the scratch wound assay (Schmidt *et al.*, 2010). A flavonoid oligocoside, kaempferol-3-*O*-[(6-caffeoyl)-β-glucopyranosyl (1⟶3) α-rhamnopyranoside]-7-*O*-α-rhamnopyranoside (22) was reported to enhance wound closure rate of keratinocytes at the concentration of 20 μM (Clericuzio *et al.*, 2012). Anthocyanins, which is another class of flavonoids, also accelerated wound healing in fibroblasts and keratinocytes. Anthocyanins isolated from black soybean seed coats at concentrations of 50 and 100 μg/ml increased the migration of keratinocytes, while at 100 μg/ml fibroblast migration was enhanced (Nizamutdinova *et al.*, 2009). The dimeric proanthocyanidin epicatechin-(4β⟶8)-catechin (23) isolated from the root bark of *Paeonia suffruticosa* increased viability and cellular proliferation of keratinocytes at the concentration of 100 nM (Wang *et al.*, 2013). At the concentration of 80 μM, rutin (26), morin (25) and chrysin (24) increased collagen synthesis, which is necessary for repairing process, in human fibroblast without affecting protein concentration (Stipcevic *et al.*, 2006). In addition, rutin enhanced the production and accumulation of extracellular matrix, and increased the contraction of wound in incision model (Tran *et al.*, 2011). 7-Carboxymethyloxy-3′,4′,5-trimethoxy flavone (DA6034) (27), a synthetic flavonoid, promoted gastric epithelial cell migration and cell motility using scratch wound and trans-well assays (Kim *et al.*, 2012).

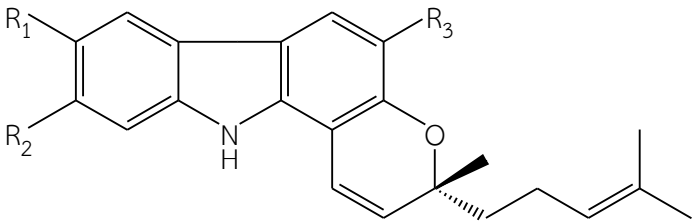

	R_1	R_2	R_3
mahanine (5)	H	OH	CH_3
mahanimbicine (6)	CH_3	H	H
mahanimbine (7)	H	H	CH_3

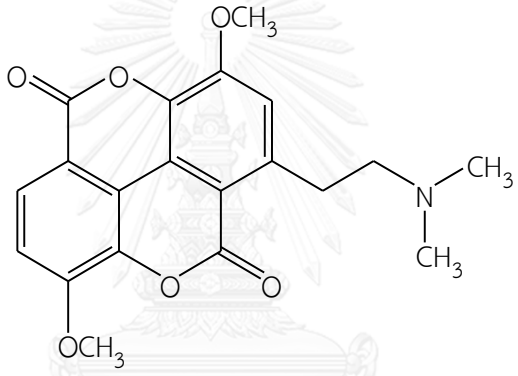

taspine (8)

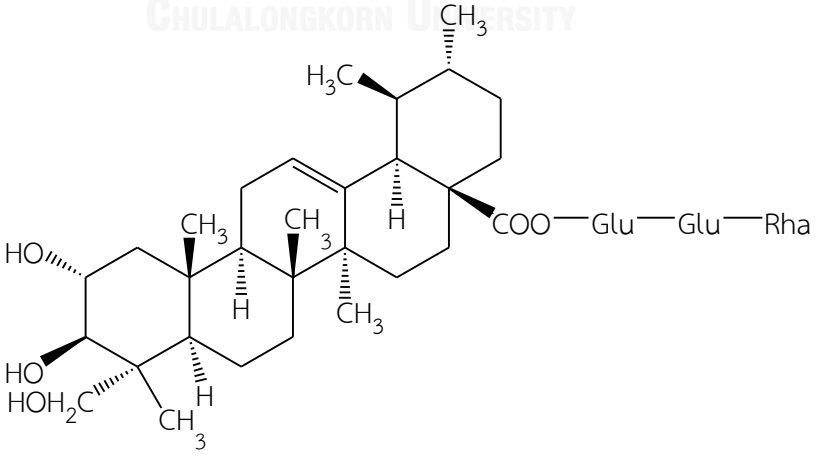

asiaticoside (9)

Figure 3 Natural compounds previously reported to have wound healing activity

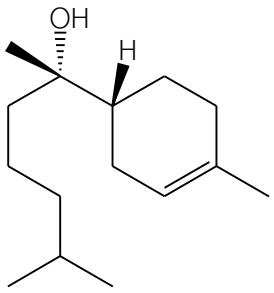

epi-alpha-bisabolol (10)

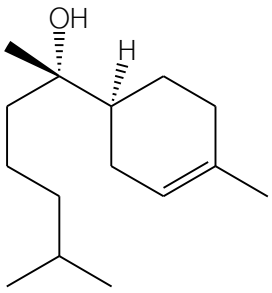

alpha-bisabolol (11)

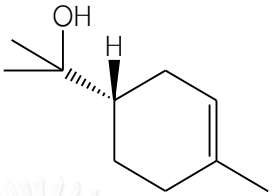

alpha-terpineol (12)

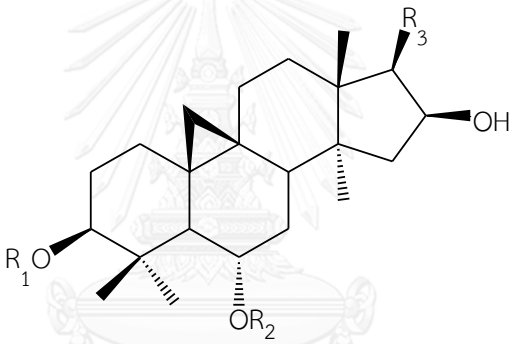

	R_1	R_2	R_3
cycloastragenol (13)	H	H	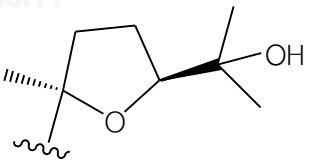
astragaloside IV (14)	Xyl	Glu	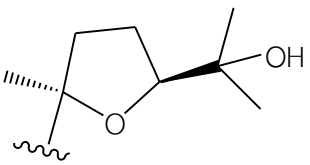
cyclocanthoside E (15)	Xyl	Glu	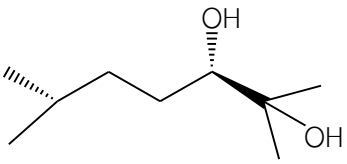

Figure 3 (continued) Natural compounds previously reported to have wound healing activity

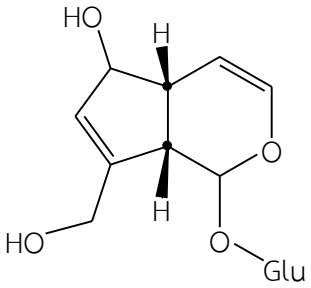

aurucin (16)

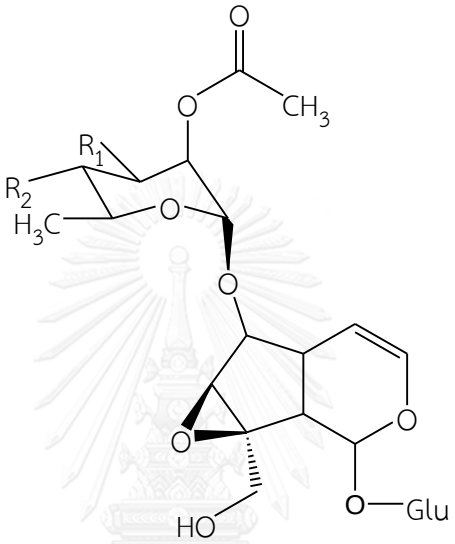

	R_1	R_2
scopolioside A (17)	p-methoxycinnamoyl	OCH_3
scrophuloside A (18)	p-methoxycinnamoyl	p-methoxycinnamoyl
scrovalentinoside (19)	OCH_3	p-methoxycinnamoyl

p-methoxycinnamoyl = 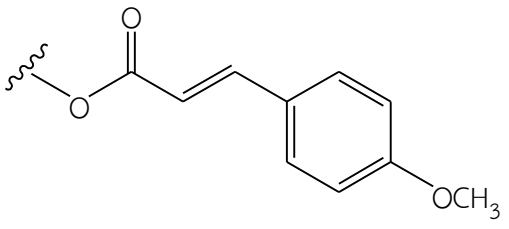

Figure 3 (continued) Natural compounds previously reported to have wound healing activity

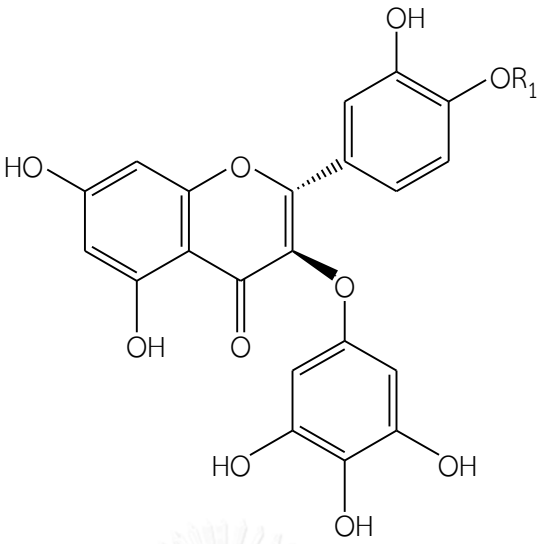

	R_1
epicatechin-3-*O*-gallate (20)	H
4′-*O*-methylepicatechin-3-*O*-gallate (21)	CH_3

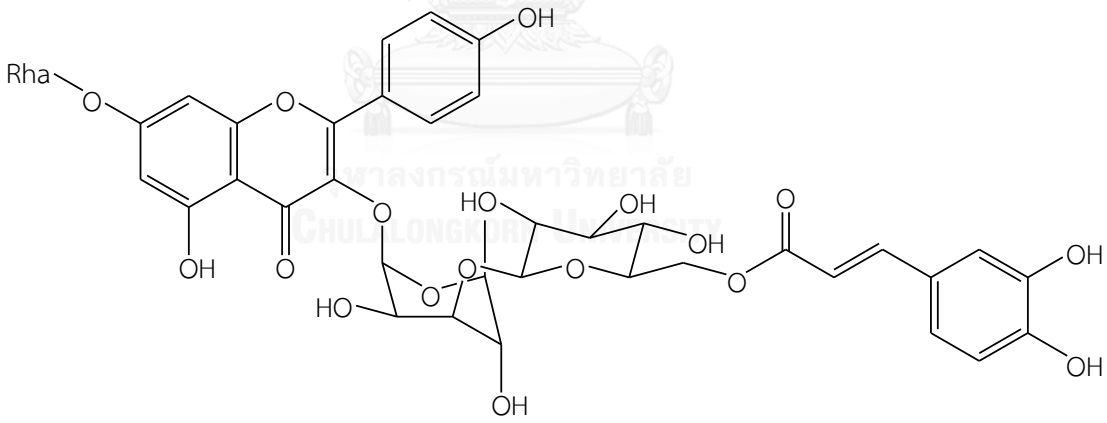

kaempferol-3-*O*-[(6-caffeoyl)-β-glucopyranosyl (1⟶3) α-rhamnopyranoside]-7-*O*-α-rhamnopyranoside (22)

Figure 3 (continued) Natural compounds previously reported to have wound healing activity

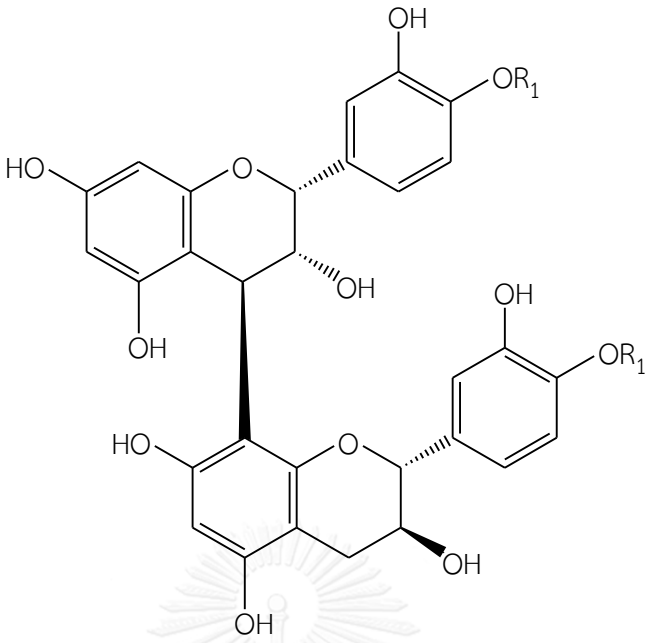

epicatechin-(4β⟶8)-catechin (23)

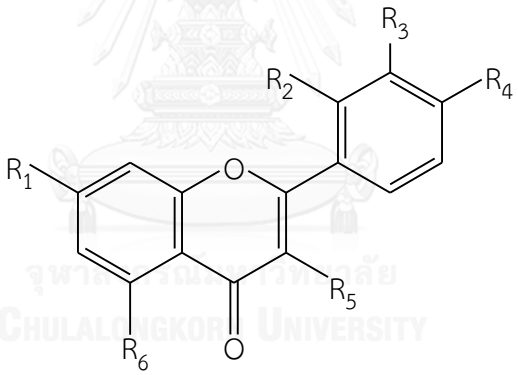

	R_1	R_2	R_3	R_4	R_5	R_6
Chrysin **(24)**	OH	H	H	H	H	OH
Morin **(25)**	OH	OH	H	OH	OH	OH
Rutin **(26)**	OH	H	OH	OH	O-Glu-Rha	OH
DA6034 **(27)**	OCOOH	H	OCH_3	OCH_3	H	OCH_3

Figure 3 (continued) Natural compounds previously reported to have wound healing activity

CHAPTER III

EXPERIMENTAL

3.1 Plant material

The leaves of *A. mahidoliae* were collected from Phu-kae Botanical Garden, Saraburi, Thailand, in July 2012. A voucher specimen (No. 5182) has been deposited at the herbarium of the Faculty of Pharmaceutical Sciences, Chulalongkorn University, Bangkok, Thailand.

3.2 General Techniques

3.2.1 Analytical Thin-Layer Chromatography (TLC)

Technique:	One dimension, ascending
Adsorbent:	Silica gel 60 F254 pre-coated plates (E. Merck)
	Silica gel RP-18 F254 pre-coated plates (E. Merck)
Layer thickness:	0.2 mm
Distance:	5 cm
Detection:	1. Ultraviolet light (254 and 365 nm)
	2. 10% Sulfuric acid and heating at 110 ºC for 10 minutes

3.2.2 Column Chromatography

3.2.2.1 Conventional Column Chromatography

Gel filter:	Silica gel 60 number 9385 (particle size 0.040-0.063 nm) and number 7734 (particle size 0.063-0.200 nm) (E. Merck)
Packing method:	Wet packing
	The adsorbent was mixed with the eluent into slurry, then poured into a column and allowed to set tightly.

Sample loading: The sample was dissolved in a small amount of the eluent, then applied gently on top of the column.

Detection: Fractions were examined by TLC technique in the same manner as described in section 3.2.1

3.2.2.2 Size-Exclusion Column Chromatography

Gel filter: Sephadex LH-20 (Pharmacia Biotech AB)

Packing method: Gel filter was suspended in the eluent and left standing to swell for 24 hours prior to use. It was then poured into the column and allowed to settle.

Sample loading: The sample was dissolved in a small amount of the eluent before being loaded gently on top of the column.

Detection: Fractions were examined by TLC technique in the same manner as described in section 3.2.1

3.2.3 Spectroscopy

3.2.3.1 Ultraviolet (UV) Spectra

UV spectra were obtained on a Shimadzu UV-160A spectrophotometer (Pharmaceutical Research Instrument Center, Faculty of Pharmaceutical Sciences, Chulalongkorn University).

3.2.3.2 Infrared (IR) Spectra

IR spectra (KBR disc) were recorded on a Perkin Elmer FT-IR 1760X spectrometer (Scientific and Technological Research Equipment Center, Chulalongkorn University).

3.2.3.3 Mass Spectra

High resolution electrospray ionization mass spectra were obtained on a JEOL JMS AX505W spectrometer in TOF MS ES+ mode (Natural Medicines Research Center, Bio-Therapeutics Research Institute, Korea Research Institute of Bioscience and Biotechnology)

3.2.3.4 Proton and Carbon-13 Nuclear Magnetic Resonance (^{1}H and ^{13}C NMR) Spectra

^{1}H (500 MHz) and ^{13}C (125 MHz) NMR spectra were obtained on a JEOL JMN-A500 spectrometer (Scientific and Technological Research Equipment Center, Chulalongkorn University).

^{1}H (400 MHz) and ^{13}C (100 MHz) NMR spectra were obtained on a Varian Unity 400 spectrometer (Natural Medicines Research Center, Bio-Therapeutics Research Institute, Korea Research Institute of Bioscience and Biotechnology).

3.3 Extraction

Dried, powdered leaves of *A. mahidoliae* Burtt et Chermsir. (1.1 kg) were macerated with methanol (3 × 10 L, 3 days each), then filtered, combined and evaporated to dryness to obtain methanol extract (172 g). The extract was re-dissolved in methanol and suspended in distilled water (1.5 L) and partitioned with *n*-hexane (3 × 1.5 L), ethyl acetate (3 × 1.5 L) and saturated *n*-butanol (3 × 1.5 L), respectively, to afford *n*-hexane extract (35 g), ethyl acetate extract (7 g), *n*-butanol extract (33 g) and aqueous extract (96 g) as shown in Scheme 1.

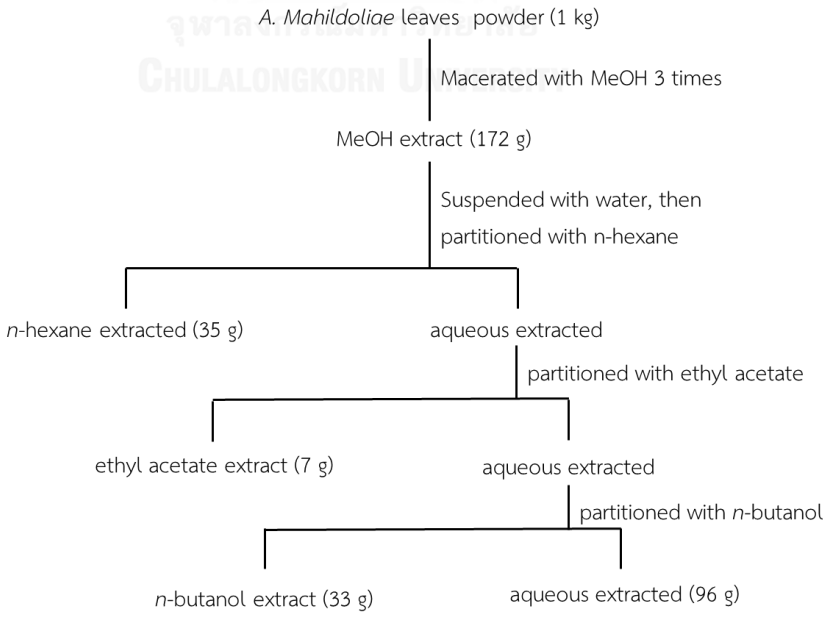

Scheme 1 Extraction of *A. mahidoliae* leaves

3.4 Isolation of compounds from the ethyl acetate extract

Ethyl acetate extract was selected for further study of its chemical constituents based on its DPPH radical scavenging activity and its ferric reducing antioxidant power. The extract (7 g) was loaded on top of a silica gel column (350 g, 4.5 × 40 cm) and eluted with increasingly polar gradient mixtures of $CHCl_3$-MeOH [from 9:1 (5.5 L) ⟶ 7:1 (2.5 L) ⟶ 5:1 (2.5 L) ⟶ 4:1 (2.5 L) ⟶ 2:1 (1.0 L) ⟶ 3:2 (1.0 L) ⟶ 1:1 (1.0 L) ⟶ 2:3 (1.0 L) ⟶ 0:1 (1.0 L)]. The eluates, about 15 ml per fraction, were collected for 820 fractions. Chemical profile of each collected fraction was visualized on TLC, then similar fractions were pooled and evaporated to give 19 combined fractions (Scheme 2): A (871 mg), B (454 mg), C (260 mg), D (421 mg), E (416 mg), F (98.5 mg), G (141 mg), H (286 mg), I (457 mg), J (477 mg), K (178 mg), L (176 mg), M (431 mg), N (632 mg), O (282 mg), P (213 mg), Q (193 mg), R (103 mg) and S (366 mg).

3.4.1 Isolation of compound 1 (juglanin)

Fraction I (457 mg) was purified by size-exclusion chromatography employing a Sephadex-LH20 column (2.5 × 170 cm) eluted with mixtures of MeOH-H_2O [from 2:3 (1.6 L) ⟶ 3:2 (1.6 L) ⟶ 4:1 (1.0 L) ⟶ 1:0 (1.0 L)] to afford 24 combined fractions (I1-I24). Compound 1 was obtained as a yellow powder (5.2 mg, 0.0005 % based on dried weight of the leaves) from fraction I18.

3.4.2 Isolation of compound 2 (astragalin)

Fraction J (477 mg) was chromatographed over a Sephadex-LH20 column (2.5 × 170 cm) using mixtures of MeOH-H_2O [from 1:1 (1.4 L) ⟶ 3:2 (0.8 L) ⟶ 4:1 (0.8 L) ⟶ 1:0 (0.8 L)] as eluents to yield 21 combined fractions (J1-J21). Compound 2 was obtained from fraction J13 as a yellow powder (11.4 mg, 0.001 % yield).

3.4.3 Isolation of compounds 3 (nicotiflorin) and 4 (isoquercetin)

Fraction N (632 mg) was gel-filtrated over a Sephadex-LH20 column (2.5 × 170 cm) washed down with mixtures of MeOH-H_2O [from 3:2 (1.0 L) ⟶ 7:3 (0.8 L) ⟶ 4:1 (0.8 L) ⟶ 9:1 (0.8 L) ⟶ 1:0 (0.8 L)] to obtain 18 combined fractions (N1-N18). Fraction N11 (87 mg) was further purified by reversed phase preparative HPLC (Atlantis Prep T3 OBD™, 5 µm, 19 × 250 mm, flow rate 10 ml/min, MeOH-H2O gradient from 3:7 to 7:3 for 45 min) to give compound 3 as a yellow powder (13.0 mg, 0.0012 % yield), whereas compound 4 was obtained from fraction N15 as a yellow powder (7.4 mg, 0.0006 % yield).

3.4.4 Isolation of compound 5 (apigenin-7-*O*-glucuronide)

Fraction R (103 mg) was subjected to gel filtration chromatography over a Sephadex LH-20 column (2.5 × 170 cm) eluted with mixtures of MeOH-H_2O [from 3:2 (1.0 L) ⟶ 7:3 (0.8 L) ⟶ 4:1 (0.8 L) ⟶ 9:1 (0.8 L) ⟶ 1:0 (0.8 L)] to afford 21 combined fractions (R1-R21). Compound 5 was obtained from fraction R5 as a yellow powder (2.1 mg, 0.0002 % yield).

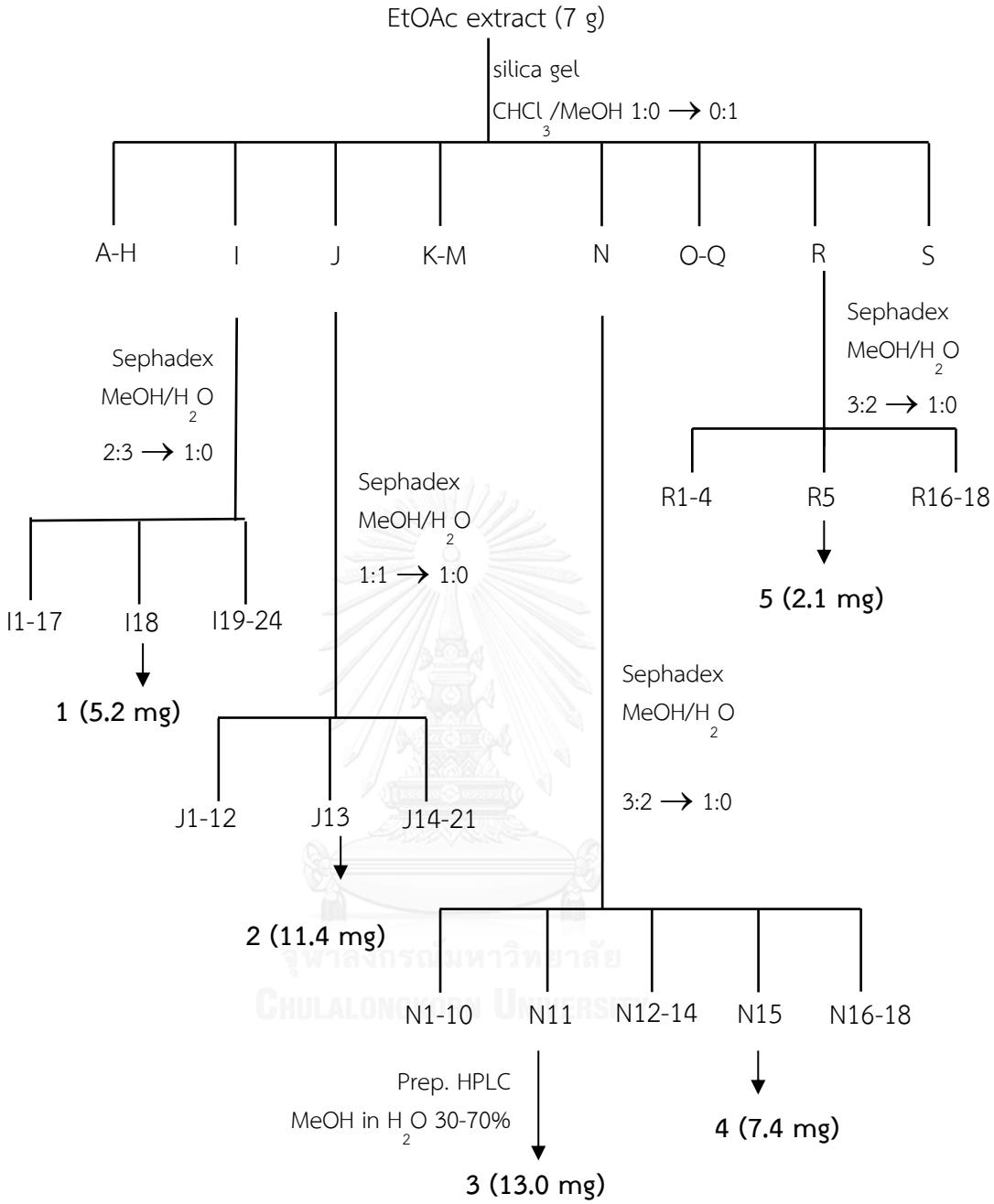

Scheme 2 Isolation of compounds 1-5 from the ethyl acetate extract of *A. mahidoliae* leaves

3.5 Isolation of compound 6 (arbutin) from the *n*-butanol extract

A portion of the *n*-butanol extract (14.6 g) was chromatographed on a silica gel column (260 g, 4 × 28 cm) eluted with gradient mixtures of dichloromethane-methanol (4:1 → 0:1) to obtain 11 combined fractions (Bu1-Bu11). Fraction Bu2 (1.5 g) was further separated on a silica gel column (75 g, 4 × 24 cm). Elution was performed using gradient mixtures of dichloromethane-methanol (3:1 → 0:1) to give 7 combined subfractions (Bu2A-Bu2G). Subfraction Bu2E was subjected to a Sephadex-LH20 column (100 × 2.5 cm) washed down with methanol to yield 5 subfractions (Bu2E1-Bu2E5). Subfraction Bu2E2 was purified on another Sephadex-LH20 column (100 cm × 2.5 cm) eluted with dichloromethane-methanol (1:1) to give 4 subfractions (Bu2E2/1-Bu2E2/4). From subfraction Bu2E2/2 compound 6 was obtained as a white powder (6.1 mg, 0.0013% yield) (Scheme 3).

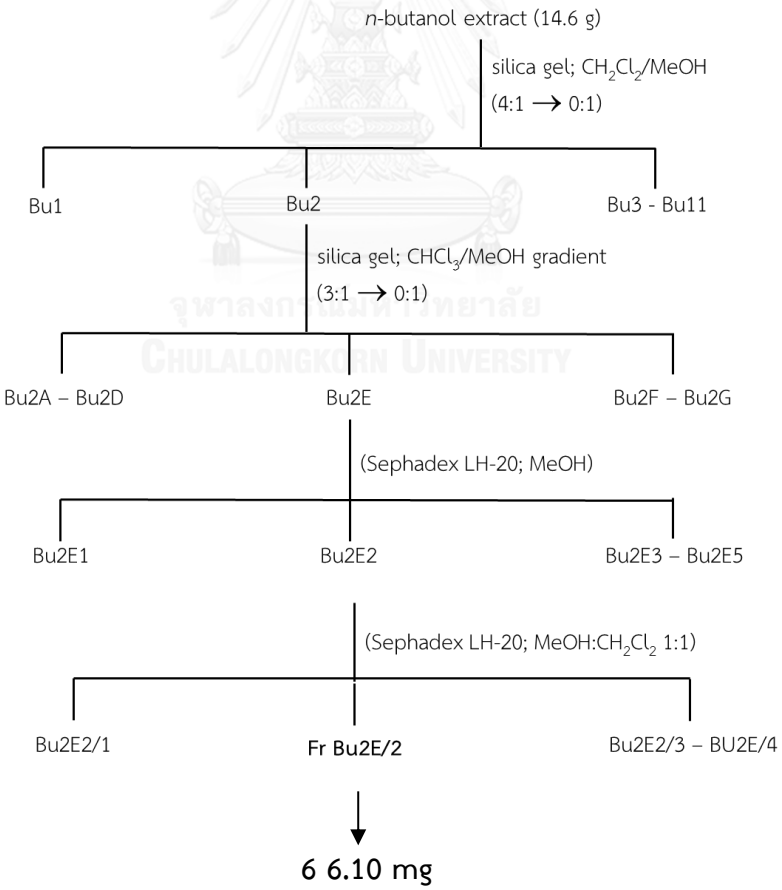

Scheme 3 Isolation of compound 6 from the *n*-butanol extract of *A. mahidoliae* leaves

3.6 Spectral data of isolated compounds

3.6.1 Compound 1 (juglanin)

Compound 1 was obtained as a yellow powder, soluble in methanol.

UV : λ_{max} (MeOH) nm (log ε): 223 (4.34), 266 (4.41), 346 (4.35); **Figure 10**.

IR: ν_{max} cm^{-1} : 3440, 1655, 1607, 1571, 1206, 1178; **Figure 11**.

HR-ESIMS : $[M+H]^+$ at *m/z* 419.0984; **Figure 12**.

^{1}H NMR : **δ** ppm, 400 MHz, in DMSO-d_6; 3.20 (1H, *dd*, 11.2, *J* = 2.8 Hz), 3.53 (1H, *dd*, 7.0, *J* = 3.0 Hz), 3.55 (1H, *dd*, 11.2, *J* = 6.0 Hz), 3.65 (*m*), 3.74 (*m*), 5.34 (1H, *d*, *J* = 4.4 Hz), 6.19 (1H, *d*, *J* = 2.0 Hz), 6.42 (1H, *d*, *J* = 2.0 Hz), 6.88 (2H, *d, J* = 9.2 Hz), 8.08 (2H, *d*, *J* = 9.2 Hz), 12.62 (*s*); **Figure 13**.

^{13}C NMR : **δ** ppm, 100 MHz, in DMSO-d_6; 64.2, 66.0, 70.7, 71.5, 93.7, 98.9, 101.2, 103.8, 115.2, 120.6, 130.9, 133.5, 156.1, 156.3, 160.0, 161.2, 164.6, 177.5; **Figure 14**.

3.6.2 Compound 2 (astragalin)

Compound 2 was obtained as a yellow powder, soluble in methanol.

UV : λ_{max} (MeOH) nm (log ε): 222 (4.44), 266 (4.42), 346 (4.14); **Figure 15**.

IR: ν_{max} cm^{-1} : 3434, 1660, 1609, 1506, 1205, 1181; **Figure 16**.

HR-ESIMS : $[M+H]^+$ at *m/z* 449.1044; **Figure 17**.

^{1}H NMR : **δ** ppm, 400 MHz, in DMSO-d_6; 3.19 (1H, *dd*, 11.4, *J* = 5.5 Hz), 3.56 (1H, *dd*, 11.4, *J* = 5.5 Hz), 5.46 (1H, *d*, *J* = 7.6 Hz), 6.19 (1H, *d*, *J* = 2.0 Hz), 6.42 (1H, *d*, *J* = 2.0 Hz), 6.88 (2H, *d, J* = 9.2 Hz), 8.08 (2H, *d*, *J* = 9.2 Hz), 12.61 (*s*); **Figure 18**.

^{13}C NMR : **δ** ppm, 100 MHz, in DMSO-d_6; 60.8, 69.9, 74.2, 76.4, 77.5 93.6, 98.7, 100.8, 104.0, 115.1, 120.9, 130.9, 133.2, 156.2, 156.4, 159.9, 161.2, 164.1, 177.5; **Figure 19**.

3.6.3 Compound 3 (nicotiflorin)

Compound 3 was obtained as a yellow powder, soluble in methanol.

UV : λmax (MeOH) nm (log ε): 224 (4.62), 267 (4.71), 346 (4.65); **Figure 20**

IR: νmax cm-1 : 3428, 1655, 1606, 1507, 1208, 1181; **Figure 21.**

HR-ESIMS : $[M+H]^+$ at m/z 595.1664; **Figure 22**.

1H NMR : δ ppm, 400 MHz, in DMSO-d_6; 0.98 (3H, *d*, *J* = 6.4 Hz), 4.40 (1H,*s*) , 5.30 (1H, *d*, *J* = 7.6 Hz), 6.19 (1H, *d*, *J* = 2.4 Hz), 6.39 (1H, *d*, *J* = 2.4 Hz), 6.87 (2H, *d, J* = 8.4 Hz), 7.98 (2H, *d*, *J* = 8.8 Hz), 12.50 (*s*); **Figure 23**.

^{13}C NMR : δ ppm, 100 MHz, in DMSO-d_6; 17.7, 66.8, 68.2, 69.9, 70.3, 70.6, 71.8, 74.1, 75.7, 76.3, 93.8, 98.8, 100.7, 101.4, 103.8, 115.1, 120.9, 130.8, 133.2, 156.5, 156.7, 159.9, 161.2, 164.5, 177.3; **Figure 24**.

3.6.4 Compound 4 (isoquercetin)

Compound 4 was obtained as a yellow powder, soluble in methanol.

UV : λ_{max} (MeOH) nm (log ε): 224 (4.52), 267 (4.51), 346 (4.25); **Figure 25**.

IR: ν_{max} cm^{-1} : 3269, 1655, 1606, 1496, 1201, 1169; **Figure 26**.

HR-ESIMS : $[M+H]^+$ at *m/z* 465.1016; **Figure 27**.

^{1}H NMR : δ ppm, 400 MHz, in DMSO-d_6; 3.19 (1H, *dd*, 11.4, *J* = 5.5 Hz), 5.45 (1H, *d*, *J* = 7.2 Hz), 6.20 (1H, *d*, *J* = 2.0 Hz), 6.40 (1H, *d*, *J* = 2.0 Hz), 6.84 (1H, *d, J* = 2.4 Hz), 6.84 (1H, *d, J* = 9.2 Hz) 7.57 (m); see **Table 4**; **Figure 28**.

^{13}C NMR : δ ppm, 100 MHz, in DMSO-d_6; 61.0, 69.9, 74.1, 76.5, 77.6 93.5, 98.6, 100.8, 104.0, 116.2, 121.1, 130.9, 144.8, 148.4, 156.1, 156.3, 159.9, 161.2, 164.1, 177.4; see Table; **Figure 29**.

3.6.5 Compound 5 (apigenin-7-*O*-glucuronide)

Compound 5 was obtained as a yellow powder, soluble in methanol.

UV : λ_{max} (MeOH) nm (log ε): 224 (4.56), 267 (4.54), 346 (4.55); **Figure 30**.

IR: ν_{max} cm^{-1} : 3419, 1656, 1609, 1497, 1174; **Figure 32**.

HR-ESIMS : $[M+Na]^+$ at *m/z* 449.3489; **Figure 31**.

^{1}H NMR : **δ** ppm, 500 MHz, in CD_3OD; 5.09 (1H, *d*, 6.0 Hz), 6.60(*s*), 6.48 (1H, *d*, *J* = 1.8 Hz), 6.81 (1H, *d*, 1.8 Hz), 6.91 (1H, *d*, 8.5), 7.85 (1H, *d*, 8.5 Hz); **Figure 33**.

^{13}C NMR : **δ** ppm, 125 MHz, in CD_3OD; 73.4, 74.5, 76.5, 77.6, 96.1, 101.4, 107.1, 101.5, 104.0, 117.1, 122.9, 129.6, 158.9, 162.7, 163.0, 164.9, 166.8, 176.2, 184.1; **Figure 34**.

3.6.6 Compound 6 (arbutin)

Compound 6 was obtained as a white powder, soluble in methanol.

UV : λ_{max} (MeOH) nm (log **ε**): 224 (3.84), 285 (3.33); **Figure 35**.

IR: ν_{max} cm^{-1} : 3338, 1650, 1513, 1213; **Figure 36**.

HR-ESIMS : $[M+Na]^+$ at *m/z* 295.0794; **Figure 37**.

^{1}H NMR : **δ** ppm, 500 MHz, in CD_3OD; 3.69 (1H, *dd*, *J* = 11.0, 5.0 Hz), 3.87 (1H, *br*. *d*, *J* = 12.0 Hz), 4.73 (1H, *d*, *J* = 7.0 Hz), 6.69 (2H, *br d*, *J* = 8.8 Hz), 6.96 ppm (2H, *br d*, *J* = 8.8 Hz, H-2 and H-6) **Figure 38**.

^{13}C NMR : **δ** ppm, 125 MHz, in CD_3OD; 62.6, 71.4, 75.0, 78.0, 103.7, 116.3, 119.6, 152.4, 153.8 **Figure 39**.

3.7 Evaluation of biological activities

3.7.1 Antioxidant and its related activities

All extracts from the leaves of *A. mahidoliae* were assessed for their total phenolic content, total flavonoid content and antioxidant activities including their DPPH radical scavenging activity and ferric reducing antioxidant power (FRAP).

3.7.1.1 Assay for total phenolic content

The total phenolic content of the extracts were quantified by using the previously described Folin-Ciocalteu assay (Herald *et al.*, 2012) with some modifications. Each 50 µl of the sample and Folin-Ciocalteu reagent were mixed together with 500 µl of distilled water. After 6 minutes, 7.5% sodium carbonate solution (400 µl) was added. The reaction mixture was incubated in the dark for 2 hours at room temperature. The absorbance of the mixture was then measured at 765 nm. Calibration curve of gallic acid at concentrations of 12.5-60 µg/ml was used as the reference. The data were expressed as mg of gallic acid equivalent per g of extract.

3.7.1.2 Assay of total flavonoid content

The total flavonoid content of the extracts were determined based on the method described by Herald *et al.* (2012). Each 25 µl of the sample was mixed thoroughly with 100 µl of distilled water and 10 µl of 5% sodium nitrite solution for 5 minutes. Then, 15 µl of aluminium chloride solution were added. After 6 minutes, a 1:1 mixture of 1M sodium hydroxide and distilled water (100 µl) was added and shaken for 1 minute. The absorbance of the sample mixture was measured against a reagent blank at 510 nm. Calibration curve of rutin at concentrations of 30-480 µg/ml was used as the reference. The data were expressed as mg of rutin equivalent per g of extract.

3.7.1.3 DPPH radical scavenging assay

2,2-Diphenyl-1-picrylhydrazyl radical (DPPH) is a stable free radical because of the paramagnetism conferred by its odd electron (the delocalization of the spare electron over the molecule as a whole). When dissolved in methanol, the DPPH solution appears as a deep violet colour which shows a strong absorption band at 515 nm. DPPH can accept hydrogen radical or an electron to become a stable diamagnetic molecule, and gives rise to the reduced form with the loss of this dark violet color. If the substance possesses strong free radical scavenging activity, its solution, when mixed with DPPH solution, can cause DPPH to lose its original colour to become yellow colour (Alam *et al.*, 2013).

In this study the DPPH free radical scavenging activity was measured using the method described by Liyana-Pathiranan and Shahidi (2005). The DPPH stock solution was prepared by dissolving DPPH with methanol. The DPPH stock solution (180 µl) was mixed thoroughly with 20 µl of positive control or sample, and incubated at room temperature in the dark for 30 minutes. The absorbance of the mixture was measured at 515 nm under a microplate reader. Trolox® and ascorbic acid were used as references. The results were reported as EC_{50} (effective concentration for the 50% elimination of total DPPH) in the unit of µg/ml.

3.7.1.4 Assay for ferric reducing antioxidant power (FRAP)

FRAP assay uses antioxidants as reductants in a redox-linked colorimetric method. Reduction of ferric tripyridyl triazine (Fe^{3+}-TPTZ) complex to ferrous form (giving an intense blue colour) can be determined by measuring change in the absorption at 595 nm. Therefore, the antioxidant effect is directly related to the total reducing power of the electron-donating antioxidants present in the reaction mixture (Moon and Shibamoto, 2009).

The ferric reducing antioxidant power was determined using the same method as Zou *et al.* (Zou *et al.*, 2011) with slightly modification. FRAP reagent was prepared by mixing 20 mM $FeCl_3 \cdot 6H_2O$, 10 mM TPTZ in 40 mM hydrochloric acid and acetate buffer pH 3.6 in the ratio of 1:1:10. The FRAP reagent (190 µl) was mixed with 10 µl of $FeSO_4 \cdot 7H_2O$ solution or sample solution. After incubation for 6 minutes at 37°C, the absorbance of the mixture was measured at 595 nm under a microplate reader. Calibration curve was constructed by using $FeSO_4 \cdot 7H_2O$ at concentrations of 0.1- 2mM. FRAP values were expressed as ferrous (Fe^{2+}) equivalent (in mM) per g of compound or extract.

3.8.2 Cytotoxicity activity

Cytotoxicity of the isolated compounds was determined against human dermal fibroblast cell line (CCD-1064sk) in order to select non-toxic concentrations for the scratch wound healing assay. Cytotoxicity was assessed by 3-(4,5-dimethylthiazol-2-yl)-2,5-diphenyltetrazolium bromide (MTT) assay (Lee *et al.*, 2012).

Fibroblasts were seeded at a density of 1×10^5/well in a 96-well plate. After 24 h incubation, cells were treated with different concentrations (1, 5, 10, 20, 40 and 80 μM) of the compounds and incubated for another 24 h. MTT solution (0.5 mg/ml, 100 μl) was dispensed in each well, followed by 4 h incubation. After removal of culture supernatants, 100 μl of DMSO was used for dissolving formazan crystals. Living cells were quantified by measuring the absorbance at 570 nm. The percentage of cell viability was calculated as follows:

$$\% \text{ Cell viability} = [\text{OD test/OD control}] \times 100$$

Whereas OD test and OD control are the absorbance from treated condition and untreated condition, respectively.

3.8.3 Scratch-wound healing assay

Human dermal fibroblast cell line (CCD-1064sk) was cultured in Iscove's Modified Dulbecco's Medium (IMDM) supplemented with 10% fetal bovine serum, 1% L-glutamine and 1% penicillin-streptomycin under a fully humidified atmosphere containing 5% CO_2 at 37°C. Non-toxic concentrations of the isolated compounds were evaluated for their ability to promote fibroblast migration into the scratch wound area (Lee *et al*., 2012). Fibroblasts (1×10^5/well) were seeded into 24-well plate and incubated for 24 hours. In order to create a scratch wound, the confluent monolayer of fibroblasts was scraped in a straight line by a 10 μl sterile pipette tip. Debris and suspended cells were removed by washing the monolayer with phosphate buffer saline. All samples were diluted with media and added into each well. Medium without sample served as a negative control. Cells were photographed by an inverted microscope at 0, 8, 16, and 24 hours after the treatment. Percentage of wound closure for each tested compound was analyzed by using Image J software.

CHAPTER IV

RESULTS AND DISCUSSION

All extracts of *A. mahidoliae* leaves were tested for their total phenolic content, total flavonoid content, DPPH radical scavenging activity, and ferric reducing antioxidant power. The most active extract in all assays was the ethyl acetate extract, followed by the *n*-butanol extract. Therefore, these extracts were selected for further investigation through the isolation of their chemical composition. Five flavonoid glycosides were isolated from the ethyl acetate extract (compounds 1-5), whereas a glycosylated hydroquinone (compound 6) was obtained from the n-butanol extract. Identification of the isolated compounds was performed based on their spectroscopic techniques, including UV, IR, MS, ^{1}H NMR and ^{13}C NMR. These compounds were examined for their DPPH radical scavenging ability and ferric reducing antioxidant power. Then, selected glycosides were assessed for their ability to promote the migration of human dermal fibroblast cells in scratch wound test.

4.1 Identification of compound 1 (juglanin)

Compound 1, isolated as a yellow powder, showed its $[M+H]^+$ peak in the high resolution ESI mass spectrum at *m/z* 419.0984 (**Figure 12**), suggesting $C_{20}H_{18}O_{10}$ as its molecular formula. The yellow colour of the compound, its UV characteristic (**Figure 10**) and the number of carbon atoms in its molecule suggested that this compound might be a flavonoid glycoside with one pentose sugar unit.

The IR spectrum (**Figure 11**) demonstrated absorption bands of hydroxyl groups at 3440 cm^{-1}, conjugated carbonyl at 1655 cm^{-1}, aromatic rings at 1607 and 1571 cm^{-1} and C-O stretching at 1206 and 1178 cm^{-1}. These absorption bands indicated commonly found groups within a flavonoid structure.

The ^{1}H NMR spectrum of compound 1 (**Figure 13** and **Table 1**) showed the signals of two *meta*-coupled aromatic protons on ring A of a flavonoid aglycone at **δ**

6.19 (1H, *d*, *J* = 2.0 Hz, H-6) and 6.42 (1H, *d*, *J* = 2.0 Hz, H-8). Other aromatic proton signals were resonances of two pairs of symmetrical, *ortho*-coupled protons of the 1,4-disubstituted ring B at **δ** 6.88 (2H, *d*, *J* = 9.2 Hz, H-3′ and H-5′) and 8.08 ppm (2H, *d*, *J* = 9.2 Hz, H-2′and H-6′). An anomeric proton of an **α**-oriented sugar moiety resonated at **δ** 5.34 (1H, *d*, *J* = 4.4 Hz, H-1″). The most downfield signal at **δ** 12.62 belongs to the chelated hydroxyl group at C-5 of the kaempferol aglycone.

The ^{13}C NMR data of compound 1 (**Figure 14** and **Table 1**) exhibited the signal of a conjugated keto-carbonyl group at **δ** 177.5 ppm (C-4), confirming its basic skeleton as a flavonol. The carbon spectrum also showed downfield resonances of 4 oxygen-linked aromatic carbons at **δ** 161.2 (C-5), 164.6 (C-7), 165.1 (C-9) and 160.0 ppm (C-4′). Other carbon signals of the kaempferol aglycone appeared at **δ** 156.2 (C-2), 133.6 (C-3), 98.8 (C-6), 93.7 (C-8), 103.8 (C-10), 120.6 (C-1′), 130.9 (C-2′/ C-6′) and 115.2 ppm (C-3′/C-5′). The rest of the signals belong to a **α**-L-arabinofuranoside moiety connected to the aglycone at C-3. A signal at **δ** 101.2 ppm corresponded with the anomeric carbon (C-1″) of arabinose. Other four signals of the sugar moiety appeared at **δ** 70.7 (C-2″), 71.5 (C-3″), 66.0 (C-4″) and 64.2 ppm (C-5″) (Agrawal, 1992). Therefore, this compound was identified as kaempferol-3-*O*-**α**-L-arabinofuranoside or juglanin and was confirmed by comparison with previously reported data (Ataa Said, 2010).

Examples of plants in the same family as *Afgekia* (Fabaceae) that also contain this flavonoid glycoside are the seeds of *Astragalus complanatus* (Xue *et al.*, 2008) and the leaves of *Indigofera hebepetala* (Hasan *et al.*, 1993). Juglanin has been demonstrated to be antioxidant in a number of assays (Jung *et al.*, 2002). In addition, this compound displayed inhibitory effect on the cellular senescence of human fibroblasts (Yang *et al.*, 2014).

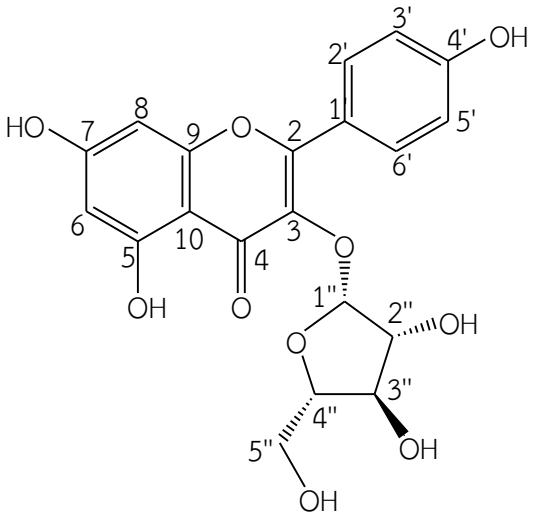

juglanin (28)

Table 1 ^{1}H and ^{13}C NMR spectral data of compound 1 and juglanin (in DMSO-d_6).

Position	compound 1		juglanin[a]	
	δ_H (mult., *J* in Hz)	δ_C	δ_H (mult., *J* in Hz)	δ_C
2	-	156.3	-	156.2
3	-	133.5	-	133.6
4	-	177.5	-	177.0
5	-	161.2	-	161.3
6	6.19 (*d*, 2.0)	98.8	6.19 (*d,* 2.0)	98.9
7	-	164.6	-	164.9
8	6.42 (*d*, 2.0)	93.7	6.42 (*d*, 2.0)	93.8
9	-	156.1	-	156.2
10	-	103.8	-	103.9
1'	-	120.6	-	120.8
2'	8.08 (*d*, 9.2)	130.9	8.08 (*d*, 8.8)	131.0
3'	6.88 (*d,* 9.2)	115.2	6.88 (*d*, 8.4)	115.3
4'	-	160.0	-	160.1
5'	6.88 (*d*, 9.2)	115.2	6.88 (*d*, 8.4)	115.3
6'	8.08 (*d*, 9.2)	130.9	8.08 (*d*, 8.8)	131.0
1''	5.34 (*d*, 4.4)	101.2	5.33 (*d*, 5.2)	101.4
2''	3.74 (*m*)	70.7	3.74 (*dd*, 6.0, 5.3)	70.9
3''	3.53 (*dd*, 7.0, 3.0)	71.5	3.52 (*dd*, 6.9, 2.7)	71.7
4''	3.65 (*m*)	66.0	3.65 (*m*)	66.1
5''a	3.55 (*dd*, 11.2, 6.0)	64.2	3.56 (*dd*, 11.6, 5.8)	64.3
5''b	3.20 (*dd*, 11.2, 2.8)		3.19 (*dd*, 11.6, 2.0)	
5-OH	12.62 (*s*)			

[a]Ataa Said 2010

4.2 Identification of compound 2 (astragalin)

Compound 2 was obtained as a yellow powder which exhibited an $[M+H]^+$ peak in the high resolution ESIMS at *m/z* 449.1044 (**Figure 17**), suggesting $C_{21}H_{20}O_{11}$ as its molecular formula. When compared with compound 1, this compound has one more carbon and oxygen atoms and two more hydrogen atoms.

The IR spectrum of compound 2 (**Figure 16**) was similar to that of compound 1 as well. The spectrum exhibited absorption bands of hydroxyl groups (3434 cm^{-1}), conjugated carbonyl (1660 cm^{-1}), aromatic rings (1609 and 1506 cm^{-1}) and C-O stretching (1205 and 1181 cm^{-1}). The colour of the compound, its UV characteristic and the number of carbon atoms indicated that this compound should be a flavonoid glycoside similar to compound 1, but with a hexose sugar instead of a pentose one.

The ^{1}H NMR spectrum (**Figure 18**, **Table 2**) of compound 2 was also very similar to that of compound 1, with the difference only in the region of sugar unit. The signals of the kaempferol aglycone appeared at **δ** 6.19 (1H, *d*, *J* = 2.0 Hz, H-6), 6.42 (1H, *d*, *J* = 2.0 Hz, H-8), 6.88 (2H, *d*, *J* = 9.2 Hz, H-3′and H-5′) and 8.08 ppm (2H, *d*, *J* = 9.2 Hz, H-2′and H-6′). A chelated hydroxyl proton resonated at **δ** 12.61 ppm (1H, *s*, 5-OH). One β-oriented sugar displayed an anomeric doublet at **δ** 5.46 ppm (1H, *d*, *J* = 7.6 Hz, H-1″).

Similar to compound 1, the ^{13}C NMR spectrum (**Figure 19**, **Table 2**) of compound 2 displayed resonances of a kaempferol aglycone including those of a keto carbonyl at **δ** 177.5 ppm (C-4), eight quaternary carbons at **δ** 156.4 (C-2), 133.2 (C-3), 161.2 (C-5), 164.1 (C-7), 156.2 (C-9), 104.0 (C-10), 120.9 (C-1′) and 159.9 ppm (C-4′) and six methine carbons at **δ** 98.7 (C-6), 93.6 (C-8), 130.9 (C-2′/ C-6′) and 115.1 ppm (C-3′/C-5′). The anomeric carbon of a β-glucose moiety appeared at **δ** 100.8 (C-1″). The rest of the carbon signals also agreed with those of a glucopyranose unit including the signals at **δ** 74.2 (C-2″), 76.4 (C-3″), 69.9 (C-4″), 77.5 (C-5″) and 60.8 ppm (C-6″) (Agrawal, 1992).

From the above data and through comparison with literature, compound 2 was identified as kaempferol-3-*O*-β-D-glucopyranoside or astragalin (Deng *et al.*, 2009).

Astragalin has previously been reported as a constituent of various plants, including members of the family Fabaceae such as the seeds of *Securigera securidacea (Ali et al., 1998)*, the roots of *Astragalus membranaceus* (Agyemang *et al.*, 2013) and the leaves of *Cassia alata* (Saito *et al.*, 2012). The flavonoid glucoside displayed several interesting biological activities relating to its anti-inflammatory effect. The compound showed inhibitory effect against the expression of lipopolysaccharide-induced inflammatory mediators through NF-κB in macrophages (Kim and Kim, 2011) and mouse mammary epithelial cells (Li *et al.*, 2014). In addition, it also reduced the activity of the enzyme myeloperoxidase and the expression of inflammatory mediators such as tumor necrosis factor-α, interleukin-6, and interleukin-1β in lipopolysaccharide-induced mastitis in murine model (Li *et al.*, 2013).

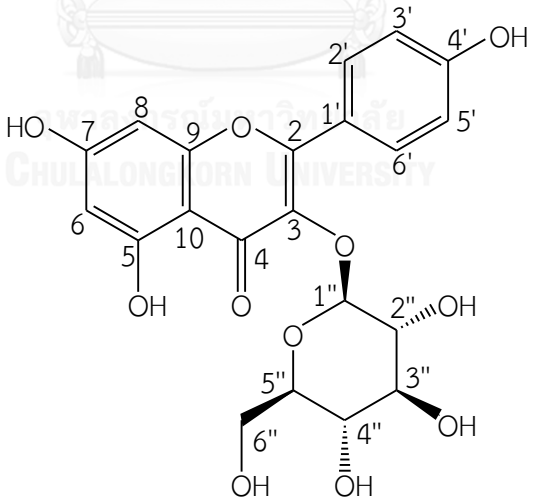

astragalin (29)

Table 2 ^{1}H and ^{13}C NMR spectral data of compound 2 and astragalin (in DMSO-d_6)

Position	compound 2		astragalin[a]	
	δ_H (mult., *J* in Hz)	δ_C	δ_H (mult., *J* in Hz)	δ_C
2	-	156.4	-	156.7
3	-	133.2	-	133.6
4	-	177.5	-	177.9
5	-	161.2	-	161.5
6	6.19 (*d*, 2.0)	98.7	6.20 (*d*, 1.8)	99.1
7	-	164.1	-	164.6
8	6.42 (*d,* 2.0)	93.6	6.43 (*d*, 1.8)	94.1
9	-	156.2	-	156.8
10	-	104.0	-	104.4
1'	-	120.9	-	121.3
2'	8.08 (*d*, 9.2)	130.9	8.03 (*d*, 8.7)	131.3
3'	6.88 (*d,* 9.2)	115.1	6.87 (*d*, 8.7)	115.5
4'	-	159.9	-	160.4
5'	6.88 (*d*, 9.2)	115.1	6.87 (*d*, 8.7)	115.5
6'	8.08 (*d*, 9.2)	130.9	8.03 (*d*, 8.7)	131.3
1''	5.46 (*d*, 7.6)	100.8	5.45 (*d*, 7.2)	101.2
2''		74.2		74.6
3''		76.4		76.8
4''		69.9		70.3
5''		77.5		77.9
6''a	3.56 (*dd*, 11.4, 5.5)	60.8		61.0
6''b	3.19 (*dd*, 11.4, 5.5)			
5-OH	12.61	-	12.61	-

[a]Deng *et al*., 2009

4.3 Identification of compound 3 (nicotiflorin)

Compound 3 was obtained as a yellow powder. Its molecular formula was determined as $C_{27}H_{30}O_{15}$ from its pseudo-molecular ion peak at *m/z* 595.1664 in the high resolution ESI mass spectrum (**Figure 22**). Its IR spectrum (**Figure 21**) exhibited absorption bands representing hydroxyl groups (3428 cm^{-1}), conjugated carbonyl (1655 cm^{-1}), aromatic rings (1606 and 1507 cm^{-1}) and C-O stretching (1208 and 1181 cm^{-1}) similar to those of compounds 1 and 2. The structure of this compound might therefore be a flavonoid glycoside with two hexose sugar units.

The aromatic region of the ^{1}H NMR spectrum of compound 3 (**Figure 23**, **Table 3**) was also similar to the previous two kaempferol glycosides. The proton signals of the kaempferol aglycone could be observed at **δ** 6.19 (1H, *d*, *J* = 2.4 Hz, H-6) and 6.39 ppm (1H, *d*, *J* = 2.4 Hz, H-8) for the *meta*-coupled aromatic ring A protons and at **δ** 7.98 (2H, *d*, *J* = 8.8 Hz, H-2′and H-6′) and 6.87 (2H, *d*, *J* = 8.4 Hz, H-3′ and H-5′) for the two pairs of symmetric, *ortho*-coupled aromatic ring B protons. Two anomeric proton signals at **δ** 5.30 (1H, *d*, *J* = 7.6 Hz, H-1″) and 4.40 ppm (1H, *s*, H-1‴) could be assigned to a glucose and a rhamnose unit, respectively. In addition, a methyl doublet at **δ** 0.98 ppm (3H, *d, J* = 6.4 Hz, H-6‴) was also characteristic of a rhamnose moiety.

The pattern of ^{13}C NMR spectrum of compound 3 (**Figure 24**, **Table 3**) was similar to that of compound 2, but with six additional carbon signals in the glycone region, indicative of one more hexose sugar unit. The signals of the glucose unit appeared at **δ** 100.9 (C-1″), 74.2 (C-2″), 76.3 (C-3″), 69.9 (C-4″), 77.7 (C-5″) and 66.8 ppm (C-6″), whereas those of the rhamnose unit resonated at **δ** 100.7 (C-1‴), 70.2 (C-2‴), 70.5 (C-3‴), 71.7 (C-4‴), 68.1 (C-5‴) and 17.6 ppm (C-6‴). The downfield shift C-6″ signal suggested that rhamnose was attached to glucose at this position. Comparison of these ^{13}C NMR data with previously published values also indicated that the disaccharide unit (rhamnose-(1→6)-glucose or rutinoside) was connected through an *O*-glycosidic linkage to C-3 of the kaempferol aglycone.

Based on the above spectral data and comparison with previous report (Leong *et al.*, 2008), compound 3 was identified as kaempferol-3-*O*-**α**-L-

rhammnopyranosyl (1→6)-β-D-glucopyranoside or kaempferol-3-*O*-rutinoside or nicotiflorin.

Nicotiflorin has been isolated from many plants in the family Fabaceae such as the aerial parts of *Astragalus ammodendron* (Khozhambergenova and Blinova, 1980) and *A. tana* (Alaniya and Chkadua, 2000), the leaves of *Paracalyx scariosa* (Nia *et al.*, 1992), and several *Vigna species* including *V. heterophylla*, *V. kirki*, *V. marina*, *V. radiata* and *V. unguiculata* ssp. *stenophylla* (Lattanzio *et al.*, 1996). Many biological activities of nicotiflolin have been reported. The compound showed neuroprotective effect against brain injury (Yu *et al.*, 2013), antiglycation activity (Lal Shyaula *et al.*, 2012), anti-inflammatory activity (Wang *et al.*, 2014), and inhibitory activity on lymphocyte proliferation (Brochado *et al.*, 2003).

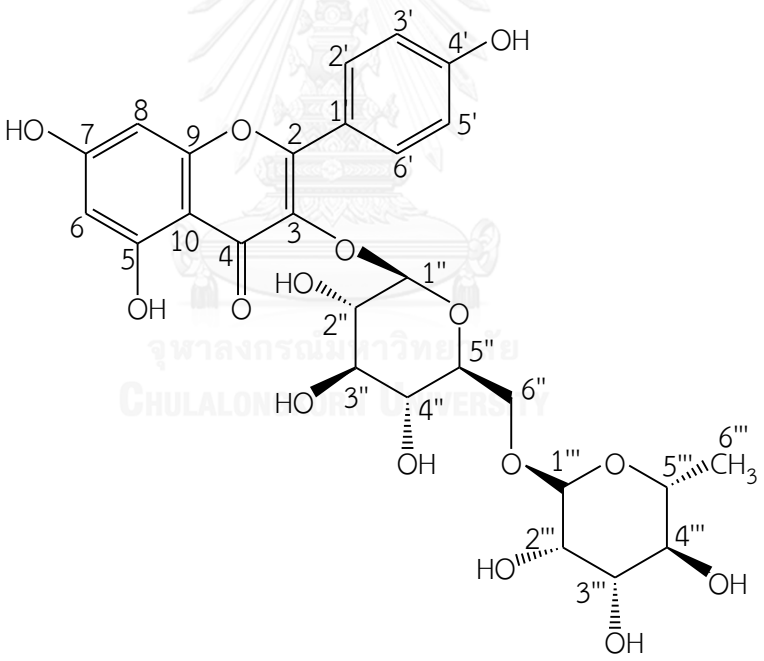

nicotiflorin (30)

Table 3 ^{1}H and ^{13}C NMR spectral data of compound 3 and nicotiflorin (in DMSO-d_6)

Position	compound 3		nicotiflorin[a]	
	δ_H (mult., *J* in Hz)	δ_c	δ_H (mult., *J* in Hz)	δ_c
2	-	156.7	-	156.4
3	-	133.2	-	133.1
4	-	177.3	-	177.3
5	-	161.2	-	161.1
6	6.19 (*d*, 2.4)	98.8	6.18 (*d*, 1.3)	98.6
7		164.5	-	164.0
8	6.39 (*d*, 2.4)	93.8	6.41 (*d*, 1.3)	93.6
9	-	156.5	-	156.7
10	-	103.8	-	103.9
1'	-	120.9	-	120.8
2'	7.98 (*d*, 8.8)	130.8	8.05 (*d*, 8.9)	130.8
3'	6.87 (*d*, 8.4)	115.1	6.86 (*d*, 8.9)	115.0
4'	-	159.9	-	159.8
5'	6.87 (*d*, 8.8)	115.1	6.86 (*d*, 8.9)	115.0
6'	7.98 (*d*, 8.8)	130.8	8.05 (*d*, 8.9)	130.8
1''	5.30 (*d*, 7.6)	101.4	5.31 (*d*, 7.6)	101.2
2''	-	74.1	-	74.1
3''	-	76.3	-	76.2
4''	-	69.9	-	69.8
5''	-	75.7	-	75.6
6''	-	66.8	-	66.8
1'''	4.40 (*s*)	100.7	4.40 (*s*)	100.7
2'''	-	70.3	-	70.2
3'''	-	70.6	-	70.5
4'''	-	71.8	-	71.7
5'''	-	68.2	-	68.1
6'''	0.98 (*d*, 6.4)	17.7	-	17.6
5-OH	12.50 (*s*)	-	12.60 (*s*)	-

[a]Leong *et al.,* 2008

4.4 Identification of compound 4 (isoquercitrin)

Compound 4 was obtained as a yellow powder. Its molecular formula was determined as $C_{21}H_{20}O_{12}$ from its pseudo-molecular ion peak at *m/z* 465.1016 in the high resolution ESI mass spectrum (**Figure 27**). Although the compound appeared to have the same number of carbon atoms as compound 2, its additional 16 mass unit suggested one more hydroxyl group in the chemical structure of this compound.

The IR spectrum (**Figure 26**) displayed absorption bands of hydroxyl groups (3269 cm^{-1}), conjugated carbonyl (1655 cm^{-1}), aromatic rings (1606 and 1496 cm^{-1}) and C-O stretching (1201 and 1169 cm^{-1}), which were similar to the previous three flavonoid glycosides.

^{1}H NMR spectral data of compounds 2 and 4 shared some similarity, especially the signals of *meta*-coupled ring A protons of a flavonol aglycone at **δ** 6.20 (1H, *d*, *J* = 2.0 Hz, H-6) and 6.40 ppm (1H, *d*, *J* = 2.0 Hz, H-8), and the **β**-glucose moiety which showed an anomeric signal at **δ** 5.45 ppm (1H, *d*, *J* = 7.2 Hz, H-1''). However, instead of the 1,4-disubstituted ring B as in compounds 1-3, the ^{1}H NMR spectrum of compound 4 (**Figure 28**) showed the signals of ring B as being 1,3,4-trisubstituted at **δ** 6.84 (1H, *d*, *J* = 2.4 Hz, H-2'), 6.84 (1H, *d*, *J* = 9.2 Hz, H-5') and 7.57 ppm (m). The difference in ring B of this compound was further supported by its ^{13}C NMR spectral data (**Figure 29**). Comparison of the data with compound 2 revealed an additional signal of a hydroxyl-substituted quaternary carbon at **δ** 144.8 ppm (C-3'), while one aromatic methine signal was absent. Therefore, both positions 3' and 4' of the B ring should be connected with hydroxyl groups and the aglycone was quercetin.

After detailed analysis of all the spectroscopic data and comparison with previous report (Kim *et al.*, 1999), it can be concluded that compound 4 is quercetin-3-*O*-**β**-D-glucopyranoside or isoquercitrin.

Isoquercitrin is a flavonoid commonly found in higher plants. For examples, in Fabaceae, this compound was reported as a constituent of the flowers of *Albizzia julibrisisin* (Kang *et al.*, 2000), the flowers of *Pterospartum tridentatum* (Paulo *et al.*, 2008), and the fruits of *Pterogyne nitens* (Regasini *et al.*, 2008). This compound

exhibited various biological activities such as ability to decrease glioblastoma cell proliferation (Amado *et al.*, 2009), inhibitory effects on melanin formation in B16 melanoma cells (Arung *et al.*, 2011), on the proliferation of human liver cancer cells and on human DNA topoisomerase II, as well as inducing effect on the apoptosis of hepatocellular carcinoma cells (Sudan and Rupasinghe, 2014).

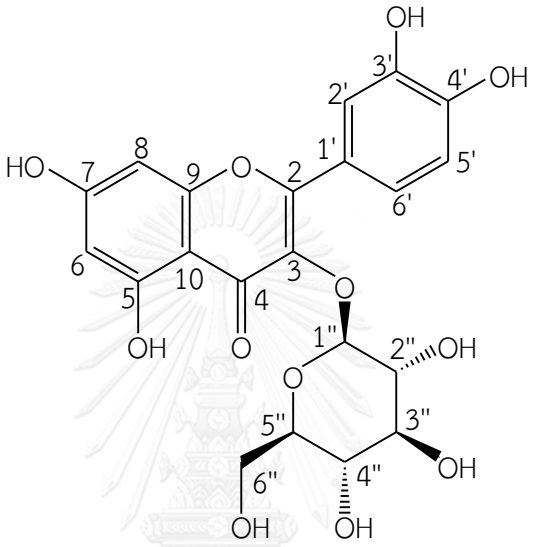

isoquercitrin (31)

Table 4 ^{1}H and ^{13}C NMR spectral data of compound 4 and isoquercitrin (in DMSO-d_6)

Position	compound 4		isoquercitrin[a]	
	δ_H (mult., *J* in Hz)	δ_C	δ_H (mult., *J* in Hz)	δ_C
2	-	156.3	-	156.1
3	-	133.3	-	133.2
4	-	177.4	-	177.4
5	-	161.2	-	161.2
6	6.20 (*d*, 2.0)	98.6	6.19 (*d*, 2.0)	98.6
7	-	164.1		164.1
8	6.40 (*d*, 2.0)	93.5	6.40 (*d*, 2.0)	93.4
9	-	156.1	-	156.3
10	-	104.0	-	103.9
1'	-	121.6	-	121.5
2'	7.57 (*d*, 2.4)	115.2	7.58 (*d*, 2.0)	115.1
3'	-	148.4	-	148.4
4'	-	144.8	-	144.7
5'	6.84 (*d*, 9.2)	116.2	6.84 (*d*, 8.8)	116.1
6'	7.57 (*dd,* 2.0, 9.2)	121.1	7.57 (*dd*, 2.0, 8.0)	121.1
1"	5.45 (*d*, 7.2)	100.8	5.45 (*d*, 7.4)	100.8
2"		74.1		74.0
3"		76.5		76.4
4"		69.9		69.9
5"		77.6		77.5
6"a	3.58 (*dd*, 11.2, 5.2)	61.0		60.9
6"b	3.18 (*dd*, 11.2, 5.2)			

[a]Kim *et al.,* 2007

4.5 Identification of compound 5 (apigenin-7-*O*-glucuronide)

Compound 5 was obtained as a yellow powder. According to its peak at *m/z* 469.0707 in the high resolution ESI mass spectrum (**Figure 31**), the molecular formula of this compound should be $C_{12}H_{16}O_7$. Its IR spectrum (**Figure 32**) was similar to that of the previously isolated flavonoid glycosides 1-4, exhibiting absorption bands of hydroxyl groups (3419 cm^{-1}), conjugated carbonyl (1656 cm^{-1}), aromatic rings (1609, 1497 cm^{-1}) and C-O stretching (1174 cm^{-1}).

The NMR spectral data of compound 5 also share similarity with previous compounds, suggesting a flavonoid glycoside skeleton as its chemical structure. Its 1H NMR spectrum (**Figure 33**) displayed aromatic proton signals of ring A at **δ** 6.48 (1H, *d*, *J* = 1.8 Hz, H-6) and 6.81 ppm (1H, *d*, *J* = 1.8 Hz, H-8) and signals of ring B at **δ** 6.91 (2H, *d*, *J* = 8.5 Hz, H-3′ and H-5′) and 7.86 ppm (2H, *d*, *J* = 8.5 Hz, H-2′ and H-6′). In addition, an addition singlet at **δ** 6.60 ppm (1H, s, H-3) indicated that the aglycone of this compound is the flavone apigenin. An anomeric proton signal could be located at **δ** 5.01 ppm (1H, *d*, *J* = 5.5 Hz, H-1″), which could be **β**-glucose on the basis of coupling constant. Therefore, the substitution as in the previous 4 flavonoid glycosides has been moved to a different position. Moreover, the ^{1}H and ^{13}C NMR spectra (**Figure 34**) also indicated the presence of a glucuronic acid moiety from the following signals at **δ** 3.86 (1H, *d*, *J* = 8.5 Hz, H-5″), **δ** 176.21 (C-6″) with four signals of methylene carbon at **δ** 73.43 (C-4″), 74.50 (C-2″), 76.56 (C-3″), and 77.56 (C-5″) ppm.

From the above data and through comparison with literature, this compound was thus identified as apigenin-7-*O*-**β**-D-glucuronopyranoside or apigenin-7-*O*-glucuronide (Cheng *et al*., 2013).

Apigenin-7-*O*-glucuronide has been isolated from various plants including a number of species in family Fabaceae. It was found in the leaves of *Dichrostachys cinerea* (Hattas *et al*., 2011), and the aerial part of alfalfa (*Medicago sativa*) (Stochmal *et al*., 2001). The compounds also showed diverse biological activities such as anti-inflammatory (Cheng *et al*., 2013) and inhibitory activity on reflux oesophagitis and gastritis (Min *et al*., 2005).

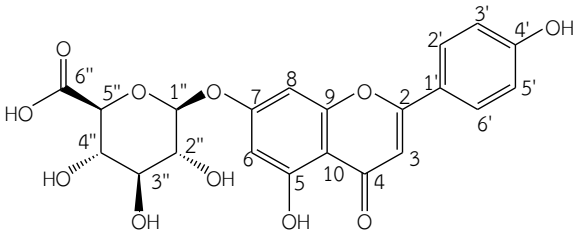

apigenin-7-*O*-glucuronide **(32)**

Table 5 ^{1}H and ^{13}C NMR spectral data of compound 5 (in CD_3OD) and apigenin-7-*O*-glucuronide (in DMSO-d_6)

Position	Compound 5		apigenin-7-O-glucuronide [a]	
	δ_H (mult., *J* in Hz)	δ_C	δ_H (mult., *J* in Hz)	δ_C
2	-	166.8	-	166.6
3	6.60 (*s*)	104.0	6.58 (*s*)	104.0
4	-	184.1	-	184.0
5	-	163.0	-	162.7
6	6.48 (*d*, 1.8)	101.5	6.44 (*d*, 2.0)	101.2
7	-	164.9	-	164.6
8	6.81 (*d*, 1.8)	96.1	6.76 (*d*, 1.6)	96.0
9	-	158.9	-	158.9
10	-	107.1	-	107.1
1'	-	122.9	-	122.9
2'	7.85 (*d*, 8.5)	129.6	7.80 (*d*, 8.8)	129.6
3'	6.91 (*d*, 8.5)	117.1	6.88 (*d*, 8.8)	117.0
4'	-	162.7	-	162.8
5'	6.91 (*d*, 8.5)	117.1	6.88 (*d*, 8.8)	117.0
6'	7.85 (*d*, 8.5)	129.6	7.80 (*d*, 8.8)	129.6
1"	5.09 (*d*, 6.0)	101.4	5.12 (*d*, 7.2)	101.4
2"		74.5		74.5
3"		76.5		76.5
4"		73.4		73..2
5"		77.6		77.4
6"		176.2		174.4

[a]Cheng *et al*., 2013

4.6 Identification of compound 6 (arbutin)

Compound 6 was isolated as a white powder. According to its peak at *m/z* 295.0794 in the high resolution ESI mass spectrum (**Figure 37**), the molecular formula of this compound should be $C_{12}H_{16}O_7$. The IR spectrum (**Figure 36**) showed absorption bands of hydroxyl groups at 3338 cm^{-1}, aromatic rings at 1650, 1603 and 1513 cm^{-1}, and C-O stretching at 1213 cm^{-1}.

The ^{1}H NMR spectrum of this compound (**Figure 38**) showed the *ortho*-coupled proton signals of a *para*-substituted aromatic ring at **δ** 6.69 (2H, *br d*, *J* = 8.8 Hz, H-3 and H-5), and 6.96 ppm (2H, *br d*, *J* = 8.8 Hz, H-2 and H-6). An anomeric proton signal of a glucose moiety could also be observed at **δ** 4.73 ppm (1H, *d*, *J* = 7.0 Hz, H-1'). The ^{13}C NMR spectrum (**Figure 39**) exhibited 10 signals representing one benzene ring and one glucose molecule. Two signals represented four aromatic methine carbons at **δ** 119.6 (C-2 and C-6) and 116.3 ppm (C-3 and C-5). One signal at **δ** 153.8 ppm (C-1) belongs to the hydroxyl-substituted quaternary carbon connected with oxygen atom, while another at **δ** 152.4 ppm was the signal of the quaternary carbon linked with *O*-glucose (C-4). The rest of the carbon signals at **δ** 104.2 (C-1'), 75.8 (C-2'), 78.4 (C-3'), 72.3 (C-4'), 78.9 (C-5'), and 63.4 ppm (C-6') belong to β-glucose moiety. From these spectral data, compound 6 could therefore be identified as arbutin. These data were also compared with reported values in literature (Sugimoto *et al.*, 2003; Lee *et al.*, 2011).

Arbutin occurs in a number of plants in the family Fabaceae such as the fodder of *Onobrychis viciifolia* (Marais *et al.*, 2000) and the epigeal part of *Onobrychis arenaria* (Yuldashev *et al.*, 1996). This compound exhibited potent tyrosinase inhibitory activity, and was used as a positive control for this activity in many studies (Chung *et al.*, 2011; Ko *et al.*, 2011; Park *et al.*, 2013). In addition, this compound has inhibitory effect on the melanogenesis in B16 melanoma cells (Akiu *et al.*, 1991) and human melanocytes (Chakraborty *et al.*, 1998). Therefore, this compound is use as a skin-lightening agent in the cosmetic industry.

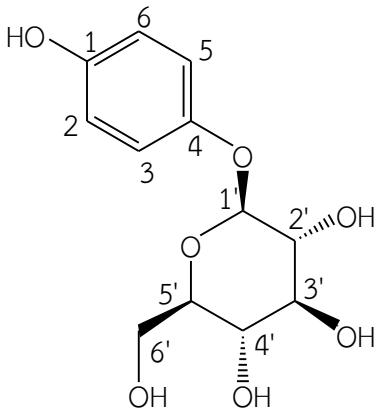

arbutin (33)

Table 6 ^{1}H and ^{13}C NMR spectral data of compound 6 in and arbutin in (CD_3OD)

Position	Compound 6		arbutin[a]	
	δ_H (mult., *J* in Hz	δ_c	δ_H (mult., *J* in Hz)	δ_c
1	-	153.8	-	154.1
2	6.96 (*br d*, 8.8)	119.6	6.96 (*br d*, 9.0)	121.3
3	6.69 (*br d*, 8.8)	116.3	6.69 (*br d*, 9.0)	119.1
4	-	152.4	-	152.7
5	6.69 (*br d*, 8.8)	116.3	6.69 (*br d*, 9.0)	119.1
6	6.96 (*br d*, 8.8)	119.6	6.96 (*br d*, 9.0)	121.3
1'	4.73 (*d*, 7.0)	103.7	4.73 (*d*, 5.0)	104.2
2'		75.0		75.8
3'		78.0		78.4
4'		71.4		72.3
5'		78.0		78.9
6'		62.6		63.4
6'a	3.87 (*br d*, 12.0)		3.88 (*br d*, 12.0)	
6'b	3.69 (*dd*, 11.0, 5.0)		3.69 (*dd*, 12.0, 5.0)	

[a]Sugimoto *et al*., 2003; Lee *et al*., 2011)

4.7 Antioxidant activities of extracts from *Afgekia mahidoliae* leaves

Extracts of *Afgekia mahidoliae* leaves with organic solvents of different polarity were investigated for their total phenolic content, total flavonoid content, DPPH radical scavenging activity, and ferric reducing antioxidant power (FRAP). Since the extract which possessed strong antioxidant activity might have wound healing potential, the purpose of the antioxidant evaluation was therefore to select extracts for further purification and isolation of their chemical constituents. The results of these assays are summarized in Table 7.

Table 7 Total phenolic content, total flavonoid content and antioxidant activity of extracts from *Afgekia mahidoliae leaves*

Extract / Control	Total phenolic (mg/g*)	Total flavonoid (mg/g**)	DPPH scavenging (EC_{50}, µg/ml)	FRAP (mM $FeSO_4$/g)
Methanol	41.93 ± 0.68	43.83 ± 7.12	>100	0.57 ± 0.02
Hexane	25.51 ± 2.34	12.00 ± 2.94	>100	0.19 ± 0.01
Ethyl acetate	248.85 ± 6.90	330.89 ± 15.40	19.52 ± 0.34	1.40 ± 0.02
Butanol	161.09 ± 7.40	171.00 ± 3.33	43.50 ± 1.52	1.17 ± 0.05
Aqueous	92.56 ± 0.80	74.33 ± 6.01	58.59 ± 1.39	0.58 ± 0.02
Trolox	-	-	46.85 ± 2.40	-
Ascorbic acid	-	-	39.92 ± 1.95	-

*mg gallic acid equivalent

**mg rutin equivalent

Total phenolic and total flavonoid contents represented the amount of phenolic compounds and flavonoids in the extracts. For total phenolic content, the results were expressed as gallic acid equivalent (GAE), while the results of total flavonoid content assay were reported as rutin equivalent (RE). The result showed that ethyl acetate extract had the highest amount of phenolic compounds (248.85 ± 6.90 mg GAE/g), followed by *n*-butanol, aqueous, methanol and hexane extracts,

respectively. These results were similar to those of the total flavonoid content assay. The amount of flavonoids in the ethyl acetate extract was 330.89 ± 15.40 mg RE/g, while *n*-butanol extract contained 171.00 ± 3.33 mg RE/g. Total flavonoid contents of the rest of the extracts were less than 100 mg RE/g. The ranking order of both the total phenolic and total flavonoid contents in these *A. mahidoliae* leaf extracts was thus ethyl acetate extract > *n*-butanol extract > aqueous extract > methanol extract > hexane extract. High total phenolic content indicates the redox ability, which contributes towards antioxidant activities and curative ability in absorbing and neutralizing free radicals.

DPPH radical scavenging assay is one of the most popular assays for screening antioxidant activity of plant extracts and constituents because it is simple, sensitive, inexpensive and reproducible. Ascorbic acid and Trolox were used as positive controls in this study. The results were expressed as effective concentration for 50% inhibition of DPPH radicals (EC_{50}). The resulted showed that ethyl acetate extract exhibited the strongest DPPH scavenging ability with an EC_{50} of 19.52 ± 0.3 µg/ml followed by *n*-butanol and aqueous extracts, respectively. Methanol and hexane extracts could be considered as inactive, since both extracts showed EC_{50} values of greater than 100 µg/ml. Interestingly, both ethyl acetate and *n*-butanol extracts displayed higher DPPH scavenging activity than the positive control, Trolox (EC_{50} of 46.85 ± 2.40 µg/ml). The ethyl acetate extract was also more active than ascorbic acid as the other positive control (EC_{50} of 39. 92 ± 1.95 µg/ml). Positive correlation could be observed between the EC_{50} values of the DPPH scavenging and the total phenolic and flavonoid contents of the tested extracts.

Reducing ability of the extracts against reactive oxygen species was measured by FRAP assay. The reducing power was expressed as ferrous equivalent (as $FeSO_4$) in mM/g. FRAP values of ethyl acetate extract was the highest (1.40 ± 0.02 mM/g), followed by *n*-butanol, aqueous, methanol and hexane extracts, respectively. The reducing antioxidant power of the samples is also correlated well with their total phenolic and total flavonoid contents.

In conclusion, ethyl acetate and *n*-butanol extracts of *A. mahidoliae* leaves were the extracts with the best antioxidant activities. Thus, chemical constituents of these fractions were investigated. The isolate compounds were expected to be antioxidant and might be able to promote fibroblast migration in the wound healing process.

4.8 Antioxidant activities of compounds from *Afgekia mahidoliae* leaves

From the ethyl acetate extract of *A. mahidoliae* leaves five flavonoid glycosides, namely, juglanin, astragalin, nicotiflorin, isoquercitrin and apigenin-7-*O*-glucuronide were isolated, whereas arbutin, a glycosylated hydroquinone, was obtained from the *n*-butanol extract. The antioxidant activities of the isolated compounds were assessed by DPPH and FRAP assays. The results are shown in Table 8. Although the DPPH radical scavenging activity of ethyl acetate and *n*-butanol extracts were both stronger than Trolox, the pure compounds isolated from these extracts showed lesser activity. Only the EC_{50} value of isoquercitrin (39.61 ± 4.08 µg/ml) was closed to those of the positive controls Trolox and ascorbic acid (46.85 ± 2.40 and 39.92 ± 1.95 µg/ml, respectively). DPPH radical scavenging activity of all isolated compounds was weaker than that of the ethyl acetate extract. Therefore, these flavonoid glycosides might work synergistically in order to eliminate DPPH radicals. However, it should be noted that isoquercitrin exhibited the strongest ferric antioxidant power (15.11 ± 0.27 mM $FeSO_4$/g), which was greater than even Trolox and ascorbic acid (FRAP values of 7.06 ± 0.36 and 10.34 ± 0.45 mM/g, respectively). The other glycosides showed weak FRAP activity. The presence of two *ortho* hydroxyl groups in ring B is important for this activity, as exemplified by the stronger antioxidant activity of isoquercitrin over that of astragalin in this study, as well as in earlier study (Rice-Evans *et al.*, 1996). In conclusion, isoquercitrin appeared to be the isolated compound with the best antioxidant activities and these flavonoid glycosides might work synergistically when combined within the ethyl acetate extract.

Table 8 Antioxidant activities of isolated compounds from *Afgekia mahidoliae*

Compound	DPPH radical scavenging (EC_{50} in μg/ml)	FRAP value (mM $FeSO_4$/g)
juglanin	> 500	0.27 ± 0.01
astragalin	390.99 ± 11.94	1.11 ± 0.04
nicotiflorin	>500	0.35 ± 0.02
isoquercitrin	39.61± 4.08	15.11 ± 0.27
apigenin-7-*O*-glucuronide	>500	0.44 ± 0.01
arbutin	>500	0.97 ± 0.05
Trolox	46.85 ± 2.40	7.06 ± 0.36
Ascorbic acid	39.92 ± 1.95	10.34 ± 0.45

4.9 Cytotoxicity of isolated compounds

Based on previous reports on the ability of flavonoids to promote cell migration (Schmidt *et al*. 2010; Kim *et al*. 2012; Clericuzio *et al*., 2012), only juglanin, astragalin, nicotiflorin, and isoquercitrin were chosen to be evaluated for their activity on the migration of human dermal fibroblasts (CCD-1064sk). Apigenin-7-*O*-glucuronide was not tested due to its limited amount. However, prior to the evaluation appropriate concentrations of the tested compounds that would not be cytotoxic to the cells needed to be determined. The isolated kaempferol glycosides and quercetin glucoside, along with kaempferol and quercetin, were assayed for their cytotoxicity against human dermal fibroblast cell line by using MTT assay. Each flavonoid was tested at concentrations of 1, 5, 10, 20, 40 and 80 μM. The results are presented in Figures 4-5.

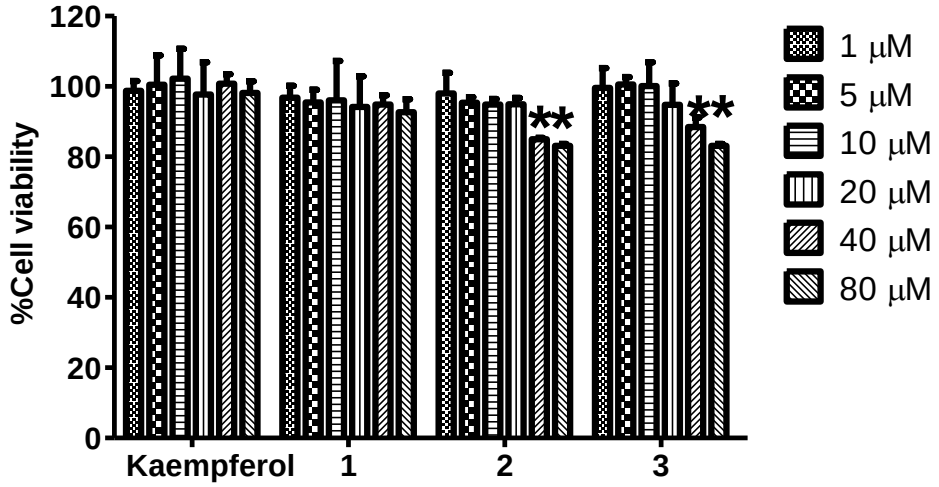

Figure 4 Cytotoxicity of kaempferol, juglanin (1), astragalin (2) and nicotiflorin (3) on human dermal fibroblast CCD-S106SK

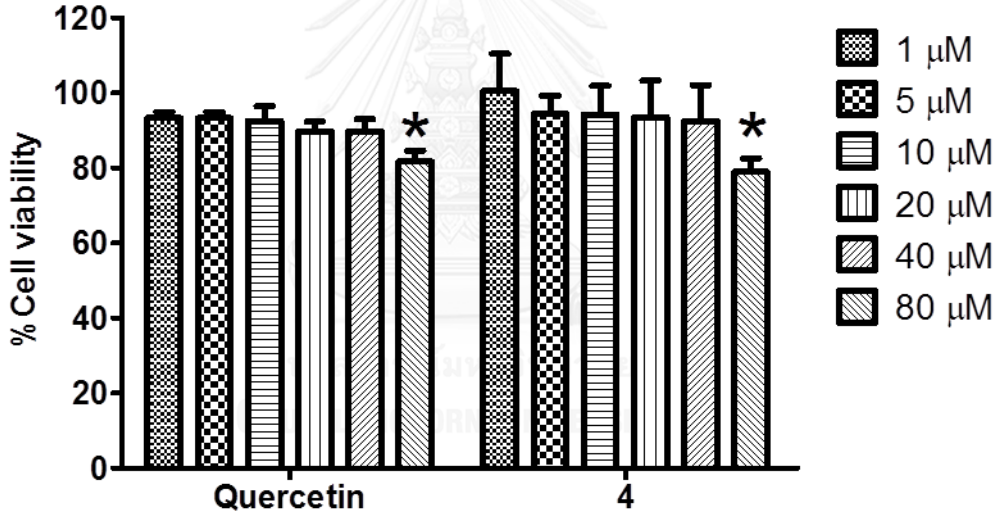

Figure 5 Cytotoxicity of quercetin and isoquercitrin (4) on human dermal fibroblast CCD-S106SK

The results of cytotoxicity assay indicated that both kaempferol and juglanin (1), were not toxic to fibroblast cells at concentrations up to 80 μM, while astragalin (2), nicotiflorin (3) appeared to reduce the viability of fibroblasts significantly ($P<0.05$) at concentrations over 40 μM. Both quercetin and its glucoside were toxic to the cells at 80 μM. Therefore, these compounds were later evaluated for their ability to promote fibroblast migration at concentrations of less than 40 μM.

4.10 Wound healing activity of isolated compounds in scratch wound assay

In scratch wound assay, layers of fibroblast cells in microplate wells were scraped by a pipette tip in order to create a scratch wound to be treated with the test compounds. After the treatment, a photo of each well was taken under an inverted microscope at 0, 8, 16 and 24 h. The ability of the isolated flavonoid glycosides and their aglycones to promote fibroblast migration into the scratch wound area was evaluated by comparison with the control (an untreated sample). The results are presented in Figures 6-9.

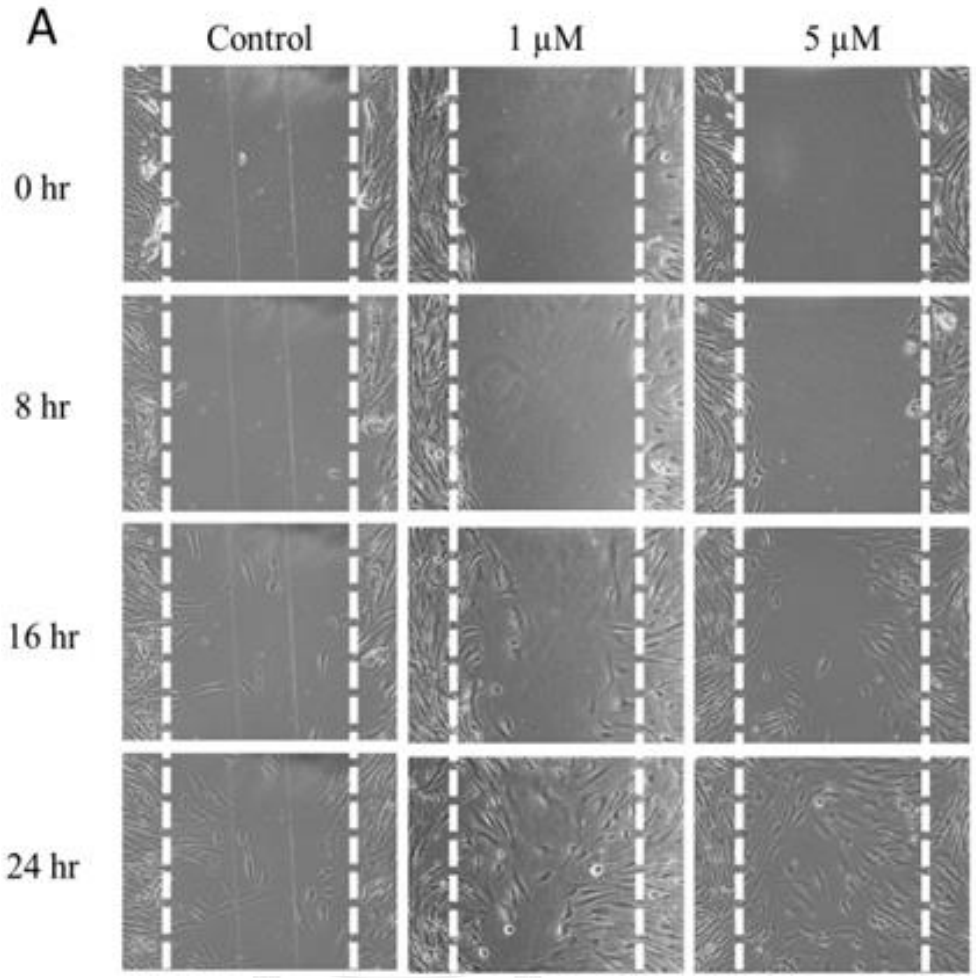

Figure 6 Ability of 1 and 5 μM juglanin to promote fibroblast migration in the scratch-wound healing assay at 0, 8, 16 and 24 h

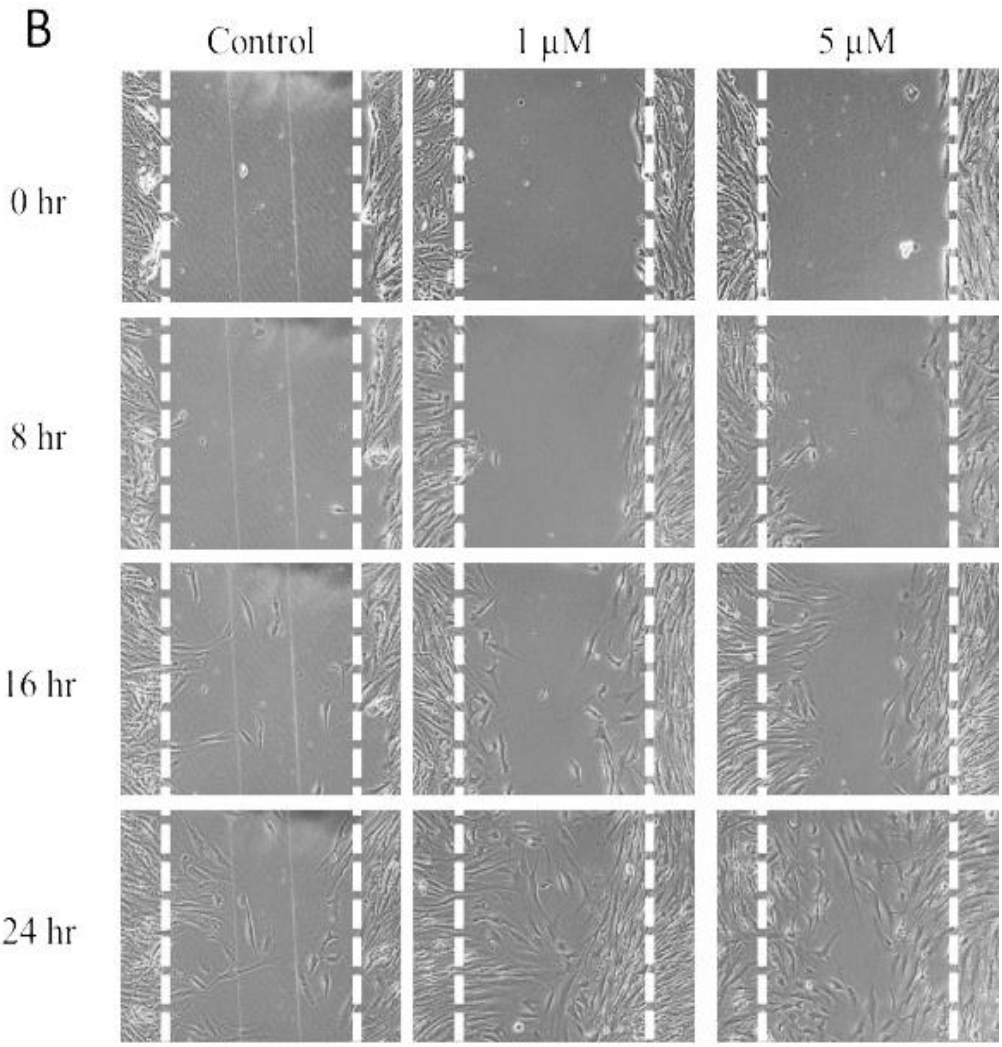

Figure 7 Ability of 1 and 5 µM nicotiflorin to promote fibroblast migration in the scratch-wound healing assay at 0, 8, 16 and 24 h

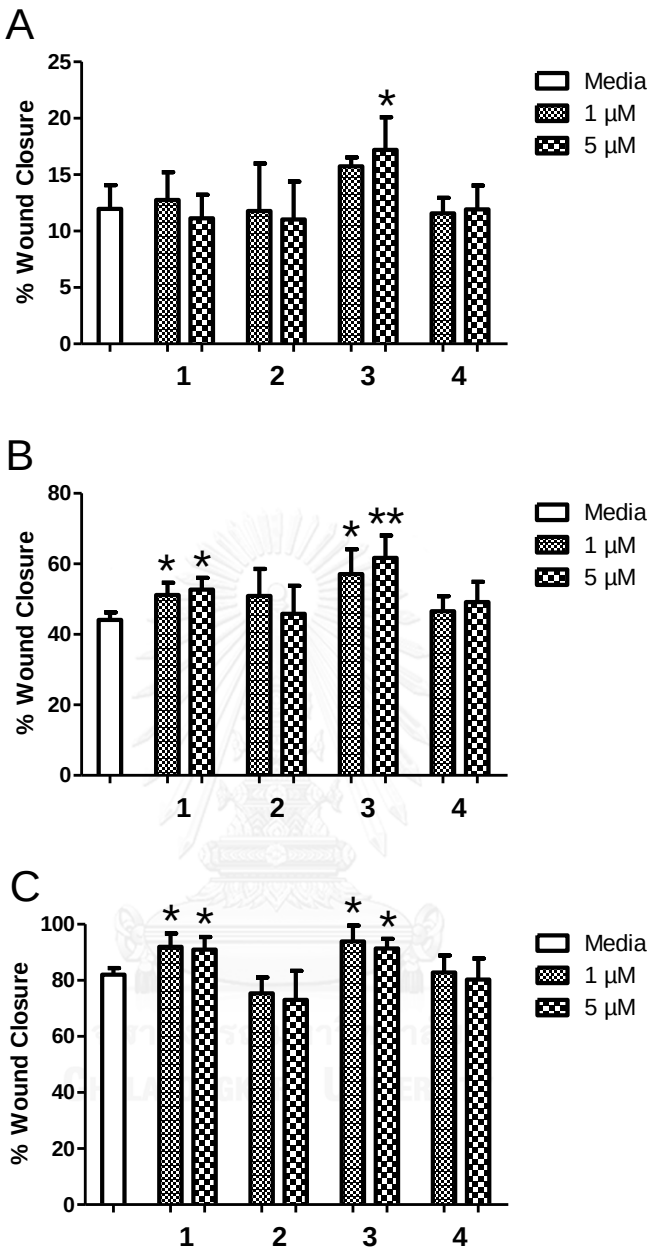

Figure 8 Effect of juglanin (1), astragalin (2), nicotiflorin (3), and isoquercitrin (4) on scratch-wound healing assay with fibroblasts at (A) 8 h, (B) 16 h and (C) 24 h. Data are expressed as percentages of wound closure in the wound area compared to the control. Bars represent the mean ± S.E.M. of three experiments, * represents $p < 0.05$, ** represents $p < 0.01$

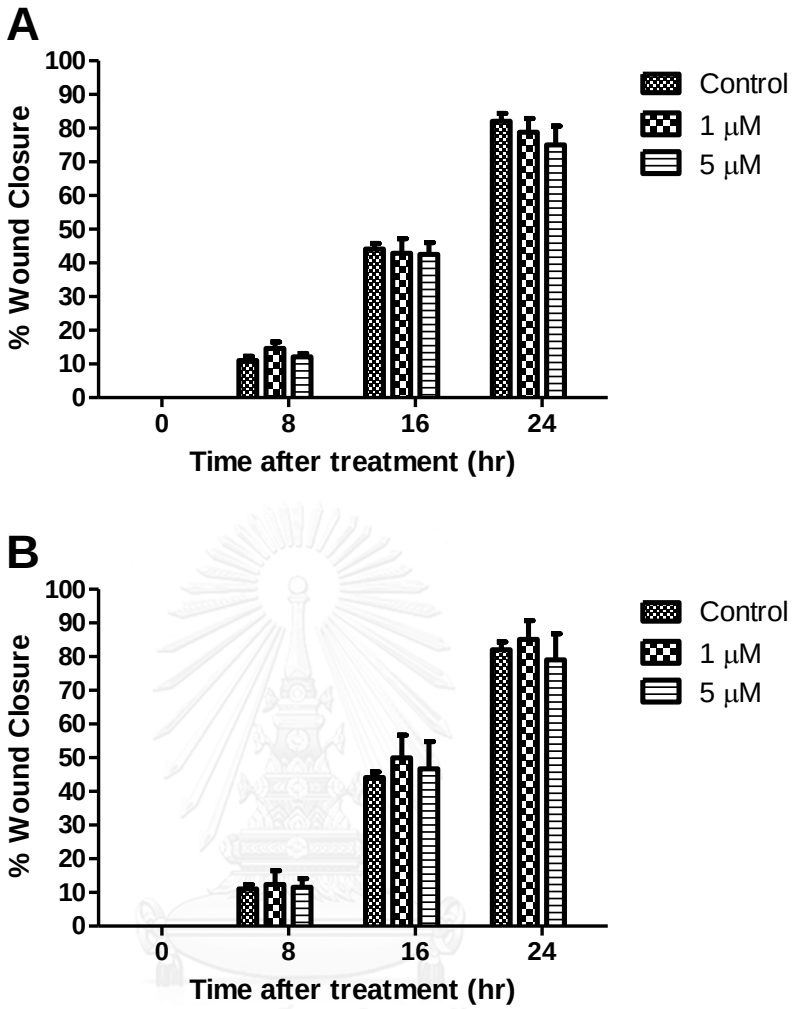

Figure 9 Effect of kaempferol (A) and quercetin (B) on scratch wound assay with fibroblasts at 0, 8, 16 and 24 h. Data are expressed as percentages of wound closure in the wound area compared to the control. Bars represent the mean ± S.E.M. of three experiments

Nicotiflorin, a kaempferol rutinoside, at the concentration of 5 μM, appeared to be the most effective promoter of fibroblast migration into the scratch wound by significantly enhancing their motility as early as 8 h after incubation (Figures 7 and 8). Both concentrations of the isolated kaempferol arabinoside, juglanin, displayed this ability at 16 and 24 h (Figures 6 and 8), whereas both kaempferol glucoside and quercetin glucoside did not display scratch-wound healing effect, giving similar or lower wound closure percentages than that of the control. Kaempferol and

quercetin themselves, when subjected to this assay, did not promote migration of the fibroblasts (Figure 9). Therefore, sugar moiety at the position 3 of these flavonol glycosides appeared to be essential to the activity and the type of sugars is also important, because glucosides of both flavonoid aglycones did not promote fibroblast migration.

Kaempferol and quercetin are flavonols widely found in higher plants and are well-known for their antioxidant and anti-inflammatory activities, both of which may contribute to an increase in the rate of wound healing (Mensah *et al.*, 2001; Jha *et al.*, 2012). Although quercetin was a strong fibroblast growth inhibitor, its glycosides such as rutin (quercetin 3-*O*-rutinoside) did not possess this activity (Koganov *et al.*, 1999). Rutin could stimulate fibroblast proliferation (Koganov *et al*., 1999), increase collagen synthesis in human fibroblasts (Stipcevic *et al*., 2006), enhance production and accumulation of extracellular matrix and has been commercially used as a drug for healing wound (Tran *et al*., 2011). In addition, a kaempferol glycoside, kaempferol-3-O-[(6-caffeoyl)-β-glucopyranosyl (1⟶3) α-rhamnopyranoside]-7-*O*-α-rhamnopyranoside, has been reported to promote keratinocyte re-epithelialization (Clericuzio *et al.,* 2012). Thus, the results of this study support the wound healing activity of these flavonoid glycosides.

CHAPTER 5

CONCLUSION

Result from preliminary wound healing assay suggested that metholic extract of *A. mahidoliae* leaves was able to promote the motility of human dermal fibroblast cell line (CCD-1064sk) at concentrations between 0.1-1 µg/ml. Thus, this study aimed to identify bioactive compounds responsible for fibroblast migration, which is an essential process in wound healing. Assays for total phenolic and total flavonoid contents, as well as antioxidant assays including DPPH radical scavenging and ferric reducing antioxidant power (FRAP), were performed using the extracts of *A. mahidoliae* leaves. Ethyl acetate and *n*-butanol extracts showed strong antioxidant activities and were further isolated for active compounds. Five flavonoid glycosides were obtained from the ethyl acetate extract i.e. juglanin, astragalin, nicotiflorin, isoquercetin and apigenin-7-*O*-glucorunide, whereas one hydroquinone glycoside, arbutin, was isolated from the *n*-butanol extract. All compounds were isolated from this plant and this plant genus for the first time. Juglanin, astragalin, nicotiflorin and isoquercetin were tested for their ability to promote fibroblast migration into scratch wound area. Juglanin and nicotiflorin were able to enhance the motility of fibroblasts. Therefore, these kaempferol glycosides may have a potential to be developed into wound healing agents.

REFERENCES

Agrawal, P. K. (1992). NMR spectroscopy in the structural elucidation of oligosaccharides and glycosides. Phytochemistry **31**(10): 3307-3330.

Agyemang, K., L. Han, E. Liu, Y. Zhang, T. Wang and X. Gao (2013). Recent advances in *Astragalus membranaceus* anti-diabetic research: Pharmacological effects of its phytochemical constituents. Evidence-Based Complementary and Alternative Medicine **2013**: 9.

Akiu, S., Y. Suzuki, T. Asahara, Y. Fujinuma and M. Fukuda (1991). Inhibitory effect of arbutin on melanogenesis--biochemical study using cultured B16 melanoma cells. Nihon Hifuka Gakkai Zasshi **101**(6): 609-613.

Akkol, E. K., I. Süntar, I. E. Orhan, H. Keles, A. Kan and G. Çoksari (2011). Assessment of dermal wound healing and *in vitro* antioxidant properties of *Avena sativa* L. Journal of Cereal Science **53**(3): 285-290.

Al-Jaber, N. A. (2011). Phytochemical and biological studies of *Sisymbrium irio* L. growing in Saudi Arabia. Journal of Saudi Chemical Society **15**(4): 345-350.

Alam, M. N., N. J. Bristi and M. Rafiquzzaman (2013). Review on *in vivo* and *in vitro* methods evaluation of antioxidant activity. Saudi Pharmaceutical Journal **21**(2): 143-152.

Alaniya, M. D. and N. F. Chkadua (2000). Flavonoids of *Astragalus tana*. Chemistry of Natural Compounds **36**(5): 537-537.

Ali, A. A., M. H. Mohamed, M. S. Kamel, M. A. Fouad and O. Spring (1998). Studies on *Securigera securidacea* (L.) Deg. et Dorfl. (Fabaceae) seeds, an antidiabetic Egyptian folk medicine. Pharmazie **53**(10): 710-715.

Amado, N. G., D. M. Cerqueira, F. S. Menezes, J. F. da Silva, V. M. Neto and J. G. Abreu (2009). Isoquercitrin isolated from *Hyptis fasciculata* reduces glioblastoma cell proliferation and changes beta-catenin cellular localization. Anticancer Drugs **20**(7): 543-552.

Arung, E. T., S. Furuta, H. Ishikawa, H. Tanaka, K. Shimizu and R. Kondo (2011). Melanin biosynthesis inhibitory and antioxidant activities of quercetin-3-*O*-

beta-D-glucoside isolated from *Allium cepa*. Zeitschrift für Naturforschung C **66**(5-6): 209-214.

Ataa Said, U. W. H., Siham El-Shenawy (2010). Flavonoids and some biological activities of *Ailanthus excelsa* leaves. IUFS Journal of Biology **69**: 41-45.

Atiba, A., M. Nishimura, S. Kakinuma, T. Hiraoka, M. Goryo, Y. Shimada, H. Ueno and Y. Uzuka (2011). *Aloe vera* oral administration accelerates acute radiation-delayed wound healing by stimulating transforming growth factor-β and fibroblast growth factor production. The American Journal of Surgery **201**(6): 809-818.

Balekar, N., N. G. Katkam, T. Nakpheng, K. Jehtae and T. Srichana (2012). Evaluation of the wound healing potential of *Wedelia trilobata* (L.) leaves. Journal of Ethnopharmacology **141**(3): 817-824.

Bian, D., J. Zhang, X. Wu, Y. Dou, Y. Yang, Q. Tan, Y. Xia, Z. Gong and Y. Dai (2013). Asiatic acid isolated from *Centella asiatica* inhibits TGF-beta1-induced collagen expression in human keloid fibroblasts via PPAR-gamma activation. International Journal of Biological Sciences **9**(10): 1032-1042.

Bickers, D. R., H. W. Lim, D. Margolis, M. A. Weinstock, C. Goodman, E. Faulkner, C. Gould, E. Gemmen and T. Dall (2006). The burden of skin diseases: 2004 a joint project of the American Academy of Dermatology Association and the Society for Investigative Dermatology. Journal of the American Academy of Dermatology **55**(3): 490-500.

Boonkerd, T. (2001). Morphometric relationships among three populations of *Afgekia sericea* Craib (Fabaceae) in Thailand. The Journal of Scientific Research Chulalongkorn University **26**(1): 1-11.

Brochado, C. d. O., A. P. d. Almeida, B. P. Barreto, L. P. Costa, L. S. Ribeiro, R. L. d. C. Pereira, V. L. G. Koatz and S. S. Costa (2003). Flavonol robinobiosides and rutinosides from *Alternanthera brasiliana* (Amaranthaceae) and their effects on lymphocyte proliferation *in vitro*. Journal of the Brazilian Chemical Society **14**: 449-451.

Burtt, B. L. and Chermsirivathana (1971). A second species of *Afgekia* (Leguminosae). Notes from the Royal Botanic Garden, Edinburgh. **31:** 131-133.

Chainok, K. (2007). Isolation of antioxidant component from petroleum ether extract of *Afgekia mahidolae* Burtt et Chermsir. Master's Thesis, Mahidol University.

Chakraborty, A. K., Y. Funasaka, M. Komoto and M. Ichihashi (1998). Effect of arbutin on melanogenic proteins in human melanocytes. Pigment Cell & Melanoma Research **11**(4): 206-212.

Cheng, H. L., L. J. Zhang, Y. H. Liang, Y. W. Hsu, I. J. Lee, C. C. Liaw, S. Y. Hwang and Y. H. Kuo (2013). Antiinflammatory and antioxidant dlavonoids and phenols from *Cardiospermum halicacabum* (Dao Di Ling). Journal of Traditional and Complementary Medicine 3(1): 33-40.

Chuakul, W., Prathanturarug, S., Saralamp, P., and Supatarawanich, P. (1994). Medicinal plants in Mahasarakham province. Thai Journal of Phytopharmacy **1**: 39 - 56.

Chung, Y. M., H. C. Wang, M. El-Shazly, Y. L. Leu, M. C. Cheng, C. L. Lee, F. R. Chang and Y. C. Wu (2011). Antioxidant and tyrosinase inhibitory constituents from a desugared sugar cane extract, a byproduct of sugar production. Journal of Agricultural and Food Chemistry **59**(17): 9219-9225.

Clark, R. A. (1993). Regulation of fibroplasia in cutaneous wound repair. The American Journal of the Medical Sciences **306**(1): 42-48.

Clericuzio, M., S. Tinello, B. Burlando, E. Ranzato, S. Martinotti, L. Cornara and A. La Rocca (2012). Flavonoid oligoglycosides from *Ophioglossum vulgatum* L. having wound healing properties. Planta Medica **78**(15): 1639-1644.

Demidova-Rice, T. N., M. R. Hamblin and I. M. Herman (2012). Acute and impaired wound healing: pathophysiology and current methods for drug delivery, part 1: normal and chronic wounds: biology, causes, and approaches to care. Advances in Skin & Wound Care **25**(7): 304-314.

Deng, S., Z. Deng, Y. Fan, Y. Peng, J. Li, D. Xiong and R. Liu (2009). Isolation and purification of three flavonoid glycosides from the leaves of *Nelumbo*

nucifera (Lotus) by high-speed counter-current chromatography. Journal of Chromatography B **877**(24): 2487-2492.

Edwards, J. V., P. Howley and I. K. Cohen (2004). *In vitro* inhibition of human neutrophil elastase by oleic acid albumin formulations from derivatized cotton wound dressings. International Journal of Pharmaceutics **284**(1–2): 1-12.

Eming, S. A., T. Krieg and J. M. Davidson (2007). Inflammation in wound repair: molecular and cellular mechanisms. Journal of Investigative Dermatology **127**(3): 514-525.

Fronza, M., B. Heinzmann, M. Hamburger, S. Laufer and I. Merfort (2009). Determination of the wound healing effect of *Calendula* extracts using the scratch assay with 3T3 fibroblasts. Journal of Ethnopharmacology **126**(3): 463-467.

Geethalakshmi, R., C. Sakravarthi, T. Kritika, M. Arul Kirubakaran and D. V. L. Sarada (2013). Evaluation of antioxidant and wound healing potentials of S*phaeranthus amaranthoides* Burm.F. BioMed Research International **2013**: 7.

Gilroy, D. W., T. Lawrence, M. Perretti and A. G. Rossi (2004). Inflammatory resolution: new opportunities for drug discovery. Nature Reviews Drug Discovery **3**(5): 401-416.

Gurtner, G. C., S. Werner, Y. Barrandon and M. T. Longaker (2008). Wound repair and regeneration. Nature **453**(7193): 314-321.

Hasan, A., M. Farman and I. Ahmed (1993). Flavonoid glycosides from *Indigofera hebepetala*. Phytochemistry **35**(1): 275-276.

Hattas, D., J. Hjältén, R. Julkunen-Tiitto, P. F. Scogings and T. Rooke (2011). Differential phenolic profiles in six African savanna woody species in relation to antiherbivore defense. Phytochemistry **72**(14–15): 1796-1803

Herald, T. J., P. Gadgil and M. Tilley (2012). High-throughput micro plate assays for screening flavonoid content and DPPH-scavenging activity in sorghum bran and flour. Journal of the Science of Food and Agriculture **92**(11): 2326-2331.

Jeong, B.-S. (2006). Structure-activity relationship study of asiatic acid derivatives for new wound healing agent. Archives of Pharmacal Research **29**(7): 556-562.

Jha, M., V. Sharma and N. Ganesh (2012). Antioxidant and wound healing potential of *Pistia stratiotes* L. Asian Pacific Journal of Tropical Disease **2, Supplement 2**(0): S579-S584.

Jung, H. A., A. R. Kim, H. Y. Chung and J. S. Choi (2002). *In vitro* antioxidant activity of some selected *Prunus* species in Korea. Archives of Pharmacal Research **25**(6): 865-872.

Kang, T. H., S. J. Jeong, N. Y. Kim, R. Higuchi and Y. C. Kim (2000). Sedative activity of two flavonol glycosides isolated from the flowers of *Albizzia julibrissin* Durazz. Journal of Ethnopharmacology **71**(1-2): 321-323.

Khozhambergenova, P. and K. F. Blinova (1980). Flavonoids of *Astragalus ammodendron*. Khimiya Prirodnykh Soedinenii (4): 566-567.

Kim, M.-S. and S.-H. Kim (2011). Inhibitory effect of astragalin on expression of lipopolysaccharide-induced inflammatory mediators through NF-**K**B in macrophages. Archives of Pharmacal Research **34**(12): 2101-2107.

Kim, S. Y., J. J. Gao, W. C. Lee, K. S. Ryu, K. R. Lee and Y. C. Kim (1999). Antioxidative flavonoids from the leaves of *Morus alba*. Archives of Pharmacal Research **22**(1): 81-85.

Kim, Y. W., W. H. Lee, S. M. Choi, Y. Y. Seo, B. O. Ahn, S. H. Kim and S. G. Kim (2012). DA6034 promotes gastric epithelial cell migration and wound-healing through the mTOR pathway. Journal of Gastroenterology and Hepatology **27**(2): 397-405.

Ko, R. K., G. O. Kim, C. G. Hyun, D. S. Jung and N. H. Lee (2011). Compounds with tyrosinase inhibition, elastase inhibition and DPPH radical scavenging activities from the branches of Distylium racemosum Sieb. et Zucc. Phytotherapy Research **25**(10): 1451-1456.

Koganov, M. M., O. V. Dueva and B. L. Tsorin (1999). Activities of plant-derived phenols in a fibroblast cell culture model. Journal of Natural Products **62**(3): 481-483.

Lal Shyaula, S., G. Abbas, H. Siddiqui, S. A. Sattar, M. I. Choudhary and F. Z. Basha (2012). Synthesis and antiglycation activity of kaempferol-3-*O*-rutinoside (nicotiflorin). Journal of Medicinal Chemistry **8**(3): 415-420.

Lattanzio, V., A. Cardinali, V. Linsalata, P. Perrino and N. Q. Ng (1996). A chemosystematic study of the flavonoids of Vigna. Genetic Resources and Crop Evolution **43**(6): 493-504.

Lee, J. H., H. L. Kim, M. H. Lee, K. E. You, B. J. Kwon, H. J. Seo and J. C. Park (2012). Asiaticoside enhances normal human skin cell migration, attachment and growth in vitro wound healing model. Phytomedicine **19**(13): 1223-1227.

Lee, K., J.-Y. Cho, H. Lee, K. Park, Y.-K. Ma, S.-H. Lee, J. Cho, W.-S. Kim, K.-H. Park and J.-H. Moon (2011). Isolation and identification of phenolic compounds from an Asian pear (*Pyrus pyrifolia* Nakai) fruit peel. Food Science and Biotechnology **20**(6): 1539-1545.

Leong, C. N. A., M. Tako, I. Hanashiro and H. Tamaki (2008). Antioxidant flavonoid glycosides from the leaves of *Ficus pumila* L. Food Chemistry **109**(2): 415-420.

Li, F., D. Liang, Z. Yang, T. Wang, W. Wang, X. Song, M. Guo, E. Zhou, D. Li, Y. Cao and N. Zhang (2013). Astragalin suppresses inflammatory responses via down-regulation of NF-kappaB signaling pathway in lipopolysaccharide-induced mastitis in a murine model. International Immunopharmacology **17**(2): 478-482.

Li, F., W. Wang, Y. Cao, D. Liang, W. Zhang, Z. Zhang, H. Jiang, M. Guo and N. Zhang (2014). Inhibitory effects of astragalin on lipopolysaccharide-induced inflammatory response in mouse mammary epithelial cells. Journal of Surgical Research **192**(2): 573-81.

Liang, C. C., A. Y. Park and J. L. Guan (2007). *In vitro* scratch assay: a convenient and inexpensive method for analysis of cell migration *in vitro*. Nature Protocols **2**(2): 329-333.

Liyana-Pathirana, C. M. and F. Shahidi (2005). Antioxidant activity of commercial soft and hard wheat (*Triticum aestivum* L.) as affected by gastric pH conditions. Journal of Agricultural and Food Chemistry **53**(7): 2433-2440.

Maenthaisong, R., N. Chaiyakunapruk, S. Niruntraporn and C. Kongkaew (2007). The efficacy of aloe vera used for burn wound healing: A systematic review. Burns **33**(6): 713-718.

Marais, J. P., I. Mueller-Harvey, E. V. Brandt and D. Ferreira (2000). Polyphenols, condensed tannins, and other natural products in *Onobrychis viciifolia* (Sainfoin). Journal of Agricultural and Food Chemistry **48**(8): 3440-3447.

Menke, N. B., K. R. Ward, T. M. Witten, D. G. Bonchev and R. F. Diegelmann (2007). Impaired wound healing. Clinics in Dermatology **25**(1): 19-25.

Mensah, A. Y., J. Sampson, P. J. Houghton, P. J. Hylands, J. Westbrook, M. Dunn, M. A. Hughes and G. W. Cherry (2001). Effects of *Buddleja globosa* leaf and its constituents relevant to wound healing. Journal of Ethnopharmacology **77**(2-3): 219-226.

Min, Y. S., S. H. Yim, K. L. Bai, H. J. Choi, J. H. Jeong, H. J. Song, S. Y. Park, I. Ham, W. K. Whang and U. D. Sohn (2005). The effects of apigenin-7-*O*-beta-D-glucuronopyranoside on reflux oesophagitis and gastritis in rats. Auton Autacoid Pharmacology **25**(3): 85-91.

Moon, J. K. and T. Shibamoto (2009). Antioxidant assays for plant and food components. Journal of Agricultural and Food Chemistry **57**(5): 1655-1666.

Nagappan, T., T. C. Segaran, M. E. Wahid, P. Ramasamy and C. S. Vairappan (2012). Efficacy of carbazole alkaloids, essential oil and extract of *Murraya koenigii* in enhancing subcutaneous wound healing in rats. Molecules **17**(12): 14449-14463.

Nia, M. A., K. V. Rao, K. Sreeramulu and D. Gunasekar (1992). Two New Prenylated Flavonoids from Paracalyx scariosa. Journal of Natural Products **55**(8): 1152-1154.

Nizamutdinova, I. T., Y. M. Kim, J. I. Chung, S. C. Shin, Y.-K. Jeong, H. G. Seo, J. H. Lee, K. C. Chang and H. J. Kim (2009). Anthocyanins from black soybean seed

coats stimulate wound healing in fibroblasts and keratinocytes and prevent inflammation in endothelial cells. Food and Chemical Toxicology **47**(11): 2806-2812.

Olczyk, P., Mencner, and K. Komosinska-Vassev (2014). The role of the extracellular matrix components in cutaneous wound healing. BioMed Research International **2014**: 8.

Pandith, H., X. Zhang, J. Liggett, K.-W. Min, W. Gritsanapan and S. J. Baek (2013). Hemostatic and wound healing properties of *Chromolaena odorata* leaf extract. ISRN Dermatology **2013**: 8.

Park, H., K. H. Song, P. M. Jung, J.-E. Kim, H. Ro, M. Y. Kim and J. Y. Ma (2013). Inhibitory Effect of arctigenin from *Fructus Arctii* extract on melanin synthesis via repression of tyrosinase expression. Evidence-Based Complementary and Alternative Medicine **2013**: 10.

Paulo, A., S. Martins, P. Branco, T. Dias, C. Borges, A. I. Rodrigues, C. Costa Mdo, A. Teixeira and H. Mota-Filipe (2008). The opposing effects of the flavonoids isoquercitrin and sissotrin, isolated from P*terospartum tridentatum*, on oral glucose tolerance in rats. Phytotherapy Research **22**(4): 539-543.

Phan, T. T., M. A. Hughes and G. W. Cherry (2001). Effects of an aqueous extract from the leaves of *Chromolaena odorata* (Eupolin) on the proliferation of human keratinocytes and on their migration in an *in vitro* model of reepithelialization. Wound Repair and Regeneration **9**(4): 305-313.

Phan, T. T., M. A. Hughes, G. W. Cherry, T. T. Le and H. M. Pham (1996). An aqueous extract of the leaves of *Chromolaena odorata* (formerly *Eupatorium odoratum*) (Eupolin) inhibits hydrated collagen lattice contraction by normal human dermal fibroblasts. Journal of Alternative and Complementary Medicine **2**(3): 335-343.

Porras-Reyes, B. H., W. H. Lewis, J. Roman, L. Simchowitz and T. A. Mustoe (1993). Enhancement of wound healing by the alkaloid taspine defining mechanism of action. Proceedings of the Society for Experimental Biology and Medicine. **203**(1): 18-25.

Priya, K. S., G. Arumugam, B. Rathinam, A. Wells and M. Babu (2004). *Celosia argentea* Linn. leaf extract improves wound healing in a rat burn wound model. Wound Repair Regeneration **12**(6): 618-625.

Regasini, L. O., J. C. Vellosa, D. H. Silva, M. Furlan, O. M. de Oliveira, N. M. Khalil, I. L. Brunetti, M. C. Young, E. J. Barreiro and V. S. Bolzani (2008). Flavonols from *Pterogyne nitens* and their evaluation as myeloperoxidase inhibitors. Phytochemistry **69**(8): 1739-1744.

Rice-Evans, C. A., N. J. Miller and G. Paganga (1996). Structure-antioxidant activity relationships of flavonoids and phenolic acids. Free Radical Biology and Medicine **20**(7): 933-956.

Ruszymah, B. H., S. R. Chowdhury, N. A. Manan, O. S. Fong, M. I. Adenan and A. B. Saim (2012). Aqueous extract of *Centella asiatica* promotes corneal epithelium wound healing *in vitro*. Journal of Ethnopharmacology **140**(2): 333-338.

Saito, S., G. Silva, R. X. Santos, G. Gosmann, C. Pungartnik and M. Brendel (2012). Astragalin from *Cassia alata* induces DNA adducts *in vitro* and repairable DNA damage in the yeast *Saccharomyces cerevisiae*. International Journal of Molecular Sciences **13**(3): 2846-2862.

Schäfer, M. and S. Werner (2008). Oxidative stress in normal and impaired wound repair. Pharmacological Research **58**(2): 165-171.

Schmidt, C. A., R. Murillo, T. Bruhn, G. Bringmann, M. Goettert, B. Heinzmann, V. Brecht, S. A. Laufer and I. Merfort (2010). Catechin derivatives from *Parapiptadenia rigida* with *in vitro* wound-healing properties. Journal of Natural Products **73**(12): 2035-2041.

Schönfelder, U., M. Abel, C. Wiegand, D. Klemm, P. Elsner and U.-C. Hipler (2005). Influence of selected wound dressings on PMN elastase in chronic wound fluid and their antioxidative potential *in vitro*. Biomaterials **26**(33): 6664-6673.

Schreml, S., R. M. Szeimies, L. Prantl, S. Karrer, M. Landthaler and P. Babilas (2010). Oxygen in acute and chronic wound healing. British Journal of Dermatology **163**(2): 257-268.

Sevimli-Gür, C., İ. Onbaşılar, P. Atilla, R. Genç, N. Çakar, İ. Deliloğlu-Gürhan and E. Bedir (2011). *In vitro* growth stimulatory and *in vivo* wound healing studies on cycloartane-type saponins of *Astragalus* genus. Journal of Ethnopharmacology **134**(3): 844-850.

Shetty, B. S., S. L. Udupa, A. L. Udupa and S. N. Somayaji (2006). Effect of *Centella asiatica* L (Umbelliferae) on normal and dexamethasone-suppressed wound healing in Wistar albino rats. The International Journal of Lower Extremity Wounds **5**(3): 137-143.

Shim, K. M., S. H. Choi, M. J. Jeong and S. S. Kang (2007). Effects of aucubin on the healing of oral wounds. In Vivo **21**(6): 1037-1041.

Shukla, A., A. M. Rasik, G. K. Jain, R. Shankar, D. K. Kulshrestha and B. N. Dhawan (1999). *In vitro* and *in vivo* wound healing activity of asiaticoside isolated from *Centella asiatica*. Journal of Ethnopharmacology **65**(1): 1-11.

Somboonwong, J., M. Kankaisre, B. Tantisira and M. Tantisira (2012). Wound healing activities of different extracts of *Centella asiatica* in incision and burn wound models: an experimental animal study. BMC Complementary and Alternative Medicine **12**(1): 1-7.

Stevenson, P. C., M. S. Simmonds, J. Sampson, P. J. Houghton and P. Grice (2002). Wound healing activity of acylated iridoid glycosides from *Scrophularia nodosa.* Phytotherapy Research **16**(1): 33-35.

Stipcevic, T., J. Piljac and D. Berghe (2006). Effect of different flavonoids on collagen synthesis in human fibroblasts. Plant Foods for Human Nutrition **61**(1): 27-32.

Sudan, S. and H. P. Rupasinghe (2014). Quercetin-3-*O*-glucoside induces human DNA topoisomerase II inhibition, cell cycle arrest and apoptosis in hepatocellular carcinoma cells. Anticancer Research **34**(4): 1691-1699.

Sugimoto, K., T. Nishimura, K. Nomura, K. Sugimoto and T. Kuriki (2003). Syntheses of arbutin-alpha-glycosides and a comparison of their inhibitory effects with those of alpha-arbutin and arbutin on human tyrosinase. Chemical and Pharmaceutical Bulletin **51**(7): 798-801.

Suguna, L., P. Sivakumar and G. Chandrakasan (1996). Effects of *Centella asiatica* extract on dermal wound healing in rats. Indian Journal of Experimental Biology **34**(12): 1208-1211.

Takzare, N., M.-j. Hosseini, G. Hasanzadeh, H. Mortazavi, A. Takzare and P. Habibi (2009). Influence of aloe vera gel on dermal wound healing process in rat. Toxicology Mechanisms and Methods **19**(1): 73-77.

Tran, N. Q., Y. K. Joung, E. Lih and K. D. Park (2011). *In situ* forming and rutin-releasing chitosan hydrogels as injectable dressings for dermal wound healing. Biomacromolecules **12**(8): 2872-2880.

Tsala, D. E., D. Amadou and S. Habtemariam (2013). Natural wound healing and bioactive natural products Phytopharmacology **4**(3): 532 - 560.

Velnar, T., T. Bailey and V. Smrkolj (2009). The wound healing process: an overview of the cellular and molecular mechanisms. Journal of International Medical Research **37**(5): 1528-1542.

Villegas, L. F., A. Marçalo, J. Martin, I. D. Fernández, H. Maldonado, A. J. Vaisberg and G. B. Hammond (2001). (+)-epi-α-Bisabolol Is the wound-healing principle of *Peperomia galioides*: Investigation of the *in vivo* wound-healing activity of related terpenoids. Journal of Natural Products **64**(10): 1357-1359.

Wang, R., M. Lechtenberg, J. Sendker, F. Petereit, A. Deters and A. Hensel (2013). Wound-healing plants from TCM: *in vitro* investigations on selected TCM plants and their influence on human dermal fibroblasts and keratinocytes. Fitoterapia **84**(0): 308-317.

Wang, Y., P. Chen, C. Tang, Y. Wang, Y. Li and H. Zhang (2014). Antinociceptive and anti-inflammatory activities of extract and two isolated flavonoids of *Carthamus tinctorius* L. Journal of Ethnopharmacology **151**(2): 944-950.

Xue, B., J. Li, Q. Chai, Z. Liu and L. Chen (2008). Effect of total flavonoid fraction of *Astragalus complanatus* R. Brown on angiotensin II-induced portal-vein contraction in hypertensive rats. Phytomedicine **15**(9): 759-762.

Yang, H. H., K. Hwangbo, M. S. Zheng, J. K. Son, H. Y. Kim, S. H. Baek, H. C. Choi, S. Y. Park and J. R. Kim (2014). Inhibitory effects of juglanin on cellular senescence in human dermal fibroblasts. Journal of Natural Medicines **68**(3): 473-480.

Yu, L., C. Chen, L.-F. Wang, X. Kuang, K. Liu, H. Zhang and J.-R. Du (2013). Neuroprotective effect of kaempferol glycosides against brain Injury and neuroinflammation by inhibiting the activation of NF-**K**B and STAT3 in transient focal stroke. PLoS ONE **8**(2): e55839.

Yuldashev, M. P., E. K. Batirov and V. M. Malikov (1996). Flavonoids of the epigeal part of *Onobrychis arenaria*. Chemistry of Natural Compounds **32**(4): 590-591.

Zou, Y., S. K. C. Chang, Y. Gu and S. Y. Qian (2011). Antioxidant activity and phenolic compositions of Lentil (*Lens culinaris* var. Morton) extract and its fractions. Journal of Agricultural and Food Chemistry **59**(6): 2268-2276.

Zubair, M., A. Ekholm, H. Nybom, S. Renvert, C. Widen and K. Rumpunen (2012). Effects of *Plantago major* L. leaf extracts on oral epithelial cells in a scratch assay. Journal of Ethnopharmacology **141**(3): 825-830.

APPENDIX

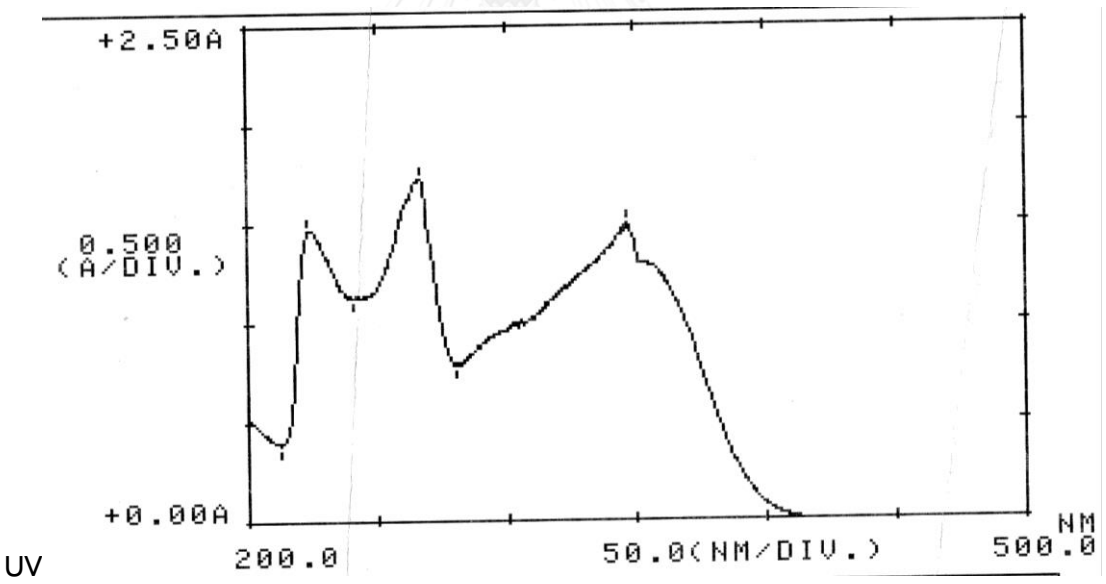

Figure 10 UV spectrum of juglanin

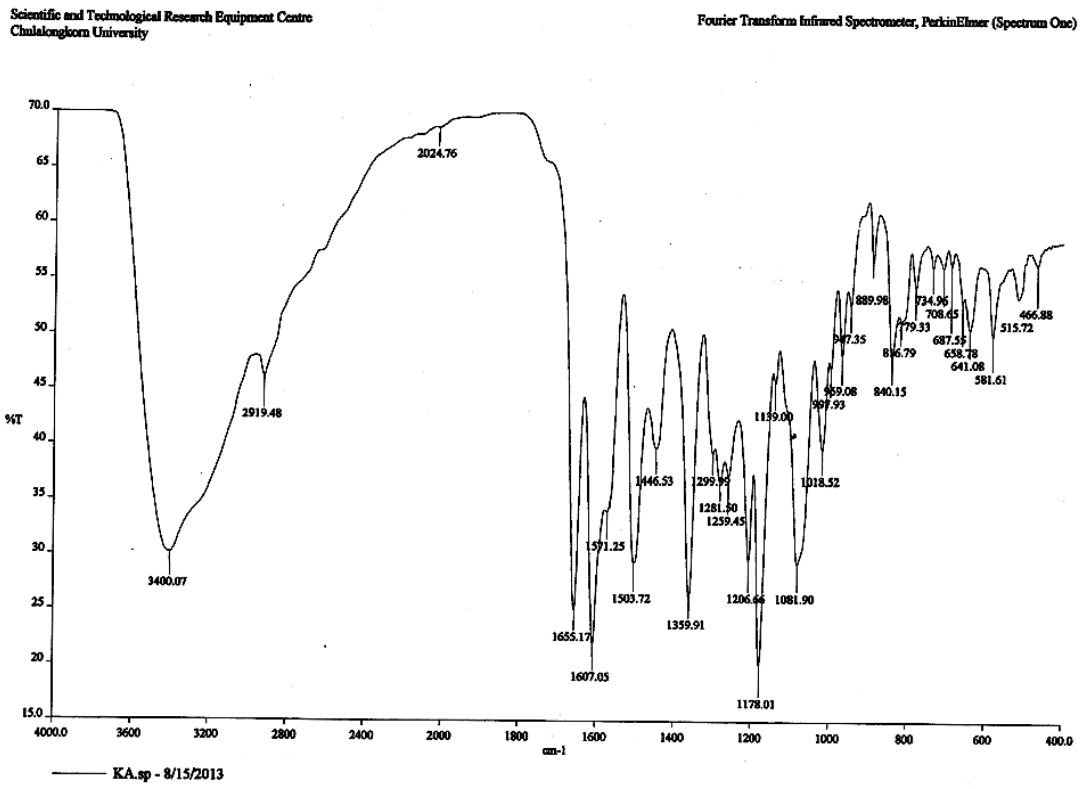

Figure 11 IR spectrum of juglanin

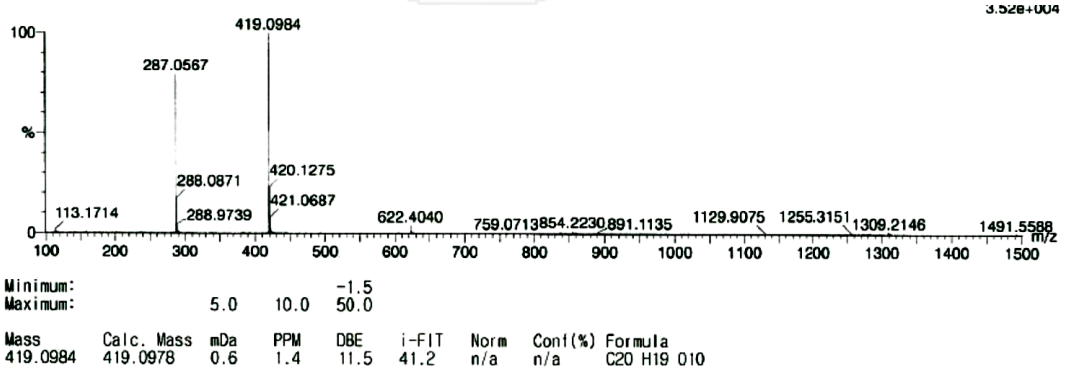

Figure 12 MS spectrum of juglanin

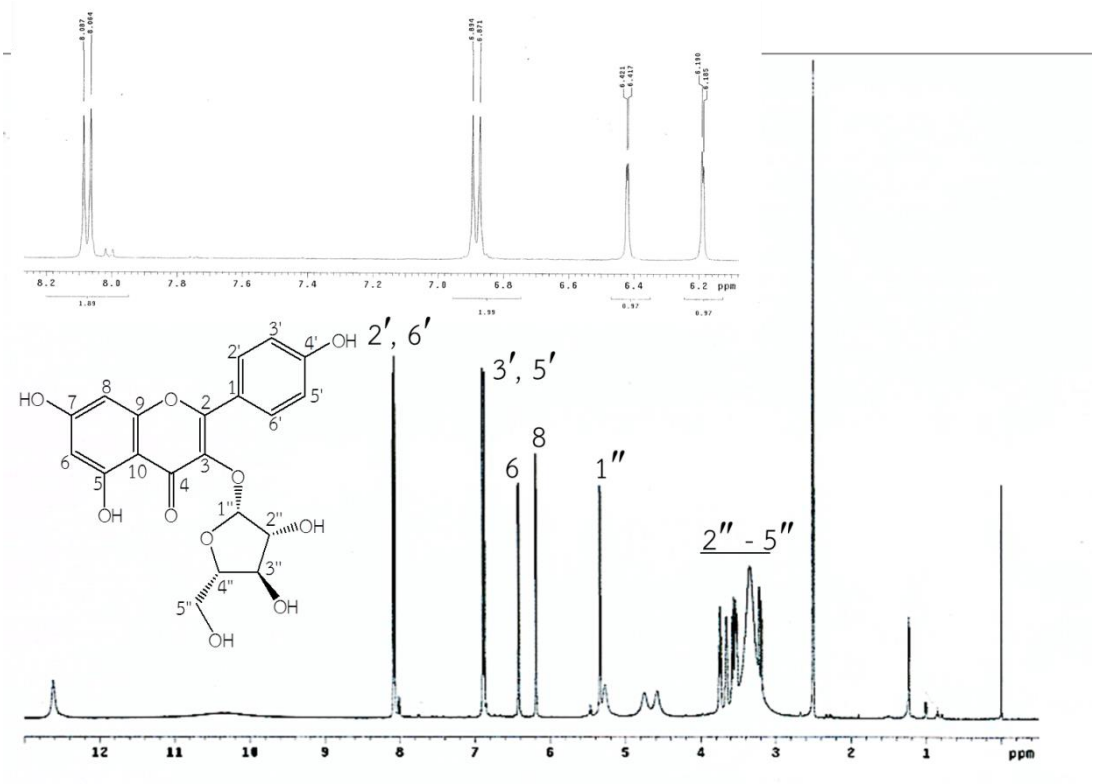

Figure 13 ^{1}H NMR (400MHz) spectrum of juglanin (in DMSO-d_6)

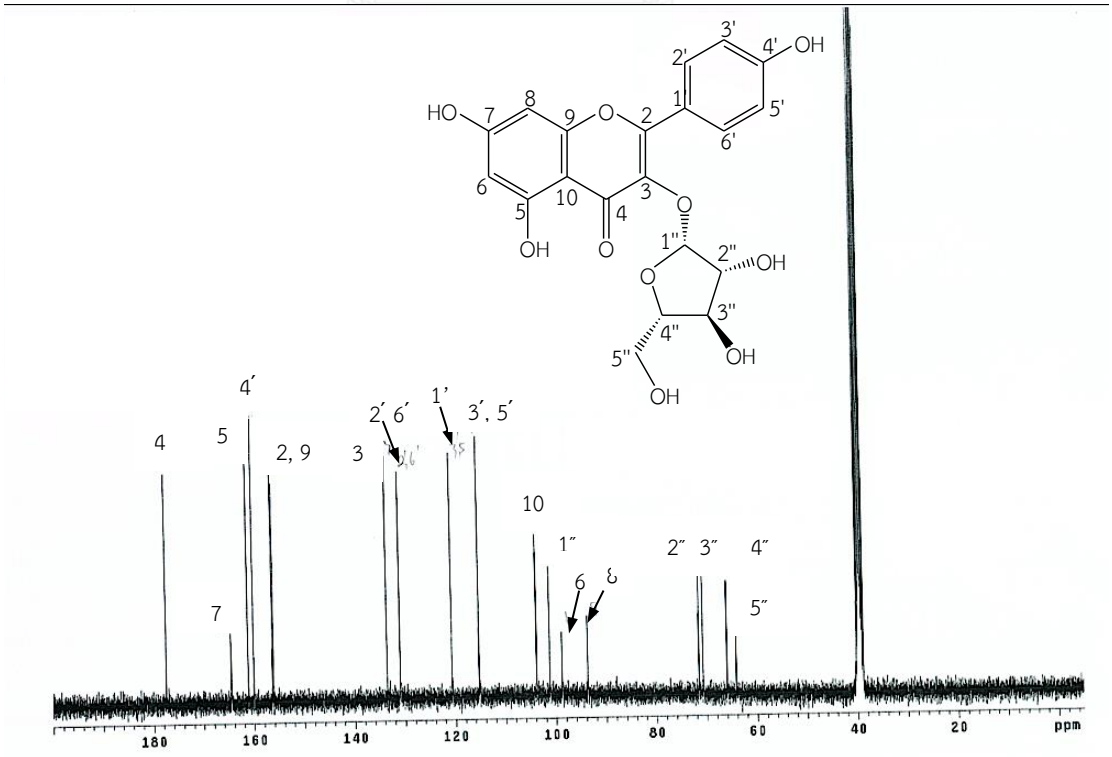

Figure 14 ^{13}C NMR (100MHz) spectrum of compound 1 (in DMSO-d_6)

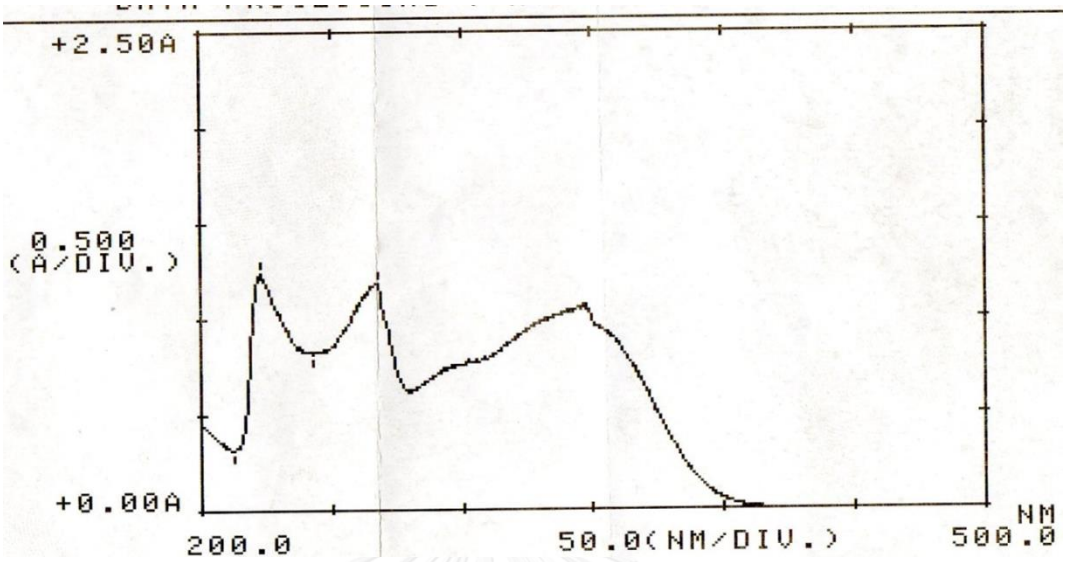

Figure 15 UV spectrum of astragalin

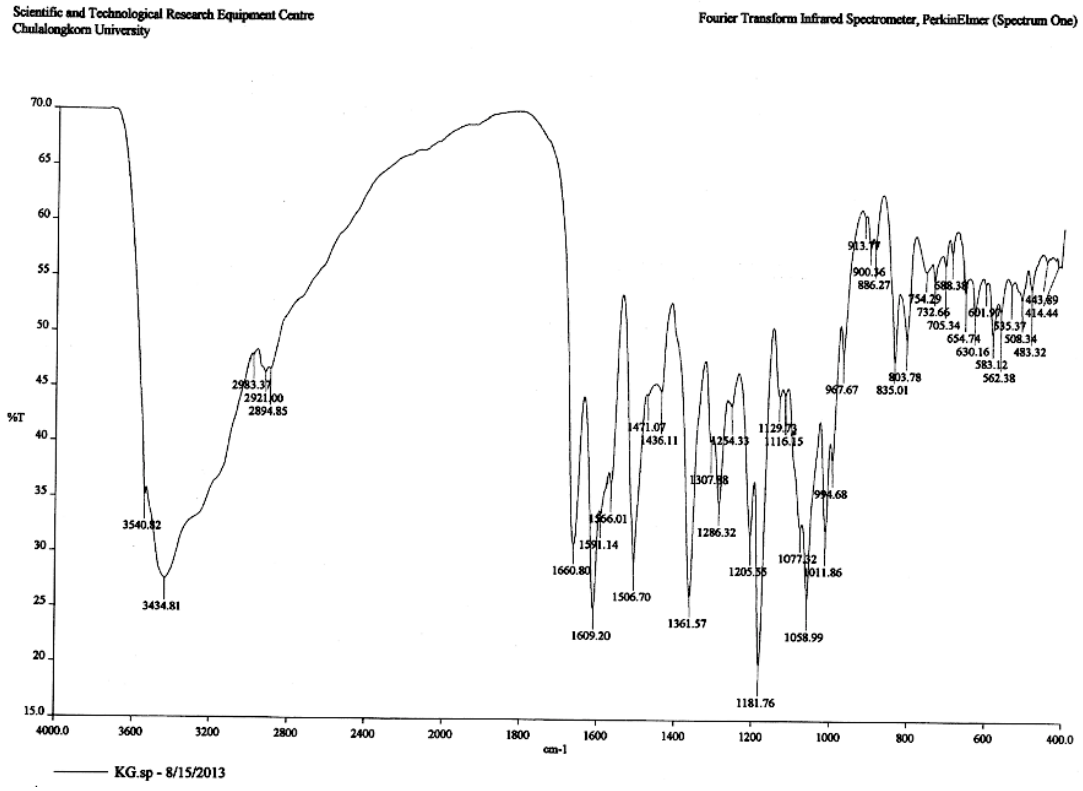

Figure 16 IR spectrum of astragalin

Mass	Calc. Mass	mDa	PPM	DBE	Formula	i-FIT	i-FIT Norm	Fit Conf %	C	H	O
449.1044	449.1025	1.9	4.2	20.5	C28 H17 O6	26.9	0.222	80.09	28	17	6
	449.1084	-4.0	-8.9	11.5	C21 H21 O11	28.3	1.614	19.91	21	21	11

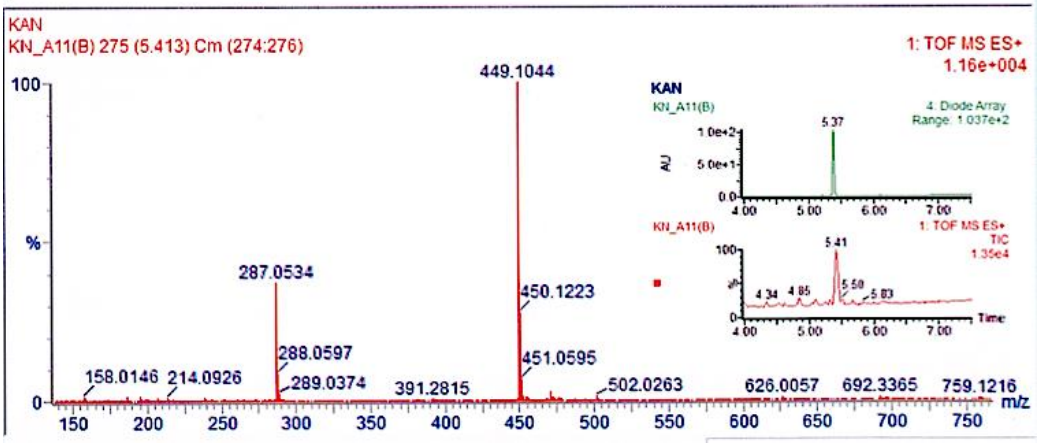

Figure 17 MS spectrum of astragalin

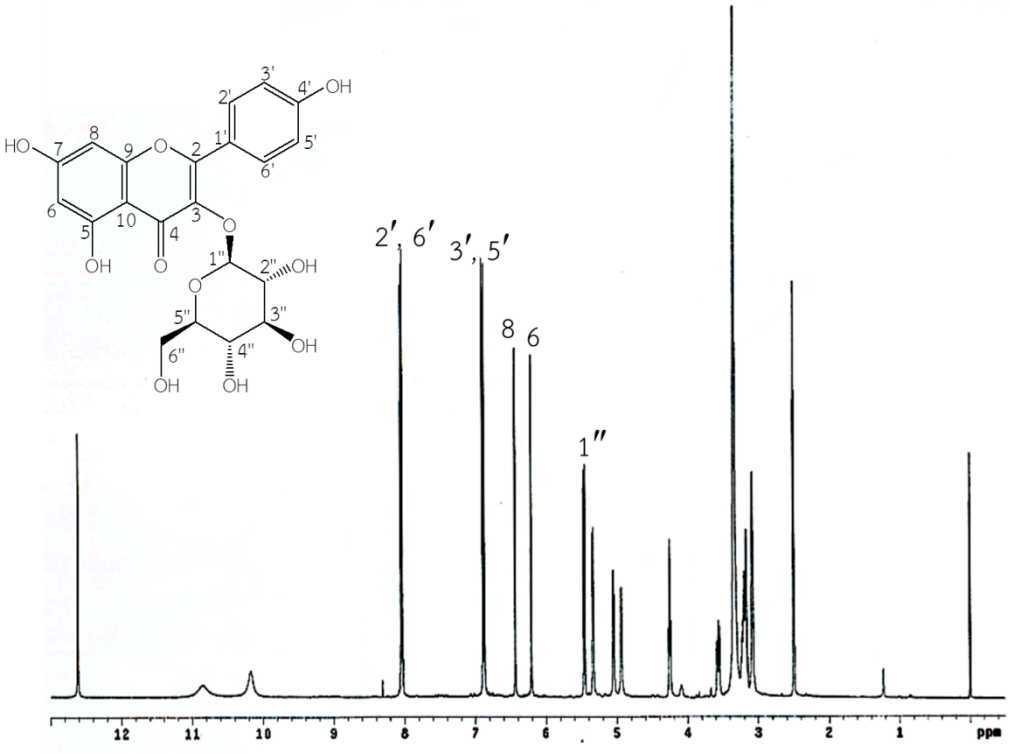

Figure 18 ^{1}H NMR (400MHz) spectrum of astragalin (in DMSO-d_6)

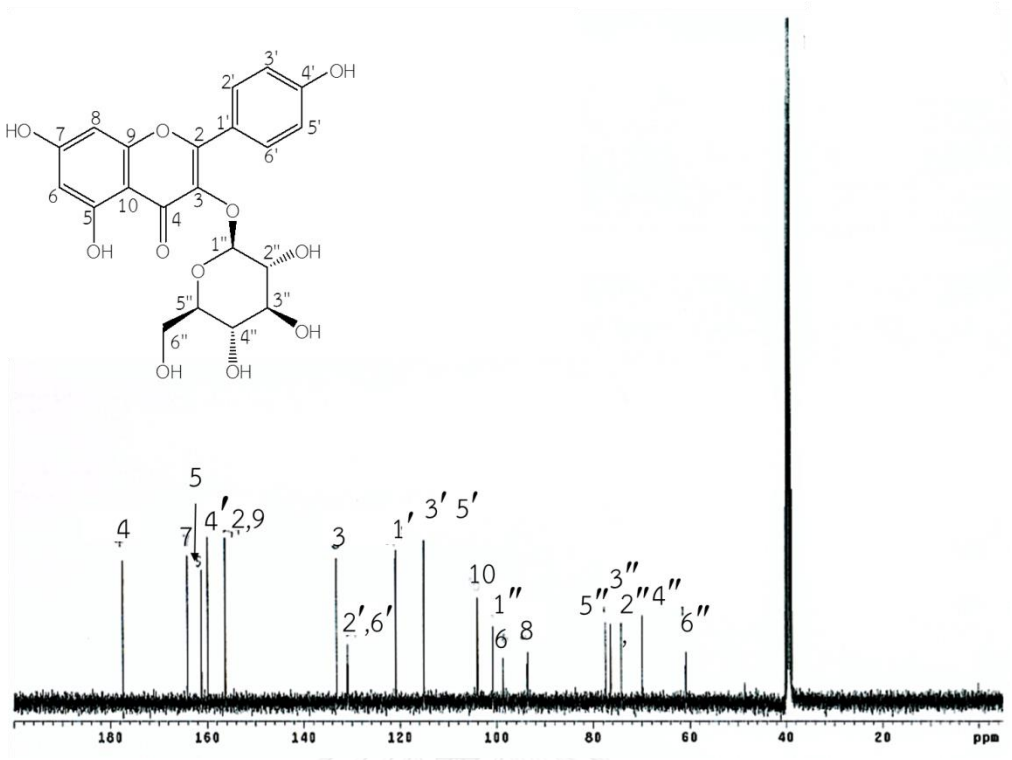

Figure 19 ^{13}C NMR (100MHz) spectrum of astragalin (in DMSO-d_6)

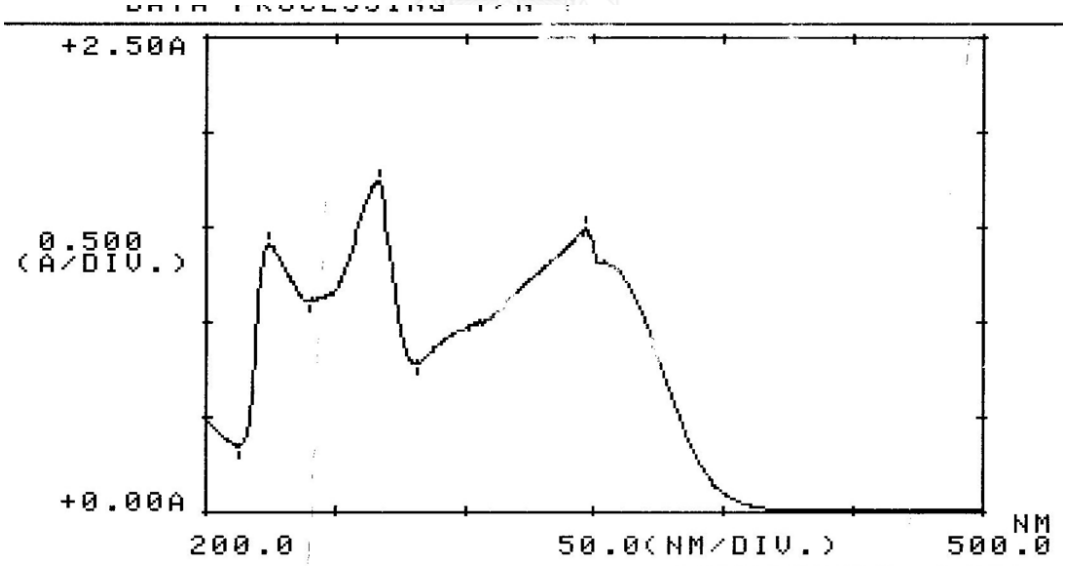

Figure 20 UV spectrum of nicotiflorin

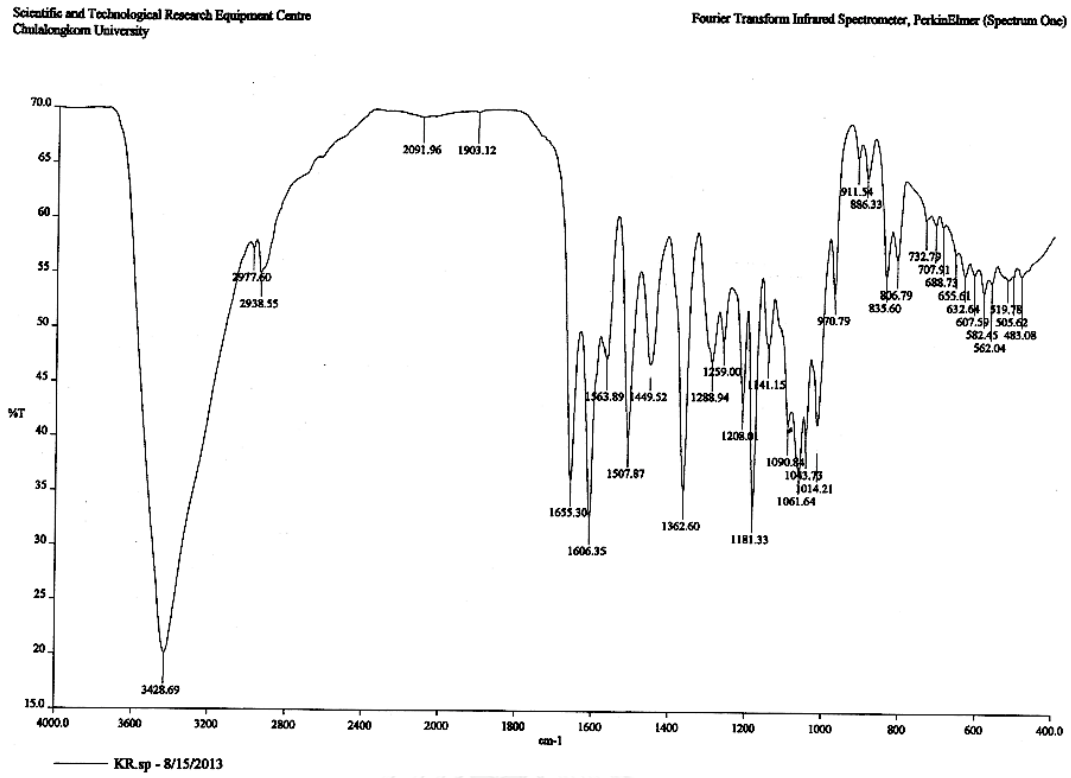

Figure 21 IR spectrum of nicotiflorin

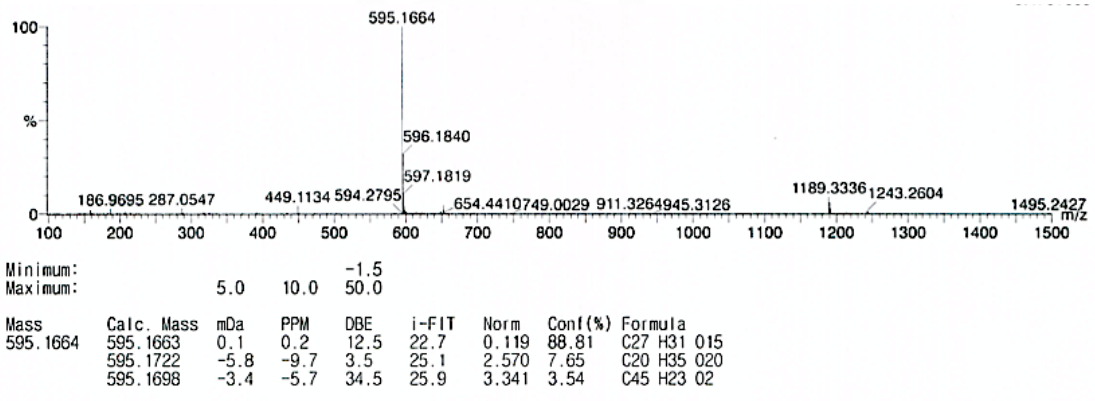

Minimum:				-1.5				
Maximum:		5.0	10.0	50.0				
Mass	Calc. Mass	mDa	PPM	DBE	i-FIT	Norm	Conf(%)	Formula
595.1664	595.1663	0.1	0.2	12.5	22.7	0.119	88.81	C27 H31 O15
	595.1722	-5.8	-9.7	3.5	25.1	2.570	7.65	C20 H35 O20
	595.1698	-3.4	-5.7	34.5	25.9	3.341	3.54	C45 H23 O2

Figure 22 MS spectrum of nicotiflorin

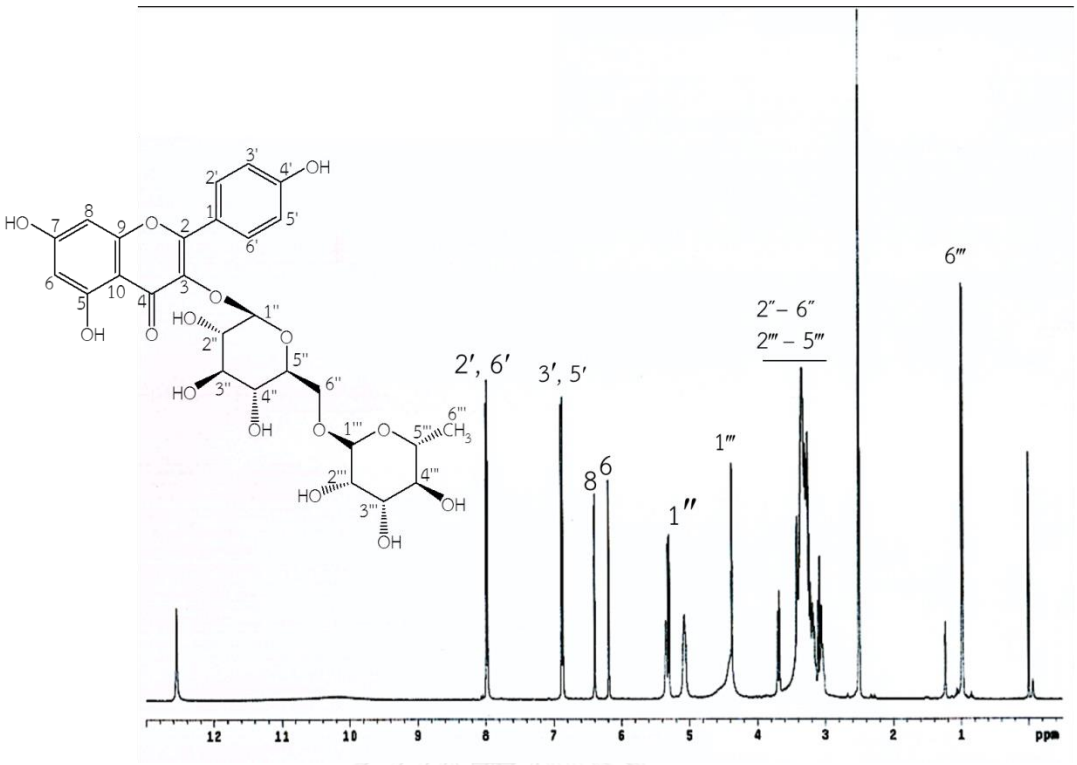

Figure 23 ^{1}H NMR (100MHz) spectrum of nicotiflorin (in DMSO-d_6)

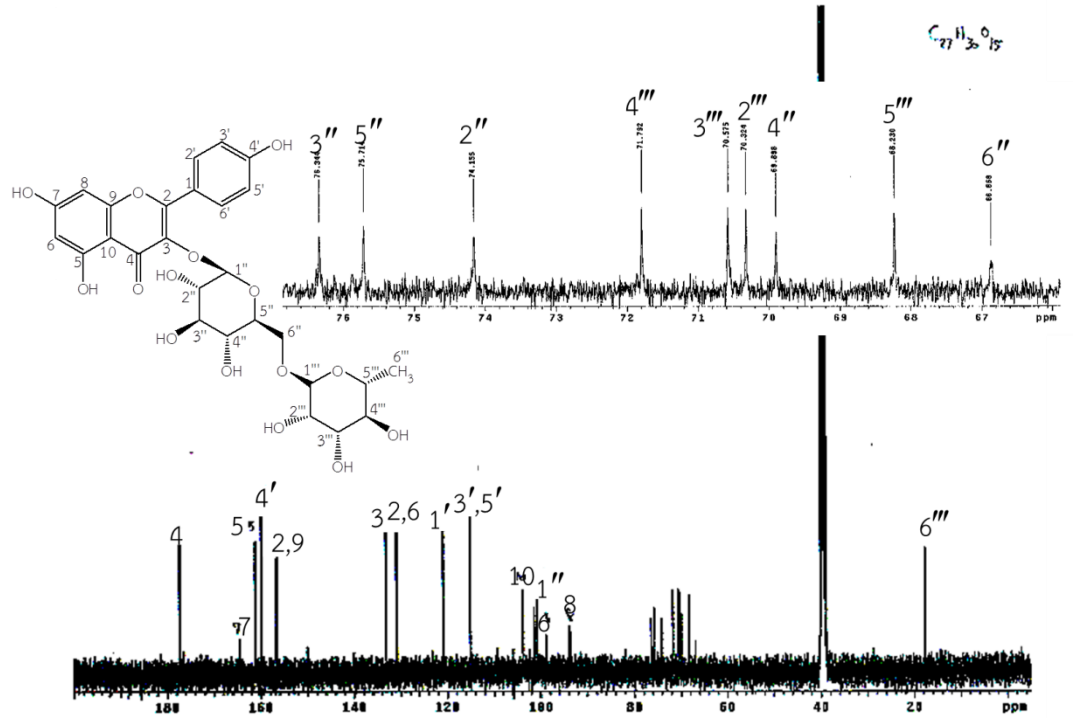

Figure 24 ^{13}C NMR (100MHz) spectrum of nicotiflorin (in DMSO-d_6)

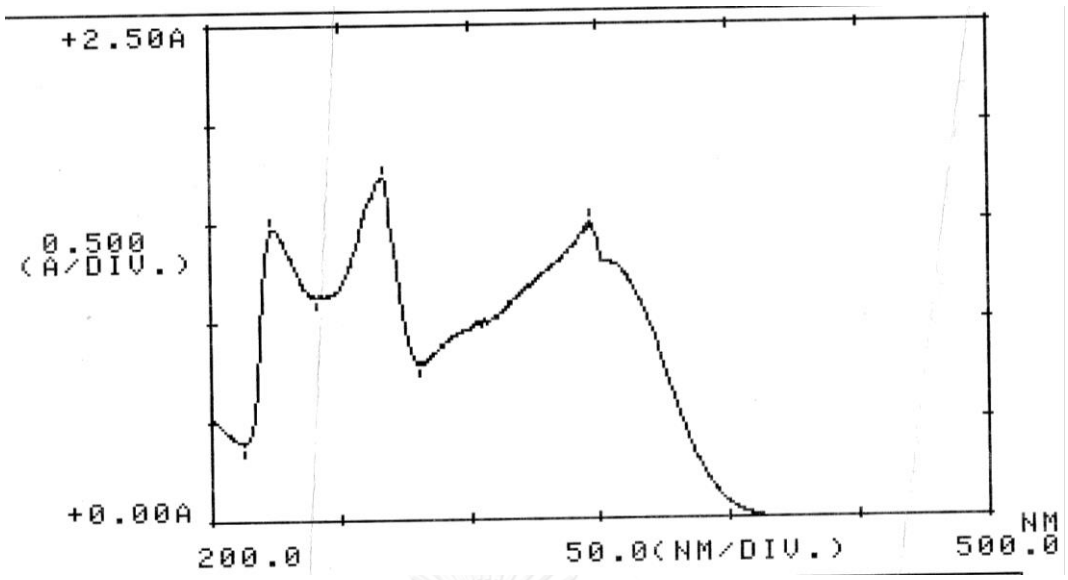

Figure 25 UV spectrum of isoquercetrin

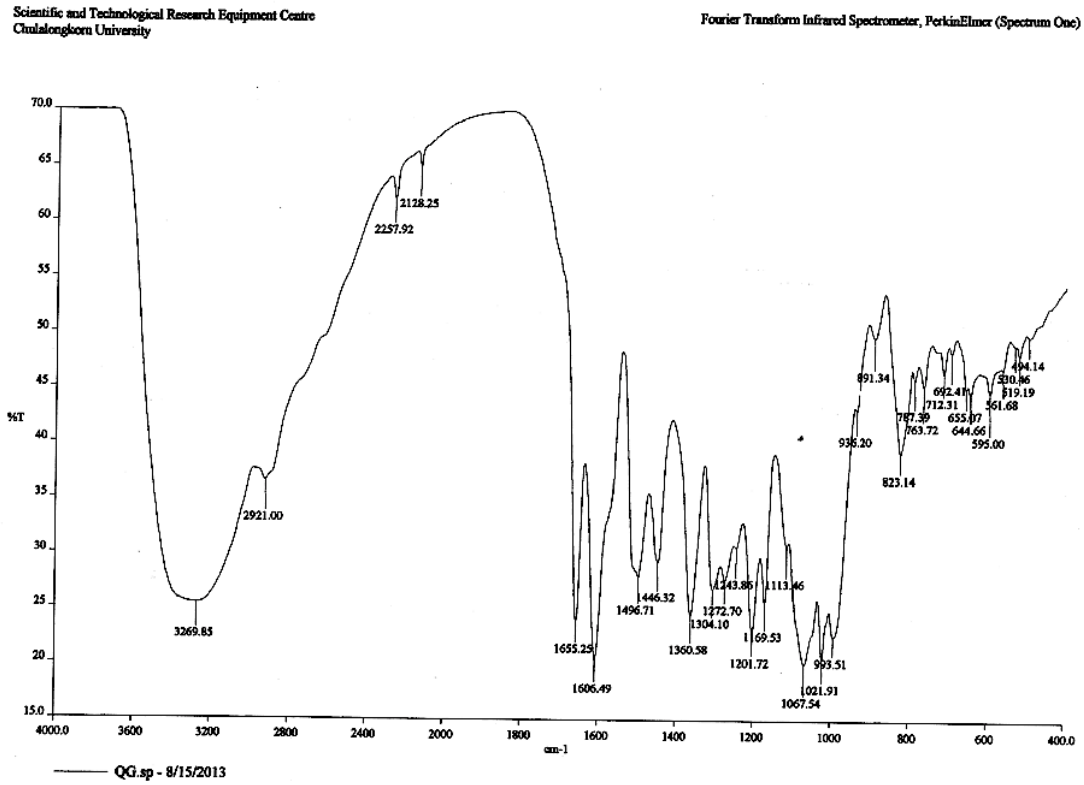

Figure 26 IR spectrum of isoquercetrin

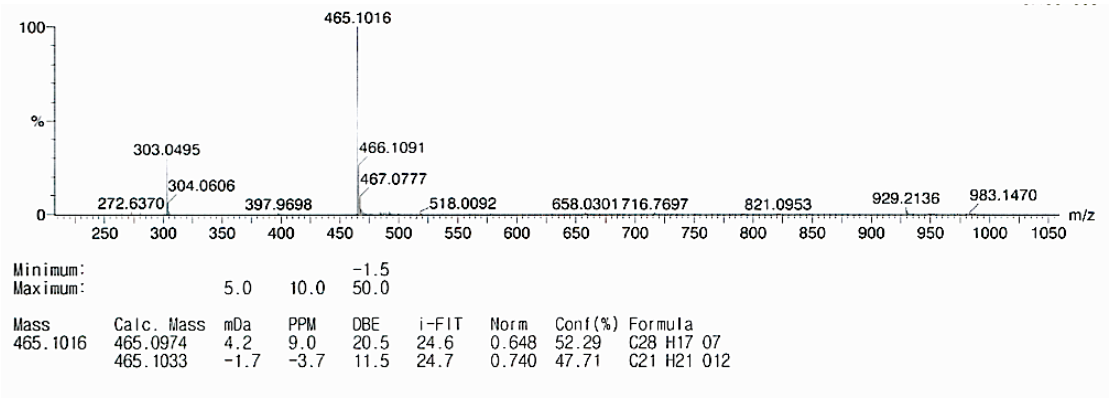

Figure 27 MS spectrum of isoquercetrin

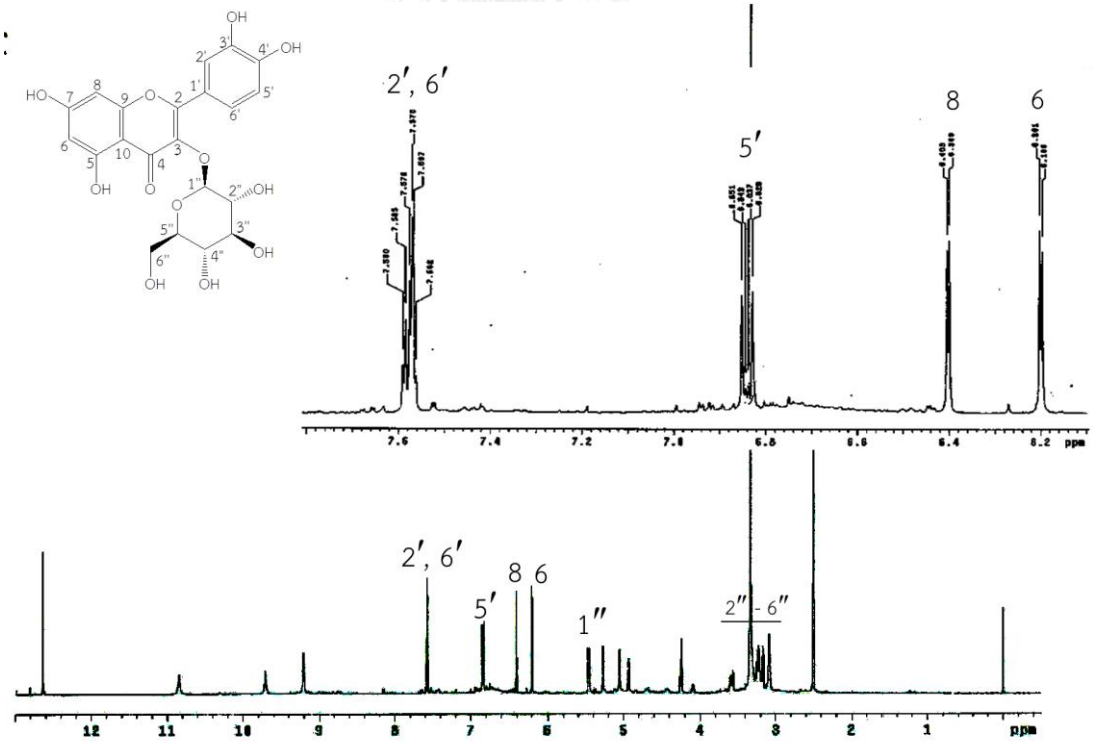

Figure 28 ^{1}H NMR (400MHz) spectrum of isoquercetrin (in DMSO-d_6)

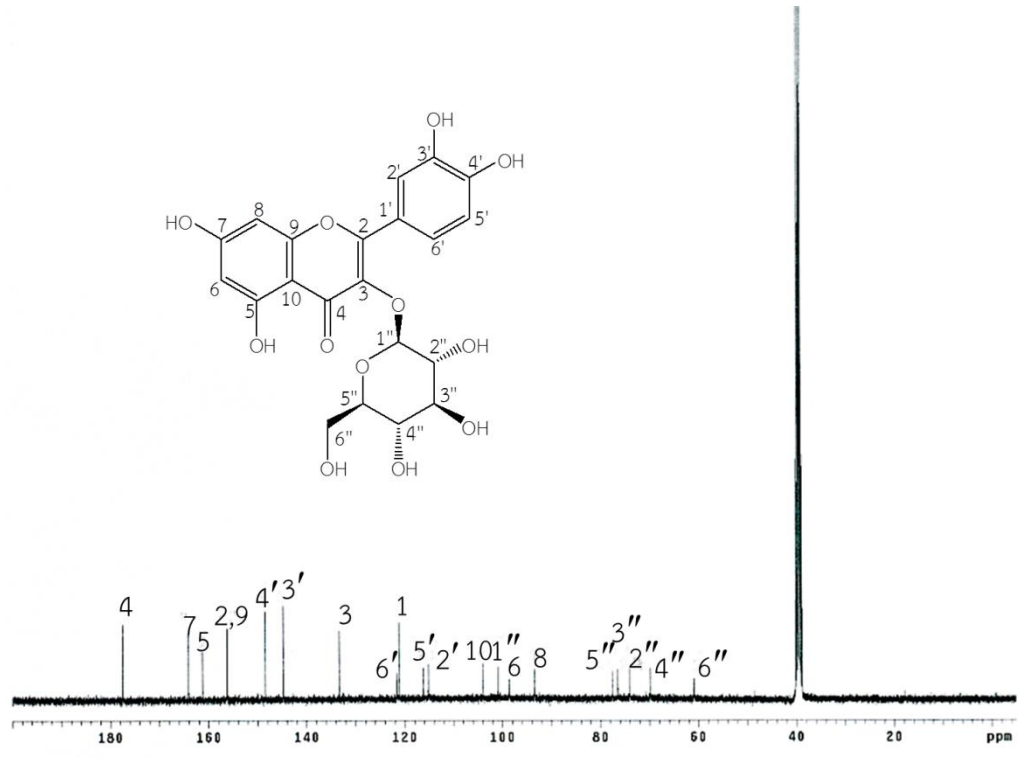

Figure 29 ^{13}C NMR (100MHz) spectrum of isoquercetrin (in DMSO-d_6)

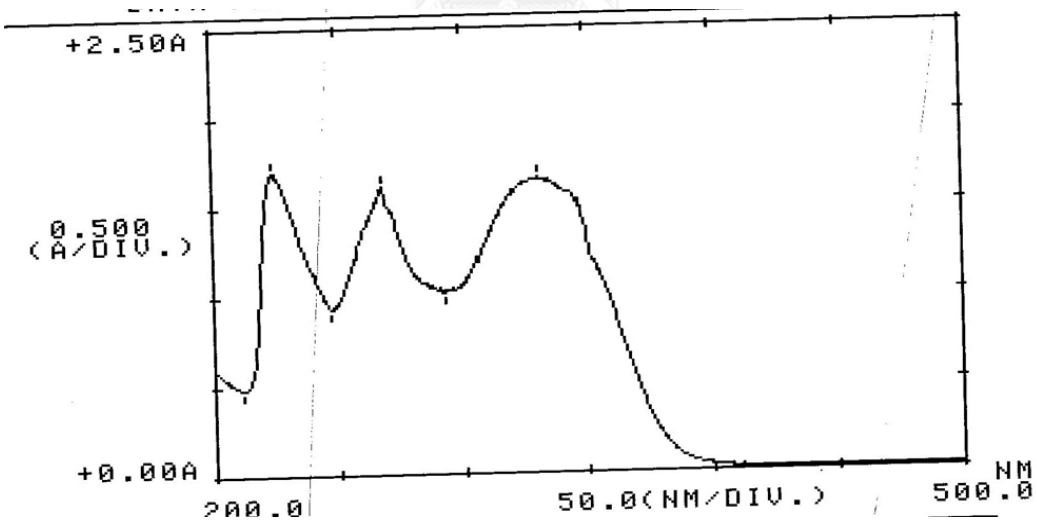

Figure 30 UV spectrum of apigenin-7-*O*-glucuronide

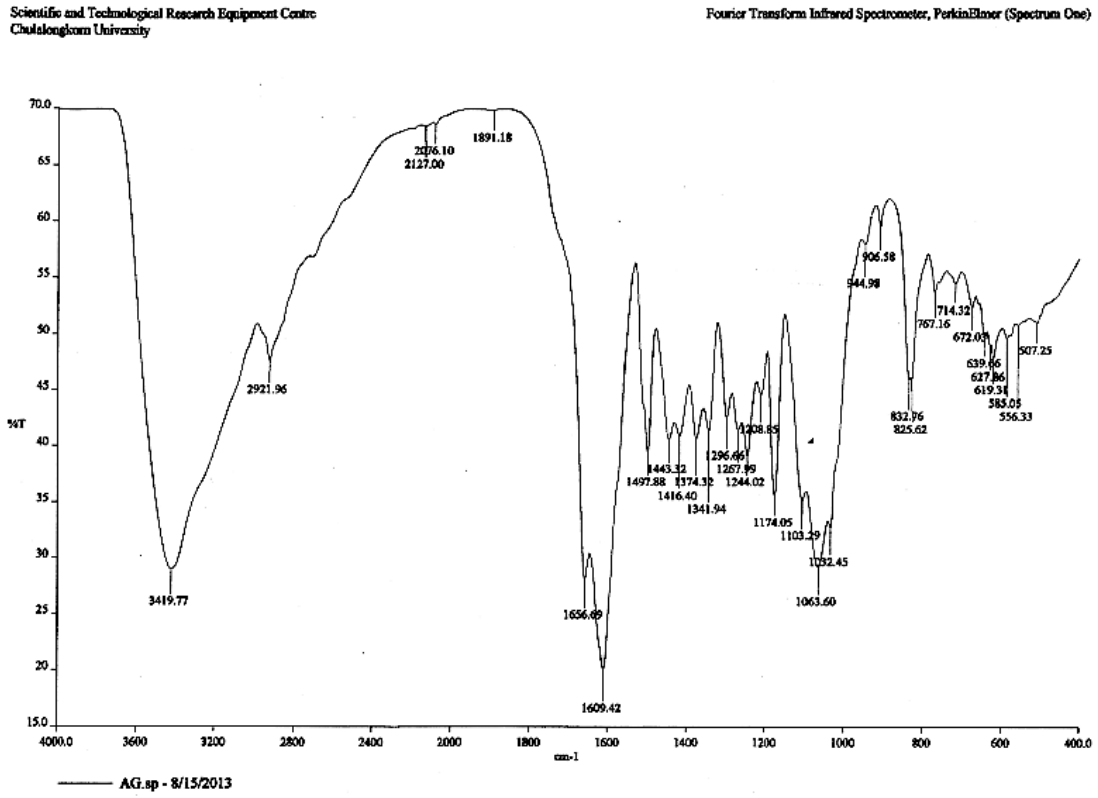

Figure 31 IR spectrum of apigenin-7-*O*-glucuronide

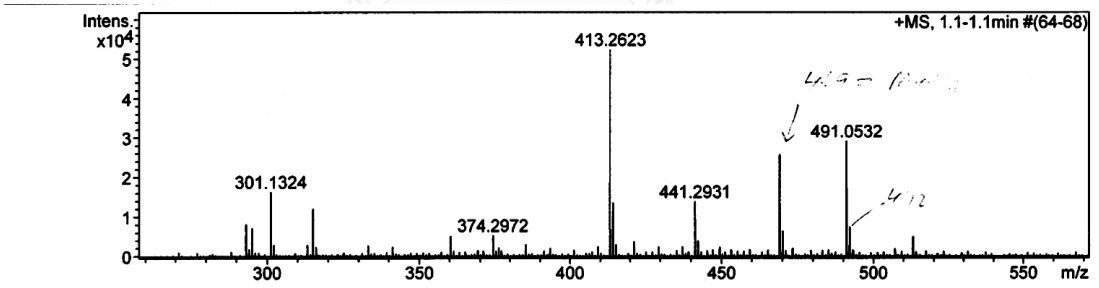

Figure 32 MS spectrum of apigenin-7-*O*-glucuronide

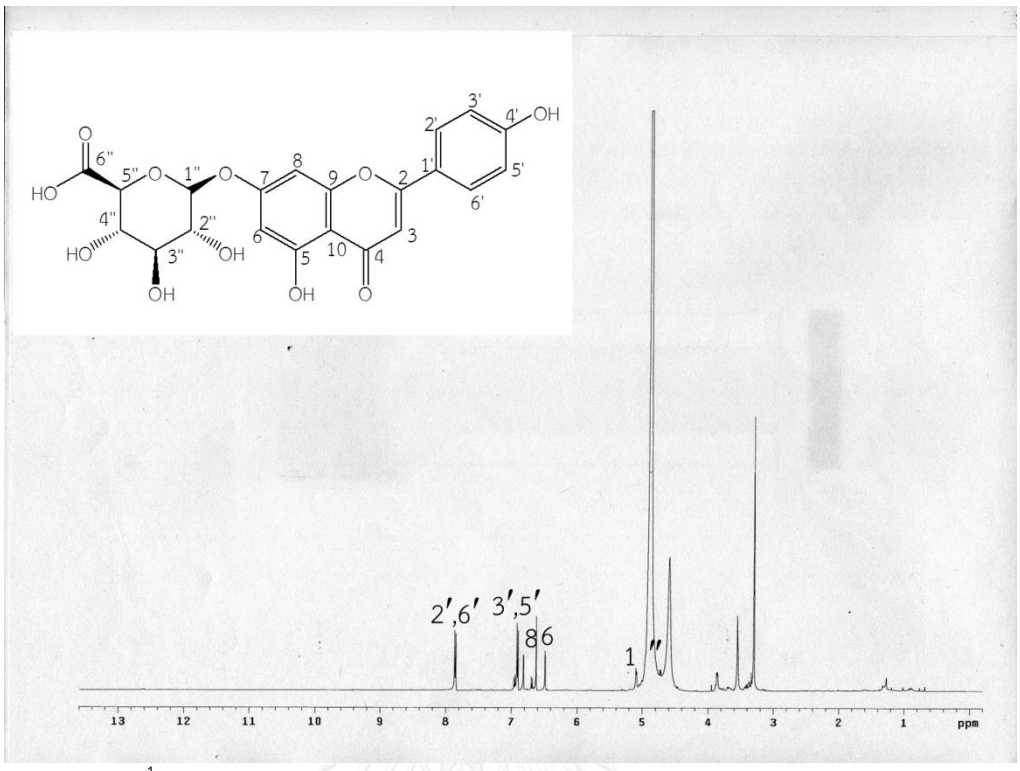

Figure 33 ^{1}H NMR (400MHz) spectrum of apigenin-7-*O*-glucuronide (in CD_3OD)

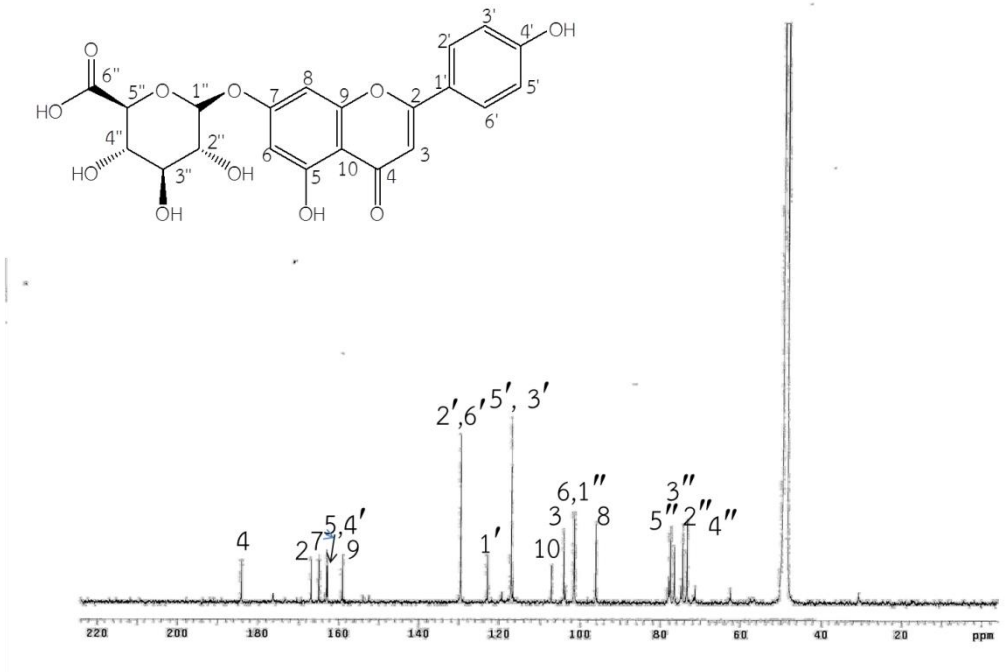

Figure 34 ^{13}C NMR (100MHz) spectrum of apigenin-7-*O*-glucuronide (in CD_3OD)

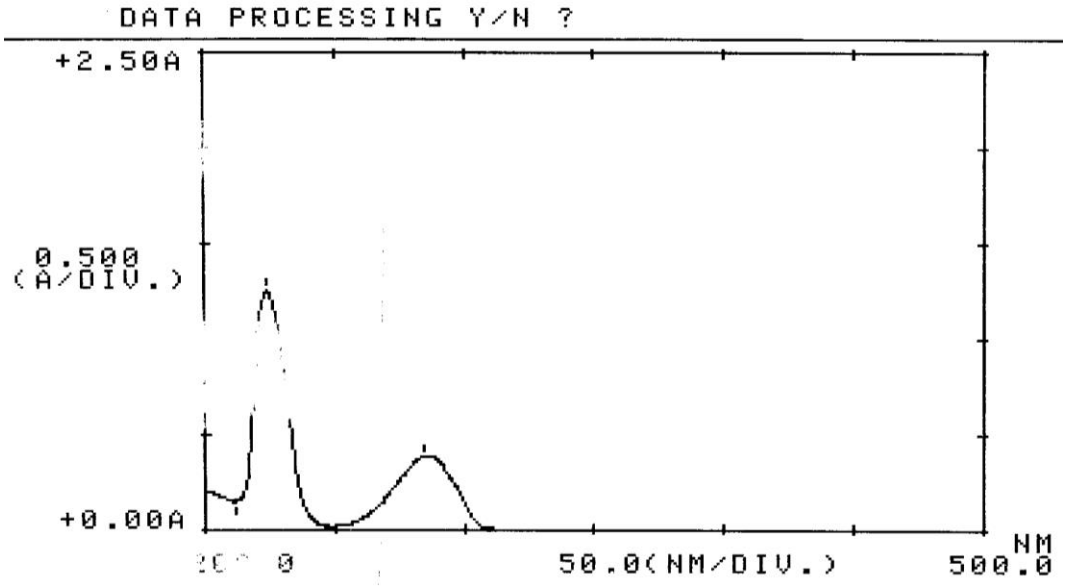

Figure 35 UV spectrum of arbutin

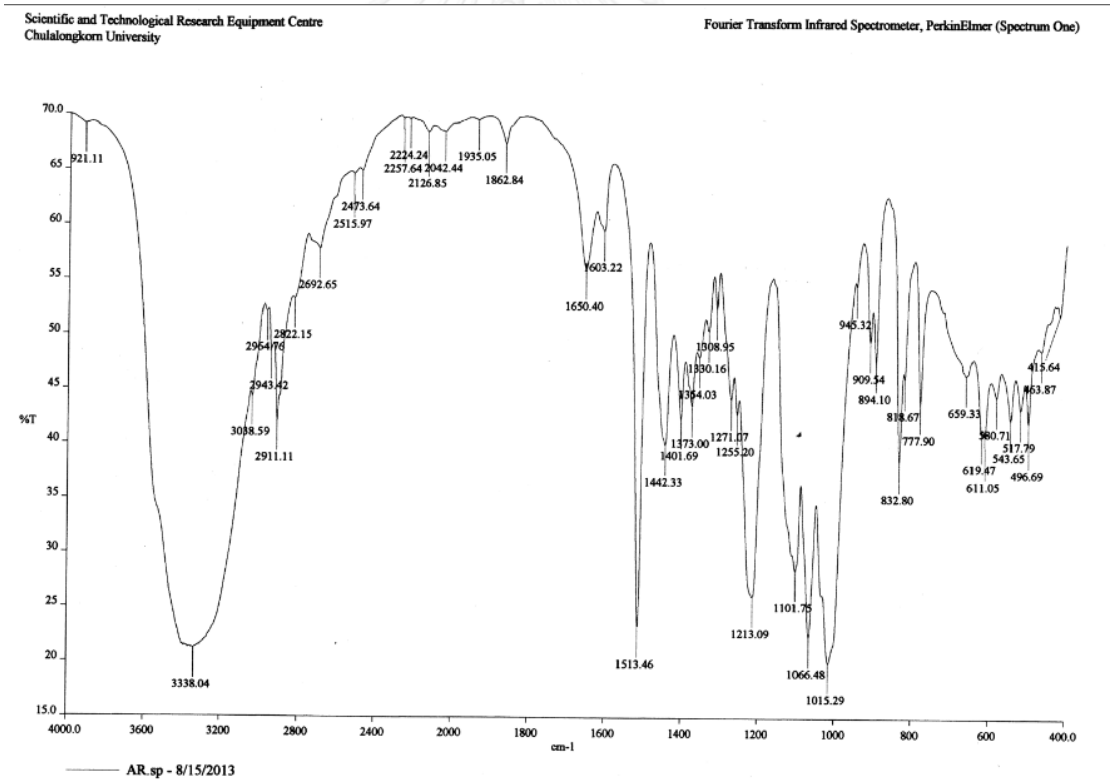

Figure 36 IR spectrum of arbutin

Mass Spectrum List Report

Analysis Info

Analysis Name	OSCUWP60911001.d	Acquisition Date	9/11/2013 2:48:55 PM
Method	MKE_tune_low_positive_20130204.m	Operator	Administrator
Sample Name	AR	Instrument	micrOTOF 72
	AR		

Acquisition Parameter

Source Type	ESI	Ion Polarity	Positive	Set Corrector Fill	75 V
Scan Range	n/a	Capillary Exit	130.0 V	Set Pulsar Pull	398 V
Scan Begin	50 m/z	Hexapole RF	90.0 V	Set Pulsar Push	380 V
Scan End	3000 m/z	Skimmer 1	45.5 V	Set Reflector	1300 V
		Hexapole 1	25.0 V	Set Flight Tube	9000 V
				Set Detector TOF	1910 V

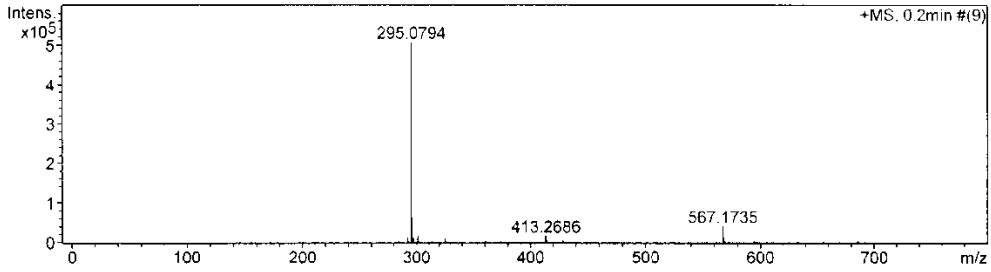

Figure 37 MS spectrum of arbutin

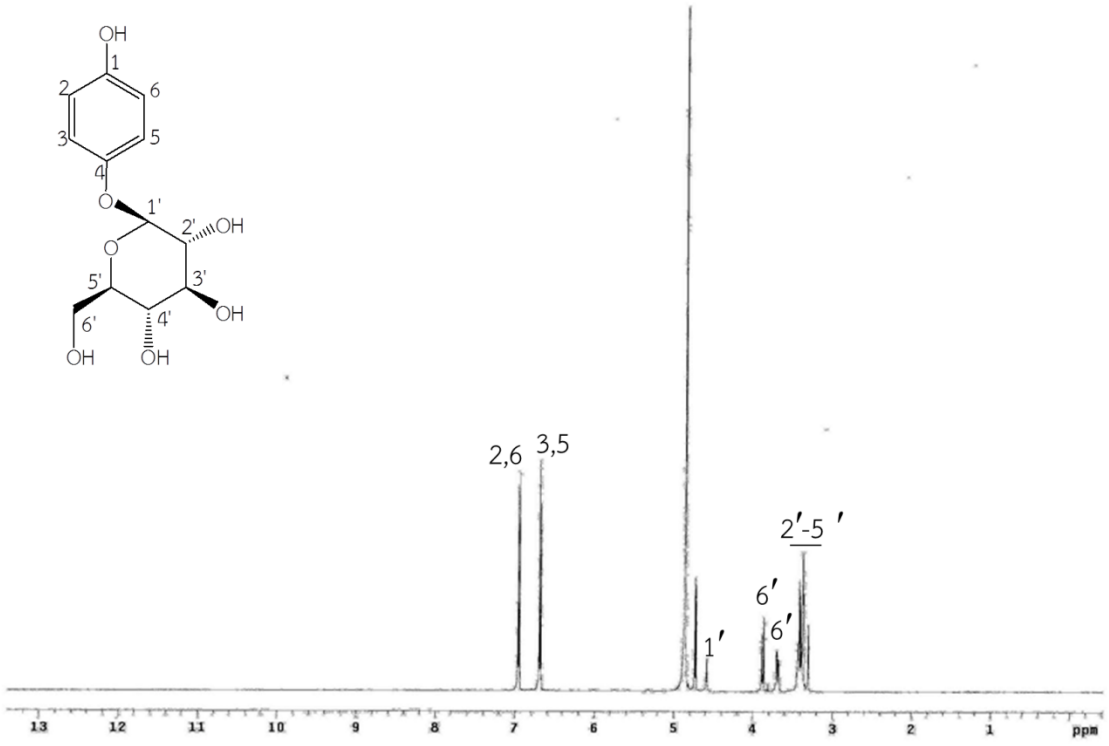

Figure 38 ^{1}H NMR (500MHz) spectrum of arbutin (in CD_3OD)

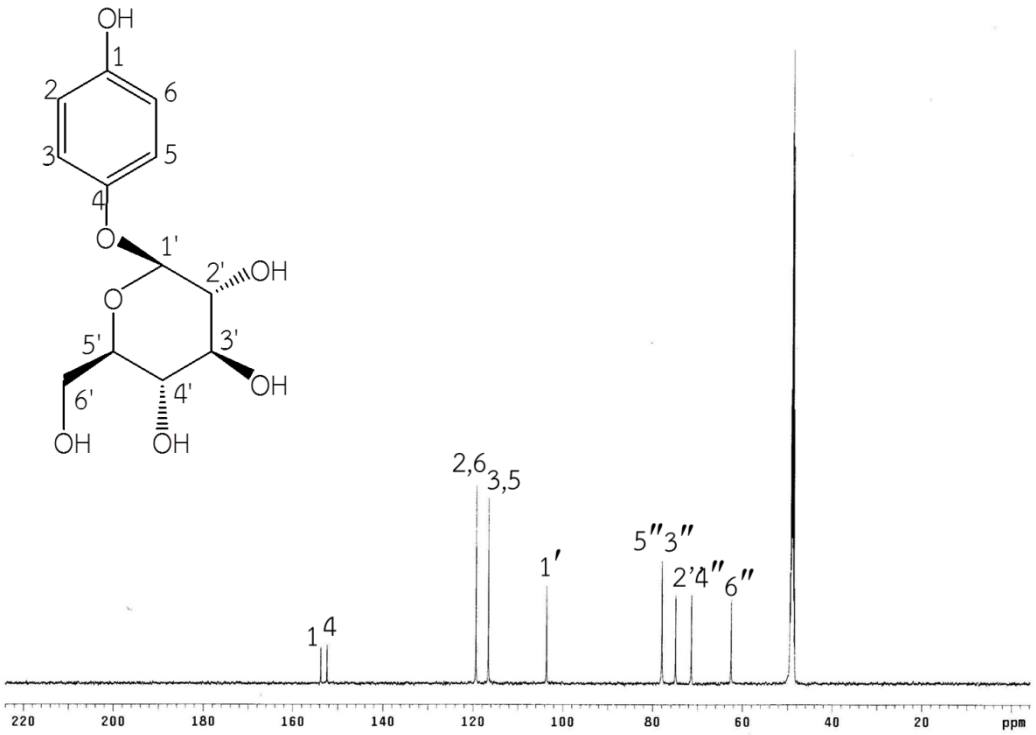

Figure 39 ^{13}C NMR (100MHz) spectrum of arbutin (in CD_3OD)

VITA

Mr. Chalermlat Suktap was born on July 2, 1988 in Rayong, Thailand. He received his B. Pharm. in 2011 from the faculty of Pharmaceutical Sciences, Khon Kaen University, Thailand.

Poster Presentation

Chalermlat Suktap, and Supawadee Daodee. Screening of tyrosinase inhibitory activity from Phyllanthus acidus skeels. Proceedings of the 3rd Annual Northeast Pharmacy Research Conference February 12th-13th, 2011. Faculty of Pharmaceutical Sciences, Ubon Ratchathani University, Ubon Ratchathani, Thailand. p. 27-31.